LPI AIR DEFENCE NOISE RADAR

by

Lazarus Molahlegi Molope

Dissertation submitted to the Faculty of Engineering and Built Environment of
The University of Cape Town, South Africa in fulfilment
of the requirements for the degree of
MSc in Radar and Electronic Defence
07 May 2022

Advisory Committee:
Dr Francois Schonken
Prof. Amit Mishra

DECLARATION

I, Lazarus Molahlegi Molope, hereby declare that "I know the meaning of plagiarism and declare that all the work in the document, save for that which is properly acknowledged, is my own. This dissertation has been submitted to the Turnitin module and I confirm that my supervisor has seen my report and any concerns revealed by such have been resolved with my supervisor."

Signature: Signed by candidate

Date: 07 May 2022

ABSTRACT

Title of dissertation: LPI AIR DEFENCE NOISE RADAR

Lazarus Molahlegi Molope
MSc Radar and Electronic Defence, 2022

Dissertation directed by: Dr Francois Schonken and Prof Amit Mishra
Department of Electrical Engineering

This dissertation is for researching the feasibility of a Low Probability of Intercept (LPI), Air Defence (AD) Noise Radar with high range and doppler resolution. The research is approached by first simulating an S-Band LPI Noise Radar detecting a flying target and determining its range and velocity. The simulated Noise Radar is then implemented in the Universal Software Radio Peripheral (USRP) B210 H/W and tested against flying targets in monostatic mode. The actual results from H/W detection of real airborne targets are finally compared with simulated results.

Dedication

This dissertation is dedicated to my family who has accommodated me waking up early in the morning doing experiments which eventually led to the final version of this document. To my wife, I say, you are the pillar of my strength and without your support, I would not have managed to spend so much time on this research. To my mother and my late father, you always taught us the importance of education. To my brother and two sisters, being the last born, I had no choice but to follow in your footsteps of putting education first. To my three children, your understanding when I spent too much time on my research is insurmountable.

Acknowledgements

I owe my gratitude to my employer, Armscor, who funded me in my studies for this Master's degree. You are one of the few organisations who support their employees in pursuing their studies, and for that, I say keep up the good work. My thanks go to my Radar colleagues at CSIR who were always available to discuss some Radar concepts I needed clarity on and for making your laboratory available for some of my experiments since you have a nice view of the highway which I couldn't finish my research without its access. To my colleague at Armscor, with whom I spent several hours discussing Radar concepts since we were both busy with our Radar research, those discussions added value to this final dissertation, and I say let our graduation not be the end of experimentation, since we both believe in life long learning through experimentation.

To my first supervisor, Prof Daniel O'Hagan, thank you for suggesting the topic of my research. Even though you left South Africa before I could complete this research, finally both my Radar and my research are complete. Next in line is my supervisor, Dr Francois Schonken, thank you for all the support during this long journey we have been through together, finally, the ultimate goal has been achieved. I spent several months focusing on my Radar to work, and your patience allowed me to finish my research with a detailed Radar understanding which can only be achieved through experimentation. Last but not least, my co-supervisor, Prof Amit Mishra, thanks for your support in providing comments timeously to make sure this dissertation is completed urgently and published.

Contents

List Of Tables

List Of Figures

List of Abbreviations

2D	Two Dimensional
3D	Three Dimensional
AD	Air Defence
APCN	Advanced Pulse Compression Noise
CERDEC	Communications-Electronics Research, Development and Engineering Center
CNS	Continuous Noise Signal
COTS	Commercial Off The Shelf
CPU	Central Processing Unit
CW	Continuous Wave
DRFM	Digital Radio Frequency Memory
EA	Electronic Attack
ELINT	Electronic Intelligence
EP	Electronic Protection
ES	Electronic Support
ESM	Electronic Support Measures
EW	Electronic Warfare
F/W	Firmware
FPGA	Field Programmable Gate Array
FMCW	Frequency Modulated Continuous Wave
GPU	Graphical Processing Unit
H/W	Hardware
IF	Intermediate Frequency
ISAR	Inverse Synthetic Aperture Radar
km	kilo meter
LFM	Linear Frequency Modulation
LPD	Low Probability of Detection
LPF	Low Pass Filter
LPI	Low Probability of Intercept
MDS	Minimum Detectable Signal
MFCR	Missile Fire Control Radar
NF	Noise Figure
NI	National Instrument
NRT	Noise Radar Technology
PRF	Pulse Repetition Frequency
PRI	Pulse Repetition Interval
RAM	Random Access Memory
Radar	Radio Detection and Ranging
RCS	Radar Cross Section
RF	Radio Frequency
ROC	Receiver Operating Characteristics
RWR	Radar Warning Receiver
S/W	Software

SAR	Synthetic Aperture Radar
SDR	Software Defined Radio
SIGINT	Signal Intelligence
SNR	Signal to Noise Ratio
SWaPC	Size Weight Power and Cost
UAV	Unmanned Aerial Vehicle
UCT	University of Cape Town
USRP	Universal Software Radio Peripheral
USRP B210	B210 Model of USRP
UWB	Ultra-Wide-Band
V.S.W.R	Voltage Standing Wave Ratio

Chapter 1
Introduction

1.1 Background

Kulpa [11] describes a Noise Radar as a Radar that uses random or pseudo-random waveforms for target illumination. It is used for various applications which include but are not limited to ground-penetration profiling, through wall surveillance, Synthetic Aperture Radar (SAR), Inverse Synthetic Aperture Radar (ISAR) and Foliage Penetration (FOPEN) [4]. Malanowski and Kulpa [16], state that some of the topics that are fundamental to the success of Noise Radar still have to be researched thoroughly. Like all Radars, noise Radar also has to overcome high target density, clutter, jamming and external interferences [4]. Their main characteristics are that they have a Low Probability of Intercept (LPI), Low Probability of Detection (LPD), high range resolution, high Doppler resolution, immunity to interference, resistance to jamming, efficient sharing of the spectrum (with both Noise Radars and all other Radio Frequency (RF) devices since they are inherently designed to filter out noise) [1, 7]. The signal is shaped like noise and covers a wide band of frequencies.

The random nature of the noise waveforms makes them very good at suppressing external interference [4, 7]. Thayaparan and Wernik [4] showed in their experiments that noise Radar can operate with a low Signal to Noise Ratio (SNR), up to -30 dB. They further showed that for Noise Radars, the signals from other Radars simply raise the noise floor. They do not interfere with other Radars in the same frequency band, whereas other Radars such as Linear Frequency Modulation Radars will cause ghost targets if they operate in the same frequency band as other Radars that are not noise Radars.

Noise Radar has been around since the 1950s but it is not widely used especially in the military environment [1, 4]. Lukin and Narayanan [7] state that the LPI and LPD characteristics of Noise Radar are very important for the military. Their efficient sharing of frequency spectrum allows them to have some overlapping coverage when used in the Air Defence role with minimal cross interference. This dissertation is limited to the performance improvements of Air Defence (AD) Radars. Some of the shortcomings of conventional AD Radar are that they use high-powered pulsed signals, have poor

range and Doppler resolutions, range ambiguity problems and are vulnerable to interference (which includes intentional and unintentional jamming). Noise Radar promises to alleviate these shortcomings since it is inherently immune to jamming, it is range unambiguous and it is immune to external interferences due to its randomness and low power characteristics which keep it within the noise and thus make it invisible to an Electronic Warfare (EW) receiver. Furthermore, the fact that its power is spread over a wide range of frequencies, makes it difficult for the Electronic Support (ES) and Electronic Intelligence (ELINT) receivers to detect it since most of them are looking for high-power narrowband signals. Its noise shape means it has no particular pattern, which contributes to its undetectable characteristic.

1.2 Statement Of Problem And Hypothesis

In the military Air Defence role, it is important to detect airborne targets of various sizes (targets with small Radar Cross Section (RCS) to targets with large RCS) sometimes at the same time. This implies that the Radar must have a high dynamic range.

It is also important for the Radar to have a high resolution in range and Doppler to distinguish between targets at various ranges and flying at various speeds. This is necessary for the AD operators to determine the threat level of each target. The Radar must also evade detection by the EW receivers by using a signal that will be within noise when received by an EW receiver at a remote distance. Therefore, the hypothesis to be tested is that an:

"LPI AD Noise Radar with high range and Doppler resolutions is realisable."

This hypothesis is tested by doing experiments which test the following:

1. Detect airborne targets
2. Test LPI characteristics
3. Test mutual interference and spectrum sharing
4. Test high-range resolution
5. Test high doppler resolution

1.3 Objectives

The objective of this dissertation is to develop an LPI AD Noise Radar with high range and Doppler resolution. A Wide-Band (WB) configurable multi-type (i.e. pulsed doppler and Modulated Continuous Wave (MCW)) noise Radar, is used to achieve the objective since it is inherently low power

and within the noise which achieves the LPI requirement, uses its WB characteristics to achieve high range resolution and achieves high Doppler resolution through its long integration time. By configurable noise Radar, it is meant that the operator can change various Radar parameters, and by multi-type noise Radar it is meant that the Radar can be used as a pulsed doppler noise Radar or as an MCW noise Radar. The choice of a pulsed signal is supported by figure 2.1 [7] which shows that for surveillance, a pulsed coherent Noise Radar must be used. Malanowski and Kulpa [16], on the contrary, demonstrated the detection of flying aeroplanes up to a few kilometres using Continuous Wave (CW) signals. They also explicitly state that they restricted their research to CW since it is more suitable for short-range surveillance. This research however focuses initially on short-range detection of flying aeroplanes with the ultimate aim of extending the range in future and hence the choice of a pulsed signal and an MCW signal whose performance will be compared.

High dynamic range is also critical to make sure small targets with weak echoes are not overshadowed by large targets with strong echoes. To achieve a high dynamic range the Analogue to Digital Converter (ADC) must have many bits. However, UWB signals require ADC with a high sampling rate and currently, ADCs with a high sampling rate have few bits resulting in a low dynamic range. Lukin et al. [9] managed to achieve high range resolution and high dynamic range using an ADC with a high number of bits and low sampling frequency. This achievement makes it possible to have a UWB Noise Radar with high range resolution and high dynamic range.

High Pulse Repetition Frequency (PRF) tends to reduce the unambiguous range. For a conventionally implemented noise radar, this will reduce its detection range. This research allows the operator to change the PRF (for pulse doppler Radar) or sweep rate (for MCW Radar) which provides flexibility in testing for various maximum unambiguous ranges and various maximum unambiguous target velocities. The use of PRF in this dissertation for pulse doppler Radar will mean sweep rate for MCW radar and the use of Pulse Repetition Interval (PRI) for pulse doppler Radar will mean sweep time for MCW Radar and vice versa. Pulse for pulse doppler Radar will mean signal duration for MCW Radar and vice versa. In future, the improved WB noise radar will be implemented in such a way that it stores several transmitted pulses in a list together with their transmitted times. A received signal from a distant target is correlated with the transmitted signals from the list until a match is found or not found. If a match is found, then the correct range of the distant target is computed since the start time of the matching transmitted signal is used instead of just using the start time of the pulse that was transmitted last, which will cause range ambiguity problems. This approach ensures that the noise radar is used in a long-range target detection role while using high PRF signals which provide high maximum unambiguous target velocity.

The objectives of this research are therefore to develop an LPI AD

Number	Characteristics	Target Values
1.	Two-dimensional (2D)	Provides only range and azimuth
2.	Low Probability of Intercept (LPI)	Use random noise waveform
3.	Low Probability of Detection (LPD)	25 W Maximum power
4.	Short Range (Ultimate goal. Start with a very short range first.)	30 km and later 80 km
5.	Wideband (WB)	limted by H/W to 25 MHz
6.	High range resolution	limited by H/W to 6m
7.	Air Defence (AD)	6 km constant detection height

Table 1.1: LPI AD Noise Radar Characteristics

Noise Radar with the following characteristics:

The selection of the target values in Table 1.1 are mainly based on specifications of operational Radars with the main deviation being the use of noise waveform in this research. In this research, the focus is on the Very Short Range Air Defence (VSHORAD) Radar with the ultimate aim of upgrading this Radar into a Short Range Air Defence (SHORAD) Radar in the future.

Ideally, this Radar should be 3 Dimensional (3D), meaning it should provide range, azimuth and height. A 3D Radar requires multiple receiver channels to determine different height levels of targets. This leads to an increase in the cost of the Radar. Due to budget constraints and the resources available to the researcher, this Radar is 2D and it does not provide height information of the targets.

It is very important that an Air Defence Radar is not classified by the enemy's Electronic Warfare (EW) systems and thus launch effective countermeasures against it, rendering it useless against the incoming threat. This feature of making it difficult for the enemy's EW system to classify one's Radar is one of the characteristics of Low Probability of Intercept (LPI). A pseudo-random noise waveform is used due to its nature of being random and thus unpredictable. This makes it difficult for it to be classified as a Radar waveform and improves the Radar LPI characteristics.

The output power of a Radar is critical for detecting small targets at longer ranges. High output power, however, makes the Radar vulnerable to Anti Radiation Missiles (ARM). To counter the threat of ARM, low transmit power is utilised and signal processing techniques such as pulse compression and pulse integration are implemented to maintain the capability of detecting small targets at longer ranges without using high output power. Weibel Doppler Radar Xenta-M5 described in [35] has a transmit power of 240W for an instrumented range of 75 km. A 25 W output power is used in this research

since it is what is available to the researcher but this will be increased to 240 W in the future for SHORAD applications.

The instrumented ranges for VSHORAD Radars and SHORAD Radars are typically 30 km and 80 km respectively. As an example, ELM-2026B from IAI [19] has an instrumented range of 25 km and Xenta-M5 from Weibel Doppler Radars [35] has the instrumented range of 75 km which represent VSHORAD and SHORAD ranges respectively. Thus the chosen instrumented ranges of 30 km and 80 km are in line with what industry norms for VSHORAD and SHORAD respectively.

Selection of bandwidth is very critical for range resolution. The higher the bandwidth the finer the range resolution. The researcher used a bandwidth of 25 MHz which resulted in a range resolution of 6 m. This bandwidth was limited by the capability of the hardware used by the researcher. For large airborne targets, this is more than good enough since they will be far apart from one another, but for the detection of humans, this range resolution will be insufficient if humans are walking very close to each other.

It is important to determine the maximum target height to be detected. SHORAD Radars normally have a maximum altitude coverage of 5 km as shown by the Revisor Radar which has a maximum height coverage of 5 km [36].

1.4 Scope And Limitations

The dissertation strictly focuses on the application of LPI Noise Radar for the AD search Radar role. Only detections are shown with no plot extractor and tracking capability implemented. The maximum detection range is limited by the 25 W power amplifier that is available to the researcher. The radar is only concerned with flying targets, however, some of the tests such as range resolution will be done using ground targets since they are easier to control. At long ranges, only targets with high Radar Cross Section (RCS) are considered. Processing is done digitally using a Software Defined Radio (SDR) architecture.

LPI at long ranges is not necessarily LPI at short to medium ranges since the signal will have to be high-power to reach long ranges. This does not pose a serious problem since for short to medium ranges, the low-power version of this noise Radar can be used as a Missile Fire Control Radar (MFCR) which will not be detectable by the target's Electronic Support (ES) receivers and thus makes it easy for the target to be taken out before it can shoot its anti-radiation missile towards the long-range LPI noise Radar. This deployment strategy makes the long-range LPI noise radar a deception radar for short to medium-range targets.

1.5 Report Structure

Chapter 2 of this research outlines the principles of noise Radar. It describes how noise Radar works and provides the latest technologies in noise Radar. It also highlights the shortcomings of noise Radar currently due to technology limitations. Some of the advancements in technology since the invention of noise Radar in the 1950s are highlighted together with the potential benefits that this research takes advantage of.

Chapter 3 looks at the design considerations of the Configurable Multi Type LPI AD Noise Radar.

Chapter 4 starts with the practical side of things by simulating an LPI noise Radar at S-Band up to a maximum flying target distance of 25 km. The design is continuously improved until desired results are achieved. The outcomes of the simulation are analysed and summarised.

Chapter 5 outlines all the steps taken in implementing the LPI noise Radar in the Universal Software Radio Peripheral (USRP) B210 H/W and summarises all the results obtained from the experiments. It then analyses the outcomes of H/W experimentation and compares them with the outcomes of simulation. This chapter ultimately determines whether or not the research objectives were achieved.

Chapter 6 summarises all activities of this research and provides conclusions and recommendations for future research work.

1.6 Chapter Summary

This chapter gave an overview of noise Radar and outlines the contents of this research. Noise Radar was shown that it is range unambiguous, it is immune to interference (e.g. jamming), it has LPI characteristics and it can be used to improve the performance of conventional Radars. The scope of this research is limited to LPI AD Noise Radars focusing only on airborne targets with a few exceptions where it is convenient to use ground targets to prove certain concepts. The problem statement and hypothesis were developed and finally, the research structure was outlined indicating that a literature review is done followed by simulation and H/W implementation of LPI Noise Radar. The next chapter goes through the various literature which will guide this dissertation.

Chapter 2
Literature Review

2.1 Introduction

Noise Radar (NRadar), also known as Random Signal Radar (RSRadar) and Chaotic Radar (CRadar), is a technology that was developed in the 1950s, has great range and Doppler resolution efficiently shares frequency spectrum, uses random noise to detect targets and achieve large range and Doppler unambiguity [1]. Lukin et al. [6] clarify the origin of the use of noise pulses for the detection of objects as being done by Alexandr Popov in 1897 when he did experiments on the detection of ships in a bistatic configuration. Later in the years after the second world war and when Radars were commonly used, the first papers on Noise Radar measuring range with coherent reception of Radar returns was by Richard Bourret in 1957 followed by B.M. Horton in 1959 [7]. Currently, there is some research being undertaken throughout the world to find applications of Noise Radar for major types of Radars and maybe even for all types of Radars [7]. Figure 2.1 shows the types of Noise Radars that are being researched throughout the world [7]. The leading countries in this type of research are the U.S., Ukraine, U.K., France, Canada, Germany, Italy, Russia, Poland, Sweden, Norway, China, South Korea and India [7].

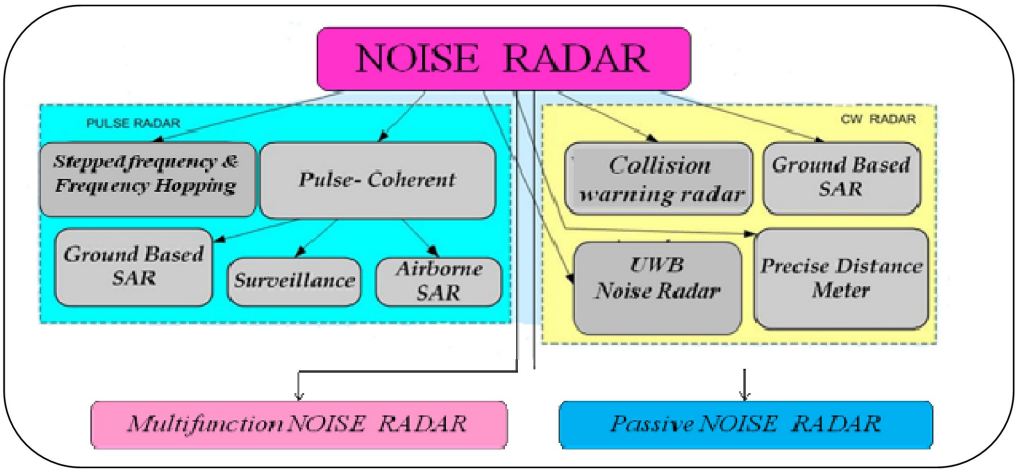

Figure 2.1: Noise Radar Types Being Researched [7]

A noise waveform is sent to the target and the received echo is correlated with the transmitted signal. A random signal is either transmitted directly or a continuous wave is a phase or frequency modulated with noise and transmitted to the target. Noise Radar is regarded as Stealth or Low Probability of Intercept (LPI) and Low Probability of Detection (LPD) Radar due to its inherent ability of covertness. It also has an ideal thumbtack ambiguity function and good Electronic Protection (EP) [4].

Typical Radars radiate high-powered signals occupying a narrow frequency band. The Ultra-Wide-Band (UWB) noise Radar occupies a wide band of frequencies at low power. This makes it difficult for traditional Radar detectors to detect it since they expect the exact opposite type of signal which is a narrow band and high power. The randomness of the Noise Radar signal makes it impossible for Electronic Intelligence (ELINT) and Electronic Support (ES) receivers to look for a certain pattern since the signal does not have a repeatable pattern and each transmitted signal is random and unique. However, for doppler processing, this noise signal is the same for a batch of pulses and only changed from scan to scan to have phase information between pulses of the same batch.

Noise Radar technology is currently mature for short-range use (less than 1 km) and pulse noise Radar is recommended for long-range [1]. This research focuses initially on VSHORAD ranges, with the ultimate goal of addressing the SHORAD ranges.

The hypothesis to be tested is that an "LPI AD Noise Radar with high range and doppler resolutions is realisable." This chapter will therefore break down this hypothesis into its parts and examine them thoroughly. First, Air Defence Radars will be analysed, followed by a description of how Radar Warning Receivers (RWR) work, an explanation of LPI and LPD Radars and then followed by an explanation of noise and Noise Radars. Different Radar noise jamming techniques are then explored, followed by mutual interference

and spectrum sharing. Range resolution, doppler resolution and dynamic range are explained in detail. Different Radar types and recent developments in Noise Radar are finally explored.

2.2 Air Defence Radars

The main aim of Air Defence Radars is to provide early warning of incoming airborne threats. These threats range from small to large, low speed to high speed, manned to unmanned and some examples are, small Unmanned Aerial Vehicles (UAVs), aeroplanes, helicopters, Rocket Propelled Grenades (RPGs), mortars and missiles. The main categories of AD Radars are two-dimensional (2D) Radars which provide a range and bearing information, and three-dimensional (3D) Radars which provide a range, bearing and height information. The types of AD Radars range from Very Short Range AD (VSHORAD) Radar with an instrumented range of roughly 25 km to long range AD Radar with an instrumented range of about 463 km. Adrian [17, p. 50] indicates a long detection range of Tactical Ballistic Missiles of at least 1000 km with a high update rate of a few seconds.

Adrian [17, p. 49] further describes the Radar missions in Extended Air Defence task as, Air Surveillance, Air Defence and Tactical Missile Defence and In Weapon Control mission. Air surveillance provides a detailed air situation picture which is the focus of this research. Air Defence and Tactical Missile Defence is air space search and track of targets including Tactical Ballistic Missiles (TBM). The Radar in weapon control mission "supply target tracking data and target pre-acquisition data for weapon systems to improve their fighting capabilities."

As mentioned above, most of the Noise Radar research has been limited to short ranges of less than 1 km, and this research will extend the Noise Radar ranges to those of VSHORAD due to the limited capability of the Hardware (H/W) resources available to the researcher. An example of the VSHORAD weapon is the RBS 70 NG from SAAB [18] which is a Man Portable Air Defence System (MANPADS) with an effective range of 9 km and an altitude of up to 5 km flying at a speed of up to Mach 2. Even though the RBS 70 NG can work independent of any VSHORAD Radar, its specification already indicates some performance expectations from a VSHORAD Radar.

A brief look at some of the operational VSHORAD Radars gives an idea of the required Radar parameters for this research. The first one to be considered is the ELM-2026B from IAI [19] with some of its performance stated as an instrumental detection range of 25 km, detection range of a fighter aircraft of 15 km, detected target velocity of 0 to 600 m/s, 60^o elevation coverage, the update rate of 2 seconds (30 rpm), the range resolution of 60 m, X Band frequency of operation, 3D and power consumption of 500 W. A 60 m range resolution requires a bandwidth of 2.5 MHz. The AN/TPQ-49

Multi-Mission Radar from SRC [20] has similar performance with a similar instrumented range of 30 km, a lower elevation coverage of 30^o, higher power consumption of 1.2 kW and uses L-Band frequency. From these two examples, as a minimum, the Noise Radar to be used for this research should have an instrumented range of around 30 km, a range resolution of better than 60 m and an update rate of 2 seconds to qualify as a VSHORAD. Considering that the VSHORAD weapon to be used against a threat has a maximum engagement range of around 9 km, having a longer instrumented range of 30 km will provide enough early warning for the weapons to engage the threat when it is within its effective range. It must be noted that instrumented range is normally the maximum range of a Radar to detect the largest possible target. Once the Radar Cross Section of a target is known, then a detection range for that particular target is determined which is normally lower than the instrumented range. This research applies Noise Radar in the VSHORAD role to benefit from some of the unique features of Noise Radar such as immunity from mutual interference, especially where VSHORAD Radars coverage overlap.

2.3 Radar Warning Receivers

VSHORAD Noise Radar must be designed in such a way that it avoids detection and interception by airborne platforms, especially those that are fitted with Electronic Support (ES) equipment such as Radar Warning Receiver (RWR). RWR enables the airborne platform to detect radars illuminating it and use its threat database to inform the operator about the type of threat posed by the Radars. Amongst other parameters, the RWR uses the Radar waveform to identify it. The fact that a Noise Radar changes its waveform every time it transmits a batch of pulses, means it will be difficult for the RWR to accurately identify it. The risk to a radar that is classified by an RWR is that the target can launch a High-Speed Anti Radiation (HARM) missile against the Radar and destroy it or it can know the type of missile associated with the VSHORAD Radar and use appropriate countermeasures to prevent a hit by the incoming missile.

To ensure that the VSHORAD Noise Radar is not intercepted by an RWR, the performance characteristics of some of the RWRs are examined and these characteristics are taken into account when specifying, designing and developing the VSHORAD Noise Radar. The Advanced RWR System from SAAB [21] has a 75 dB dynamic range, 100% Probability Of Interception (POI), can intercept both pulsed and CW Radars and covers all potential Radar frequencies from 0.5 GHz to just over 60 GHz. The ALR-400 RWR from Indra [22] has similar technical specifications as the Advanced RWR System from SAAB, with it also claiming 100% POI including LPI Radars which poses a serious challenge for the VSHORAD Noise Radar to avoid being intercepted by these types of RWRs. Its frequency coverage is however

from 0.5 GHz to 42 GHz. It can also intercept both pulsed and CW Radars. The third RWR to be analysed is the SEER Advanced Radar Warning Receiver from Leonardo [23] which covers a frequency range from 0.5 GHz to 40 GHz, can intercept pulsed, pulse doppler and CW Radars and it has a sensitivity of -55 to -60 dBm. Assuming a Signal to Noise Ratio (SNR) of 15 dB, the noise floor of the RWR can be deduced to be -75 dBm. The fact that the VSHORAD Noise Radar will behave like the Noise Jammer to the RWR and thus raise its noise floor means that the VSHORAD Noise Radar has a better chance of not being intercepted by the RWR.

2.4 LPI Radars

The previous section dealt with the concept of RWR and this nicely leads to the concept of LPI and LPD Radars. Jarpa [24] defines LPI Radar as "a class of radar systems that have certain characteristics that make them nearly undetectable with most common digital receivers." In the dissertation, it is further stated that LPI emitters are difficult to detect or identify using passive intercept devices because of their low power, wide bandwidth, frequency variability or other design attributes. Low power can be achieved through long pulses which leads to a high duty cycle and long integration times. Long pulses degrade the range resolution and this is corrected by pulse compression which uses a wide bandwidth within the pulses and this improves the range resolution.

LPI is divided into two categories of Low Probability of Detection (LPD) and Low Probability of Exploitation (LPE) [27, 1]. One main feature of LPD is that it is difficult to capture due to things like low power. LPE deals with making it difficult for an ES receiver to make sense of the captured signal. The signal cannot be recognised. It is therefore more convenient to talk about LPI since it addresses either LPD or LPE. Schleher [28, p. 3] states that a Radar can never be completely undetectable since there is a maximum distance at which the Minimum Detectable Signal (MDS) of the ES receiver will be exceeded. It must be noted that Schleher used a minimum range but the researcher believes it must be a maximum range because the signal will always be detectable for all ranges lower than this range. Therefore it is the maximum distance between the LPI Radar and the ES receiver beyond which the ES receiver will not detect the LPI Radar signal. Schleher [28, p. 4 - 5] further shows that an LPI Radar does not necessarily have LPI characteristics against all ES receivers and a detailed calculation must be done for each ES receiver that the LPI Radar is expected to encounter to determine whether or not the Radar has LPI characteristics against that ES receiver.

Low Probability of Detection (LPD) deals with the concept of making it difficult for an ES receiver to even know that there is a Radar signal. Hashemi and Nayebi [26, p. 134] state that random PRF and staggered PRF

are similar methods for improving the LPD feature of a Radar, but random PRF is better than staggered PRF since it changes randomly and is therefore unpredictable, whereas staggered PRF is predictable.

To ensure that Noise Radar LPI characteristics are achieved, this research implements some of the LPI measures such as high duty cycle configurable up to 100%, low power output, long integration time through a configurable number of pulses (or sweeps in the case of MCW mode), wide bandwidth limited only by the used Software Defined Radio (SDR) capabilities and configurable transmit frequency. Even though these LPI features can be implemented in non-Noise Radars, implementing them in a Noise Radar ensures that the Noise Radar is truly an LPI Radar.

The use of pulse compression in this research helps the Noise Radar to achieve LPI characteristics by having longer pulses and thus low peak power. It also makes the Noise Radar have high range resolution due to the wide bandwidth used in pulse compression, which gives the benefit of narrow pulses while using long pulses with low peak power. This results in a pulse compression gain defined by a time-bandwidth product greater than unity [25, p. 1351] whereas an uncompressed pulse has a unity pulse compression gain.

Govoni et. al. [25, p. 1351] state that deterministic radar operational parameters are easily compromisable by an Electronic Intelligence (ELINT) receiver. The paper state that the chirped waveform is one of these deterministic parameters and is a poor form of LPI. The ideal noise waveform is random and therefore non-deterministic which makes it a good LPI waveform [25, p. 1351]. However, a random noise waveform from pulse to pulse will make doppler processing impossible since doppler processing is dependent on phase change from pulse to pulse due to target movement. With a random signal from pulse to pulse, phase change due to target movement cannot be measured. Therefore this research changes the random noise signal between batches of pulses (or sweeps) so that within a batch of pulses the same random noise signal is used and thus enabling doppler processing. Govoni et. al. [25, p. 1355] successfully showed through simulation that the Advanced Pulse Compression Noise Radar (APCN) waveform, which is a combination of a chirp signal with noise, is nondeterministic and cannot be intercepted by an ELINT receiver. This research takes the concept of APCN waveform further by implementing it in simulation and hardware.

Using a configurable large number of pulses or (sweeps) achieves the goals of lower power transmission (LPI Feature) and high doppler resolution. A large number of pulses are integrated coherently to improve the processing gain of the Noise Radar and thus reduce the transmit power and the required Signal to Noise Ratio (SNR) at the input of the Noise Radar receiver, making it a truly LPI Radar. A Radar with a large integration gain will improve its LPI properties since the ratio of ES interception range to the Radar detection range will be lower [28, p. 4]. The other benefit of a large number of pulses is that the measured velocity of objects is more accurate due to finer doppler

resolution.

2.5 Noise Radar

A noise waveform also contributes to the LPI features of a Radar since it is nondeterministic and all systems are designed to get rid of the noise. Electronics-Notes [29] describes noise as a random fluctuation of an electrical signal. It further categorises RF noise into three categories of white noise, pink noise and band-limited noise based on their frequency distribution. In the same article, white noise is described as a random signal with the same amplitude in all frequencies of interest. Pink noise is described as the type of RF noise whose power density is biased towards the lower frequencies. Lastly, band-limited noise is described as the type of RF noise whose frequencies are limited to a certain range.

Electronics-notes [29] further categorise RF noise according to the way it is generated and these sub-categories are avalanche noise, flicker noise, phase noise, shot noise, thermal noise and burst noise. Avalanche noise is generated when the "junction diode is operated close to the point of avalanche break down." Flicker noise has a "frequency spectrum that falls off into the higher frequencies." Phase noise causes phase jitter in the RF signal. Shot noise is described as being "from the time-dependent fluctuations in electrical current." Thermal noise is caused by "thermal agitation of charge carriers" and is mitigated by lowering the temperature of the device. Lastly, burst noise is an impulse from a semiconductor. All of these types of noise collectively combine to form a noise floor of the RF receiver whereby the minimum detectable signal (MDS) has to be above this noise floor unless advanced processing techniques are used to extract the signal out of the noise.

Now that noise has been thoroughly described, it is time to focus on Noise Radar. Noise Radar is regarded as one of the modern LPI Radars which are difficult to intercept and classify by an Electronic Support Measures (ESM) receiver [10]. The goal is to detect a target before it detects you. Kulpa [10] states that different estimation methods in conjunction with PRF staggering are used to counter range and Doppler ambiguities. This is supported further by [12] whereby it is stated that in addition to avoiding range and Doppler ambiguities, PRF staggering also helps to prevent jammers from locking onto the Radar's PRF. PRF staggering can be implemented in two ways. The first one is changing PRFs sequentially during each scan period, and the other is the use of a single PRF during a scan period followed by a different PRF during the next scan period to resolve ambiguities [12]. The target dynamics from scan to scan make the latter technique problematic [12].

Kulpa [11] states that noise Radars can be divided into three major groups, short, medium and long integration time Radars. Short integration time Radar is Radar with negligible Doppler effect during integration time

and has very simple signal processing. Medium integration time Radar is a Radar that processes signals in which the "target remains in both range and Doppler resolution cell during integration period" and has medium complex signal processing [11]. A long integration time Radar is characterised by a target that changes the range and Doppler resolution cells during integration time and has a highly complex signal processing [11]. This research focuses on a medium integration time Radar.

A CW Noise Radar transmits a Continuous Noise Signal (CNS) to a target and performs signal processing on the received signal [3]. Figure 2.2 shows various signal processing techniques employed in Noise Radars [7]. A brief description of the correlation and double spectral processing techniques is provided below.

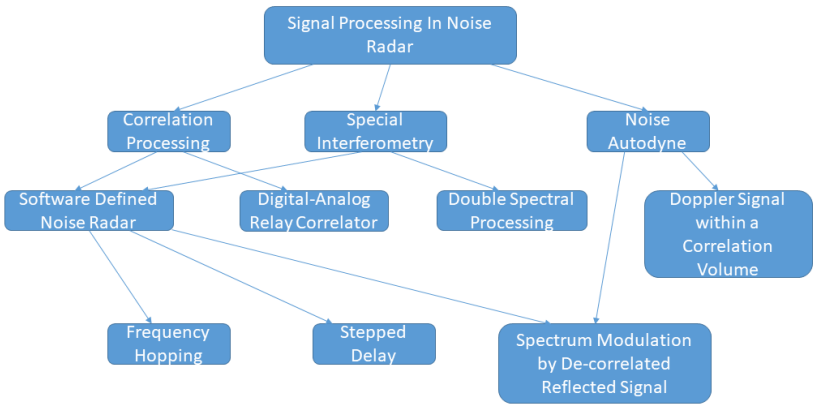

Figure 2.2: Signal Processing Techniques Used In Noise Radar [7]

The Noise Radar with a correlation receiver extracts a portion of the transmitted noise signal, and uses it to coherently down-convert the received signal to Intermediate Frequency (IF), and then uses the digital delay line to delay the reference signal before it multiplies it with the reflected signal from a target that has been converted to IF [4]. The product of the multiplication is then passed through a Low Pass Filter (LPF) to produce a correlation function [4]. The time delay found from the position of the correlation function's maximum is used to determine the range of the target [4]. Target velocity is determined from the output of the Doppler filters after correlation [4].

On the other hand, the noise Radar with double spectral processing uses two options to process the signal. The first one adds the reference signal with the received signal before down converting the sum to IF. The time delay is determined by the Fourier transform of the power spectrum that results from the sum that is fitted into a spectrum analyser [4].

2.6 RF Interference And Spectrum Sharing

What is described above as Noise Radar, can be viewed as a noise jammer by other Radars. Noise is another type of interference which can be intentional or unintentional. A Radar jammer is a device that belongs to the Electronic Attack (EA) leg of Electronic Warfare (EW) and its main objective is to prevent the Radar from detecting and tracking a target. It achieves this by raising the noise floor of the Radar or by deceiving the Radar by changing some of the parameters that are measured by the Radar such as range. Therefore a Noise Radar will raise the noise floor of other Radars, and thus jam them unintentionally.

Three types of noise jamming are spot, sweep and barrage. Spot jammer focuses its output power on a single frequency. It can be overcome by a Radar that is frequency agile. Sweep jamming takes spot jamming further by jamming several frequencies sequentially. The only problem with this method is that these frequencies are not jammed concurrently and thus the jammer may not always be effective. Barrage jamming is an advancement of sweep jamming whereby it jams several frequencies almost concurrently through fast frequency changes and sweeps the spectrum to jam a wide bandwidth. The disadvantage of a barrage jammer is that its output power is spread across a wide bandwidth and thus making it less effective against individual frequencies. However, when a powerful transmitter is used for a barrage jammer, the Radar will be rendered useless since all of its frequencies will be jammed.

Noise Radar can be an inadvertent jammer to other Radars. However, due to its low power radiation, most likely it will be filtered out by other Radars and they can share the spectrum. Mutual interference for Radars occurs when two Radars operating in the same frequency are located next to each to an extent that they can receive each other's transmit signals and/or reflected signals from targets. If the transmit signal from one Radar is too strong, then the adjacent Radar will be jammed. This will jam all types of Radars including the Noise Radar. However, if an ordinary Radar receives its reflections from a target and it also receives reflections from the same target due to an adjacent Radar's transmissions, then the target will be shown at the correct range and doppler and a ghost target will also appear at an incorrect range and doppler. This problem is known as mutual interference. Noise Radar is immune to this problem since the two Radars adjacent to each other will have unique noise waveforms and each of them will display a target at the correct range and doppler because reflections from a target due to another Radar will not correlate with its own transmit signal. Ordinary Radars use the same waveforms in all their Radars of the same type and that is why reflections from Radars of the same type correlate with their transmit signals and thus create ghost targets. Therefore Noise Radars can share the spectrum with other Noise Radars using the same frequency without severely degrading each other's performance and thus leading to efficient usage of the

RF spectrum.

Previously in this dissertation, it was mentioned that Noise Radar is immune to interference including jamming. A noise-modulated Radar signal raises the noise floor around the centre frequency, making it difficult for its transmit frequency to be discovered by jammers during their look-through window. The reason this works is that a jammer has an ES receiver associated with it. The ES receiver is used to discover all the threat Radars in its vicinity. Once these Radars are discovered and deemed to be threats, then a jammer will be activated for the applicable frequency band. Therefore if the ES receiver cannot discover the Radar signal, then the jammer will not be activated and thus the Noise Radar is immune to jamming.

2.7 Radar Types

Radar design has a lot of tradeoffs and wrong choices can result in over or under-design. The main requirement of this Radar is that it must not be detectable and interceptable by EW systems and it must search and acquire targets at long distances.

Waveform selection has a direct impact on the performance of the Radar. The two choices of waveforms for Radars are Continuous Wave (CW) and Pulse Waveforms which can be modulated or unmodulated. CW waveforms are used for short ranges and they have no blind range. Long-range Pulsed Waveforms are typically used but they have a blind range that is determined by the pulse width. They also require a low PRF for a large unambiguous range. Modulating the pulsed waveform improves its range resolution and allows the Radar to reduce its peak transmit power by having a pulse width that is longer. This research will focus on both pulse doppler noise radar and MCW noise radar.

2.8 Recent Noise Radar Developments

The US Army Materiel Command's Communications-Electronics Research, Development and Engineering Center (CERDEC) is developing an Advanced Pulse Compression Noise (APCN) Radar which among other things encrypts its waveforms to prevent opposing forces from intercepting and exploiting their emissions [2]. Encryption of transmitted waveforms is another technique of LPE which makes it difficult for an ESM receiver to exploit the Radar signal since an encrypted signal will be random.

The current implementation of long-range Radars is based on pulsed signals which have range and Doppler ambiguities due to a trade-off that must happen when choosing the Pulse Repetition Frequency (PRF). A high PRF gives a high unambiguous velocity but a small maximum unambiguous range, and a low PRF gives a large maximum unambiguous range but a low unambiguous velocity and thus ambiguous in Doppler. Lukin et al. [5],

mention two methods that are used to detect fast targets at long ranges, but warn that these methods use complex algorithms and are costly in terms of implementation and computational resources. One of the methods uses several bursts with various PRF and the other one uses PRF jitter to overcome the range ambiguity problem that is associated with high PRF signals. Lukin et al. [5] propose the use of high variable PRF noise Radar to detect long-range fast targets and overcome the blind range interval of high PRF noise pulsed Radar with constant Pulse Repetition Interval (PRI).

The air threat of today ranges from small Unmanned Aerial Vehicles (UAVs) to large aircraft carriers such as the A400. This vast difference in size means that a Radar must have a high dynamic range and it must also be able to resolve them in range. A low dynamic range will cause targets with strong reflections to mask targets with much weaker reflections. Lukin et al. [6] have done experiments with a Noise Radar with high range resolution and high dynamic range.

The advent of Software Defined Radio (SDR) has meant that most of the functions that were performed in H/W can now be performed in S/W and F/W. This approach has led to a significant reduction in Size, Weight, Power and Cost (SWaPC). Lukin et al. [6] successfully demonstrated the implementation of Noise Radar in SDR with most of their processing functions implemented in the Field Programmable Gate Array (FPGA) of the SDR. FPGA offers high-speed parallel computing which is critical for Radar signal processing. Malanowski and Kulpa [16] have also successfully implemented clutter filtering, correlation and detection using digital processing schemes and they were able to detect moving cars and flying aeroplanes in their experiments. Kulpa [10] states that due to the high computational demands of noise Radars, it cannot be effectively implemented in analogue H/W. In this research, a USRP B210 is used for the implementation of Noise Radar in SDR. It has a frequency range of 70 MHz to 6 GHz with up to 56 MHz instantaneous bandwidth. A transmit frequency of 2.45 GHz (S band) is used for this research.

2.9 Summary

This chapter looked at some of the literature to determine the current trends in Noise Radar research. It was shown that the US military is already researching the use of Noise Radar for military purposes. It was also shown that the use of SDR makes it possible to implement a Noise Radar with low SWaPC. The next chapter looks at the design consideration of the LPI VSHORAD Noise Radar.

Chapter 3
Design Methodology Of LPI AD Noise Radar

3.1 Introduction

This chapter designs the LPI AD Noise Radar at S-Band for a flying target that is within a 25 km range. It starts by first determining the minimum SNR required to meet the specified P_d and P_{fa}. Table 3.1 contains a list of all requirements and the derived requirements. For each calculated value there is an equation that was used to compute the value. This equation is stated under the equation column. The ambiguity function is used to confirm that the chosen waveform meets the required unambiguous values and resolution values for range and doppler.

3.2 Requirement Analysis And Motivation

In this section, an analysis of requirements is performed and the reasons for these requirements are provided. As previously explained, most of these parameters are configurable by the operator, but chosen values in this dissertation are used to make sure the experiment is repeatable. The reason for making the Radar configurable is to make sure the Radar can work as different types of Radars, using the same hardware for an extremely low cost. The best way to achieve this objective was to use an SDR since it has configurable parameters with most of the processing being software based. The USRP B210 SDR was used for experiments of this dissertation since it is one of the SDRs available to the researcher.

The guideline in choosing the frequency of operation was based on getting a frequency that is licence free and within the specification of USRP B210 and with peripherals that are low cost due to economies of scale. International Telecommunications Union (ITU) Radio Regulations have defined the Industrial, Scientific and Medical (ISM) frequency bands which can be

used without requiring a licence [34]. The USRP B210 frequency range is from 70 MHz to 6 GHz. Some of the ISM bands within the capability of the USRP B210 are 2.4 to 2.5 GHz and 5.725 to 5.875 GHz [34]. These bands are of interest to the researcher since they are used for Wireless Fidelity (WiFi) networks which are ubiquitous throughout the world, which results in low cost of peripheral components. The researcher chose the frequency of 2.45×10^9 Hz since it is used for WiFi technology and is part of the ISM band plus it will require less power than the 5 GHz frequency for the same range and target.

Other Radar parameters that were determined in no particular order of importance include maximum radial velocity, noise figure, system loss, probability of false alarm, probability of detection, range resolution and RCS. The maximum radial velocity of 270 m/s is chosen since this is the typical cruising speed of commercial aeroplanes and it will thus be easy to test it. The Noise Figure of 8 dB is the maximum value stated in the USRP B210 datasheet. To compute system loss, the first step was to determine the total loss from the two 10 m low loss cables of 0.2 dB per meter per cable which came to 4 dB. The inflexible low loss cables were connected to the B210 via flexible lossy cables 1.5 m x two cables which have a combined loss of 3 dB. This brings the total loss so far to 7 dB. An additional 3 dB loss was provided to cater for any other unmeasured losses which brought the total System Loss to 10 dB. Most Radars have a probability of false alarm of 1.00×10^{-6} and a probability of detection of 0.9. These values ensure that the Radar will have extremely low false alarms and a high probability of detecting targets. The researcher decided to use these values as well. A typical room temperature of 290.00 K was chosen which is in line with the researcher's room temperature in his environment. Even though the Radar is designed for airborne targets where the range resolution is of the order of 150 m and thus requires a 1 MHz bandwidth, this Radar is also tested against humans and vehicles which require range resolutions of 1 m (bandwidth of 150 MHz) and 6 m (bandwidth of 25 MHz) respectively. The USRP B210 was tested for different bandwidths at full duplex and the maximum bandwidth that was found to work well in full duplex mode was 25 MHz. Therefore due to hardware limitations, the chosen bandwidth is 25 MHz which results in the finest range resolution of 6 m. Since the Radar is transmitting and receiving in a full duplex mode for both pulse and continuous Radar mode, the theoretical blind range is at least the range resolution which is 6 m. The Radar Cross Section (RCS) is critical in determining the detection range of different target sizes. The typical RCS of a human being is about $1m^2$, that of a car is about $5m^2$ and that of the small aeroplanes flying in the vicinity of the researcher's house is $3m^2$. Since human beings are detected at much shorter ranges compared to aeroplanes due to line of sight issues, it is best to use the RCS of $3m^2$ of a small aeroplane because they must be detected at much longer ranges and thus will determine the maximum power of the Radar.

Normally, from an operator's perspective, the requirement for the Radar will be to detect a target of a certain RCS and at a certain maximum range. These values together with other variables found in the Radar range equation will be used to determine the maximum transmit power required. In the case of the researcher who has limited resources, the maximum transmitting power is limited by the power amplifier available to him which is a 25 W power amplifier. From this limitation, the maximum range for pulse Radar mode and MCW Radar mode were computed to be 7.15×10^3 m and 1.05×10^4 m respectively. These are less than the typical VSHORAD Radar ranges of 25 km but are acceptable considering the limited resources of the researcher. There are other ways of increasing the target detection range with the same maximum output power, such as integrating more pulses, but this will require more processing resources. This will be looked at in future work by the researcher.

An analysis of flightradar24 around the researcher's area was done for different times of the day over several months using the software's playback feature to determine among other things the type of aeroplanes, the range from the researcher's house, the speed at different ranges and height at different ranges. It was found that the aeroplanes in this region flew below 6000m. Therefore the maximum height of this Radar is designed to be 6000m. The best way to achieve this height over a longer range is to use a cosecant squared (csc^2) antenna. Unfortunately, the use of the csc^2 antenna will have to be part of future work by the researcher due to time constraints. As an interim solution, a grid antenna with model number KB-2424-GRIDW was chosen due to its low cost, a frequency range of 2.3 GHz to 2.5 GHz, 24 dBi gain, low Voltage Standing Wave Ratio (VSWR) of less than 1.5, maximum power of 100 W and maximum wind velocity of 60 m/s. It has horizontal and vertical beam widths of 10^o and 14^o respectively.

Further values such as minimum PRF, maximum unambiguous range, integration time, the number of pulses, pulse width, duty cycle and SNR were determined as well. The minimum PRF is computed using the maximum radial velocity and the wavelength of the centre frequency which comes to a value of 8.82×10^3 Hz. Using the minimum PRF and speed of light, the maximum unambiguous range is calculated to be 1.70×10^4 m. Computing the integration time is done using half the range resolution and maximum radial velocity and comes to a value of 1.11×10^{-2} s. The reason for using half the range bin (range resolution) is to make sure the target does not leave the range bin during integration time and to implement a simple signal processing algorithm. The number of pulses is computed using the integration time and PRI (determined from the inverse of PRF) and comes to a value of 98. A pulse width of 2.50×10^{-5} s in pulse Radar mode is chosen to make sure a duty cycle of 0.22 is achieved. This high duty cycle improves the average power on the target which gives a better target detection range for the same peak transmit power. MCW radar mode has a duty cycle of 1.00 whose sweep length is similar to the PRI value of 1.13×10^{-4} s. Last but not least,

the SNR is computed using the P_{fa} and P_d.

3.3 Requirements

Below are the requirements:

Description	**Variable**	**Equation**	**Pulse Mode**	**MCW Mode**
Centre frequency (Hz)	f_c		2.45×10^9	2.45×10^9
Maximum radial Velocity (m/s)	V_{rmax}		270	270
Noise Figure (dB)	F		8	8
System Losses (dB)	L_s		10	10
Probability of false alarm	P_{fa}		1.00×10^{-6}	1.00×10^{-6}
Probability of detection	P_d		0.9	0.9
Speed of light (m/s)	c		3.00×10^8	3.00×10^8
Boltzmann constant ($\frac{J}{K}$)	k		1.38×10^{-23}	1.38×10^{-23}
Temperature (K)	T_0		2.90×10^2	2.90×10^2
Range Resolution (m)	R_{res}		6	6
Blind Range (m)	$Blind_{range}$		6.00	6.00
Target Radar Cross Section (m^2)	T_{RCS}		3	3
Target range (m)	R_{target}		7.15×10^3	1.05×10^4
Maximum Target Height (m)	$T_{heightmax}$		6000	6000
Gain in dB	G_{dB}		24	24
Gain	G	$10^{\frac{GdB}{10}}$	251.18	251.18
Antenna 3 dB elevation beamwidth (°)	θ_e		14.00	14.00

Continued on next page

Table 3.1 – *Continued from the previous page*

Description	**Variable**	**Equation**	**Pulse Mode**	**MCW Mode**
Antenna 3 dB azimuth beamwidth (°)	θ_a		10.00	10.00
Range Error (m)	δR	$-\frac{c\tau f_{dmax}}{2\beta}$	-6.61×10^{-1}	-3.00
Wavelength (m)	λ	$\frac{c}{f_c}$	0.12	0.12
Minimum PRF or Sweep Rate (Hz)	$\mathrm{PRF_{min}}$	$\frac{4V_{rmax}}{\lambda}$	8.82×10^3	8.82×10^3
Maximum Doppler frequency shift (Hz)	$\mathrm{f_{dmax}}$	$\frac{PRF_{min}}{2}$	4.41×10^3	4.41×10^3
Maximum unambiguous range (m)	$\mathrm{R_{max}}$	$\frac{c}{2PRF_{min}}$	1.70×10^4	1.70×10^4
Pulse Repetition Frequency or Sweep Rate (Hz)	PRF	PRF_{min}	8.82×10^3	8.82×10^3
Pulse Repetition Interval or Sweep Time (s)	PRI or T_s	$\frac{1}{PRF}$	1.13×10^{-4}	1.13×10^{-4}
Range bins [gates]	$\mathrm{R_{gates}}$	$\frac{R_{max}-Blind_{range}}{R_{res}}$	2 833	2 833
Integration Time (s)	$\mathrm{T_{int}}$	$\frac{0.5*Range_{res}}{V_{rmax}}$	1.11×10^{-2}	1.11×10^{-2}
Velocity Resolution (m/s)	$\mathrm{V_{res}}$	$\frac{\lambda}{2T_{int}}$	5.51	5.51
Number of pulses or sweeps	$\mathrm{N_{pulses}}$	$\frac{T_{int}}{PRI}$	98	98
Doppler Resolution (Hz)	$\mathrm{Doppler_{res}}$	$\frac{PRF}{N_{pulses}}$	90.00	90.00
Pulse or Sweep Bandwidth (Hz)	$\mathrm{P_{BW}}$	$\frac{c}{2R_{res}}$	2.50×10^7	2.50×10^7
Pulse or Sweep Width (s)	τ		2.50×10^{-5}	1.13×10^{-4}

Continued on next page

Table 3.1 – *Continued from the previous page*

Description	**Variable**	**Equation**	**Pulse Mode**	**MCW Mode**
Time Bandwidth Product	TB	$P_{BW} * T_{dwell}$	277 775	277 775
Duty Cycle	D_{cycle}	$\tau * PRF$	0.22	1.00
Minimum Signal to Noise Ratio	SNR_{min}	$log_{10}(\frac{P_{fa}}{P_d}) - 1$	131.10	131.10
Minimum Signal to Noise Ratio (dB)	SNR_{mindB}	$10\log_{10}(SNR_{min})$	21.18	21.18
Peak transmit power (W)	P_t	$\frac{SNR(4\pi)^3(R_{max})^4}{G^2\lambda^2\sigma * n_p * Sig_{time}} + \frac{kT_0FL_s}{G^2\lambda^2\sigma * n_p * Sig_{time}}$	24.69	24.84
Peak transmit power (dBm)	P_{dBm}	$10\log(P_t) + 30$	43.93	43.95
Average transmit power (W)	P_{ave}	P_tD_{cycle}	5.44	24.84
Reflected power at target (W)	P_{refl}	$\frac{P_tG\sigma}{4\pi(R_{target})^2}$	2.90×10^{-5}	1.36×10^{-5}
Reflected power at target (dBm)	P_{reflBm}	$10\log\frac{P_{refl}}{10^{-3}}$	-15.38	-18.65
Received power (W)	P_r	$\frac{P_tG^2\lambda^2\sigma}{((4\pi)^3) * (R_{target})^4}$	1.35×10^{-14}	2.98×10^{-15}
Received power (dBm)	P_{rdBm}	$10\log\frac{P_r}{10^{-3}}$	-108.69	-115.26

Table 3.1: Pulse and MCW Mode Calculations

3.4 Design Discussion

The main requirement of this Radar is that it is a configurable LPI VSHORAD Noise Radar. Making it configurable makes it possible to test the Radar with different parameters. To make the final implementation configurable, a Software Defined Radio (SDR) is used whose parameters can be changed in software (S/W) and firmware (F/W) without changing the hardware (H/W). The S/W is currently designed to use three SDR H/Ws one at a time but it can be expanded to accommodate additional SDRs by just writing their dedicated driver S/W. The Radar operates in quasi-monostatic (separate transmit and receive antennas that appear to be at the

same location from a target perspective) full duplex mode by using dedicated transmit and receive channels with their separate antennas. The antennas are just under 2 meters apart from each other. It is up to the user to make sure the transmit and receive configurable parameters are the same for the Radar to work properly.

The approach is to design the software that is first tested in simulation mode and thereafter use the same software with an SDR to detect actual targets in the air. The main difference between simulation mode and H/W in the loop mode is that in the simulation mode targets are simulated whereas with H/W in the loop mode actual targets are detected. H/W in the loop mode can also be used in simulation mode by generating false targets and connecting the transmit antenna port to the receive antenna port via an attenuator. The simulation mode is used to confirm the proper functioning of S/W, the H/W in the loop simulation mode is used to test the integration of H/W with S/W and the H/W in the loop mode, tests if the complete Radar can detect targets as designed. Using the same S/W for simulation mode and field testing ensures that all the bugs are sorted out in a controlled environment with known simulated targets and during field tests, only a few new variables are introduced and it thus becomes easier to solve any new performance issues.

Configuration of the Radar happens at two parameter groupings and the default values are allocated when the Radar S/W is started. Changing of parameters is non-sequential and the order in which they are addressed in this design section of the dissertation does not imply any order of importance. The first group changes parameters that affect the transmitted signal henceforth known as RF parameters and they can only be changed while the Radar is not transmitting. A compute button is pressed to capture these changes and compute new values of other parameters that are affected by new RF parameters entered by the user. The second group can be changed at any time and henceforth they are known as display parameters. Once the user presses a start transmit button, only the display parameters can be changed. Pressing the stop transmit button stops the Radar transmission and all parameters can be changed. The exit button closes the Radar S/W and can be pressed at any time.

Most of the changeable parameters are the RF parameters and they are hereby examined in detail. Even though the current focus is VSHORAD which is limited to 25 km, the long-term objective is to make this Radar a long-range air defence Radar. For this reason, the Radar can operate in either a pulsed mode or Continuous Wave mode. In pulse mode either a Pulsed Linear Frequency Modulated wave (PLFMW) or Pulsed Linear Frequency Noise Modulated wave (PLFNMW) or a Pulsed Noise Waveform (PNW) can be used. For the modulated continuous wave mode, the user can either use the Frequency Modulated Continuous Wave (FMCW) or a Frequency Modulated Continuous Noise Wave (FMCNW) or a Continuous Noise Waveform (CNW). Furthermore, it is possible to select either a positive

up chirp waveform or a symmetric up chirp waveform for the baseband signal. The user must enter an amplitude value other than zero if the noise waveform must be generated.

For the positive up chirp and symmetric up chirp waveforms, LFM and FMCW waveforms are used for pulse mode and continuous mode respectively since they are easier to generate and they are some of the most popular waveforms for LPI Radars and will therefore be beneficial to compare their performance against that of a noise waveform. Modulating a pulse with a waveform of a certain bandwidth helps in the achievement of the desired range resolution, and this concept is known as pulse compression. Pulse compression ensures that the range resolution depends on the bandwidth of the signal and not on the pulse width. Pulse compression makes it possible to have a long pulse width to achieve the desired average power with the same range resolution as a short pulse. A long pulse also leads to low output peak power. Govoni et al. [14] state that another benefit of a chirp waveform is that it is Doppler tolerant. They furthermore conclude that the "LFM noise waveform offers advantages over the random noise waveform and performs comparably with the conventional chirp waveform." Figure 3.1 shows a single pulse of this waveform with a 2.50×10^7 Hz bandwidth. Its spectrogram is shown in figure 3.2.

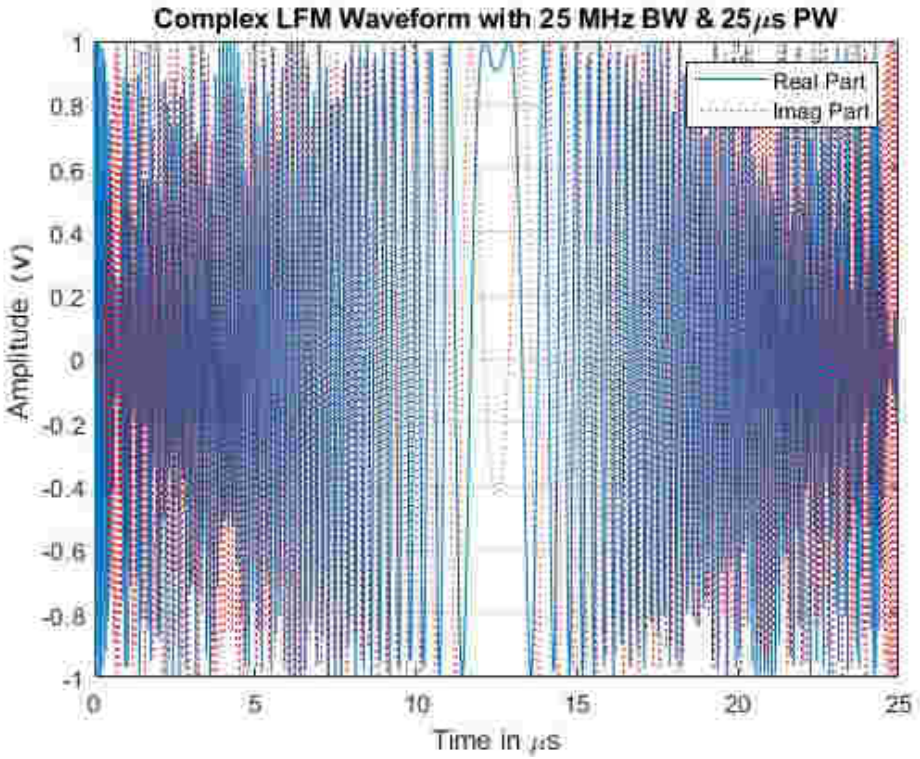

Figure 3.1: Linear Frequency Modulated Pulse

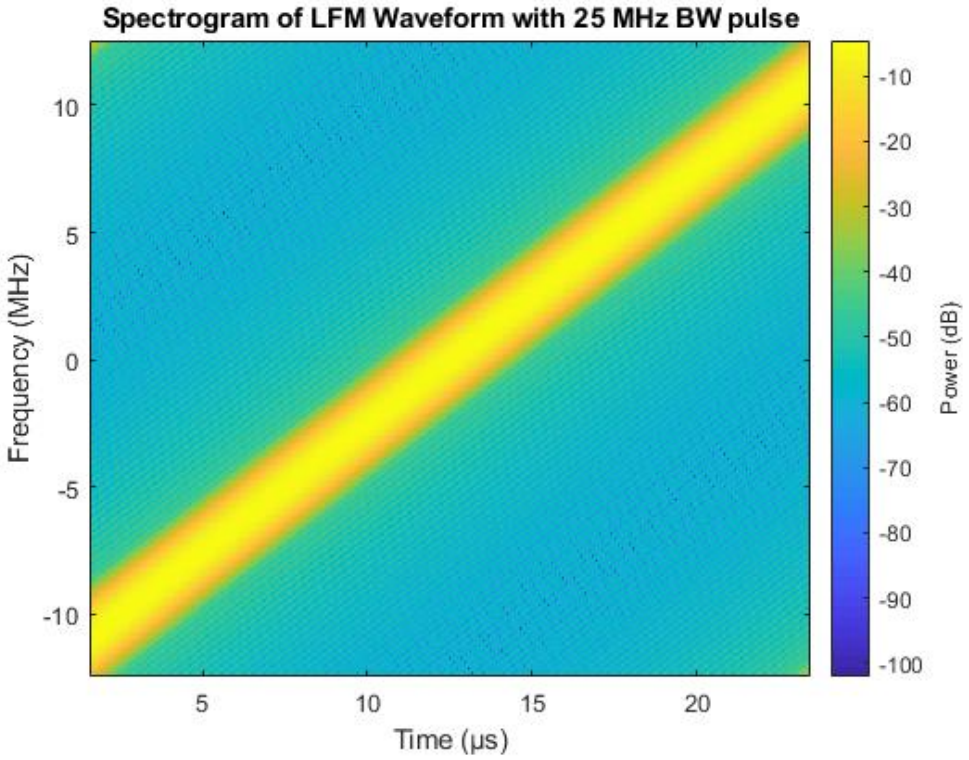

Figure 3.2: Linear Frequency Modulated Pulse Spectrogram

A typical Radar waveform equation is shown in equation 3.1 from [30] which is a modulated carrier signal whereby a(t) is the amplitude modulation of the frequency and/or phase modulated RF carrier, $e^{j\omega t}$ is the complex RF carrier signal and $e^{j\theta(t)}$ represents the signal that modulates the frequency and/or phase of the RF carrier signal. This signal is also known as the complex baseband signal and its amplitude modulated equation is shown in equation 3.2 [30].

$$\overline{x}\left(t\right) = a\left(t\right) e^{j[\omega t + \theta(t)]} \tag{3.1}$$

$$x\left(t\right) = a\left(t\right) e^{j\theta(t)} \tag{3.2}$$

Equation 3.3 [30] which is the frequency and/or phase function is used to generate the LFM waveform. It is further expanded by equation 3.4 derived from [31]. Its derivative yields the instantaneous frequency given by equation 3.6 [30].

$$x\left(t\right) = e^{j\pi\beta t^2/\tau} = e^{j\theta(t)},\ 0 \leq t \geq \tau \tag{3.3}$$

$$\theta\left(t\right) = \theta_0 + 2\pi\left(f_0 t \pm \frac{k}{2}t^2\right) \tag{3.4}$$

where,

$$k = \frac{f_1 - f_0}{\tau} \tag{3.5}$$

$$F_i(t) = \frac{1}{2\pi}\frac{d\theta(t)}{dt} = \frac{\beta}{\tau}t \ hertz \tag{3.6}$$

The next step is to determine if the chosen waveform will meet the requirements related to range and velocity resolution and their respective unambiguous values. The ambiguity function was used to achieve this objective. The ambiguity function is a two-dimensional function that determines the range and velocity (or delay and doppler) resolutions of a waveform used in a Radar application. It also determines if there is range doppler coupling whose presence means there are range errors at different doppler frequencies. Its output can be plotted in different graphs which must be interpreted to predict the expected performance of the Radar waveform. Range resolution determines the minimum distance between at least two targets in the direction of the Radar for them to be distinguished as distinct targets by the Radar. Whereas velocity resolution is the minimum radial velocity in the direction of the Radar between at least two distinct targets that are equidistant from the Radar for them to be distinguished as distinct targets. The amplitude of the ambiguity function must be large enough to be able to detect targets in the presence of noise. The ultimate aim is to detect multiple targets even if they are very close in terms of range and velocity, and the ambiguity function determines if the chosen waveform can help in achieving this objective. The ambiguity function equation is shown in equation 3.7.

$$|\chi(\tau_d, f)|^2 = \left|\int_{-\infty}^{\infty} r(t)\, u^*(t - \tau_d)\, e^{j2\pi f t}\, dt\right|^2 \tag{3.7}$$

In equation 3.7, τ_d is the time delay of the received signal, f is the frequency of the received signal, r(t) is the received signal and u^*(t - τ_d) is the time-reversed complex conjugate of the reference signal (the transmit signal in this case) delayed by time τ_d.

The ambiguity function of an LFM waveform is shown in figure 3.3 which is slanted to the right. This implies that this waveform produces range doppler coupling which means range errors will occur at different doppler frequencies. The maximum range error of the chosen LFM waveform for the maximum possible doppler frequency is computed using equation 3.8 [30] which is equal to -0.66148m and it is extremely small considering the chosen range resolution of 6 m.

Ambiguity function with doppler cut provides information such as range resolution, PRI and pulse length. Figure 3.4 shows the high-level view of the ambiguity function for 0 Doppler cut in the top graph and maximum doppler frequency doppler cut for an LFM signal with 98 pulses. The 98 pulses lead to 1.11×10^{-2} s integration time. In the top graph, the pulse length of 24.26 μs

and the PRI length of 113.3 μs are indicated. The bottom graph shows that at maximum doppler frequency, the signal is attenuated by 40 dB. In figure 3.5 the first null occurs at 40.03 ns which translates to a range resolution of 6 m as designed.

A view at the ambiguity function 0 delay cut shown in figure 3.6 shows that the first null occurs at 95.3 Hz, which is the doppler resolution (f_{dres}). Using the formula $V_{res} = \frac{\lambda * f_{dres}}{2}$, velocity resolution, $V_{res} = 5.83$ m/s, and it is very close to the design value velocity resolution of 5.51 m/s.

$$\delta R = -\frac{c\tau f_{dmax}}{2\beta} \tag{3.8}$$

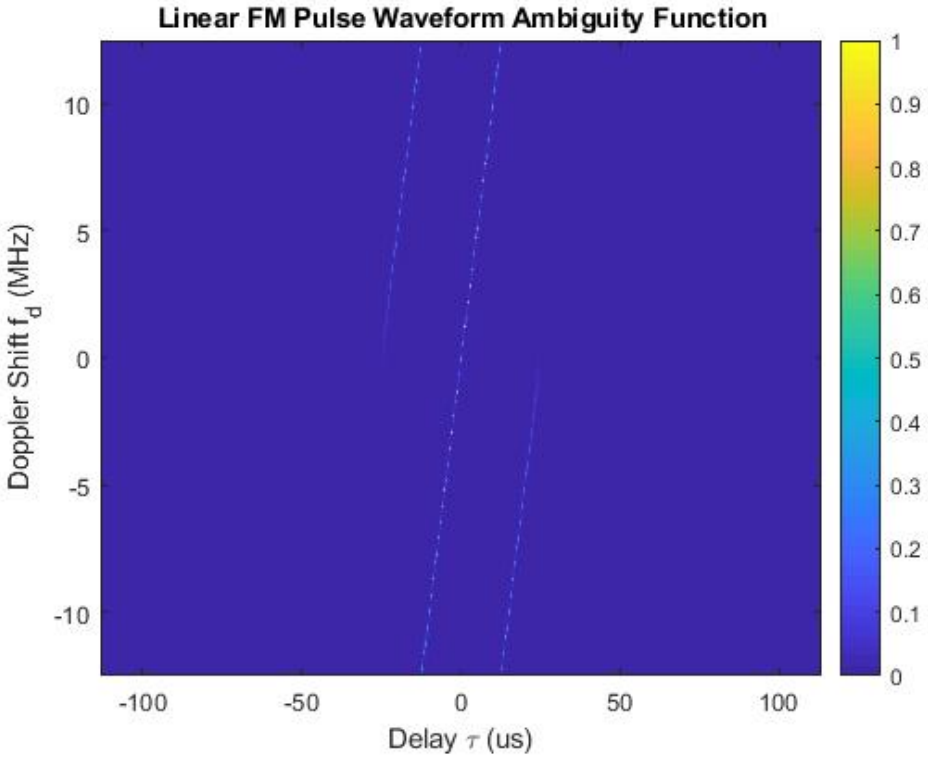

Figure 3.3: Ambiguity Function Of LFM Waveform

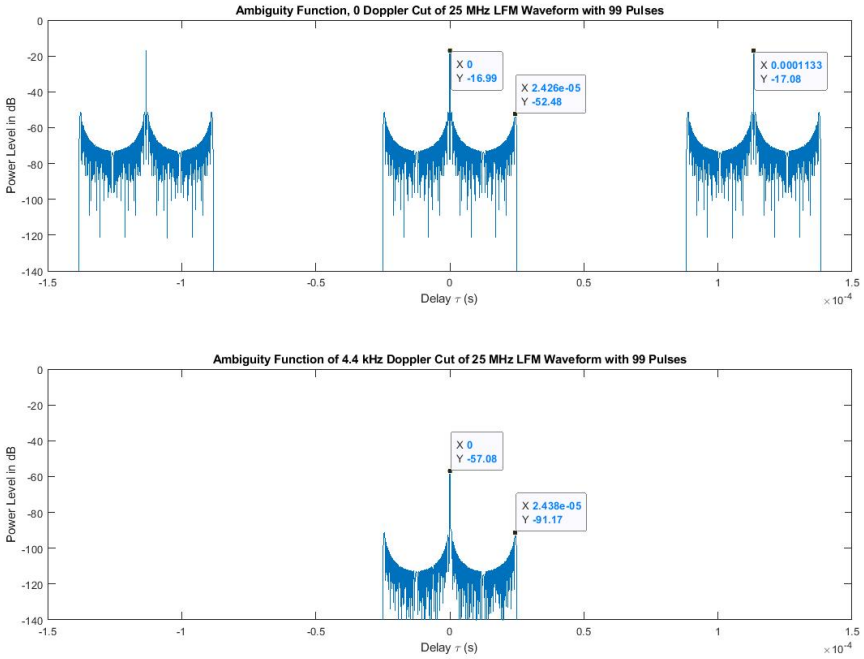

Figure 3.4: Ambiguity Function LFM With Multiple Pulses: Doppler Cut

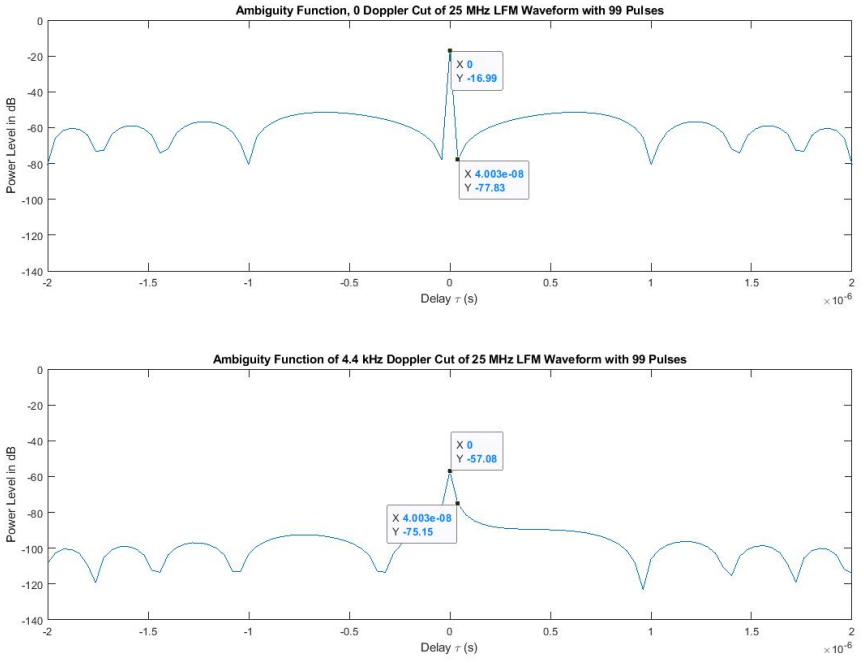

Figure 3.5: Ambiguity Function LFM With Multiple Pulses: Doppler Cut : $2\mu s$ View

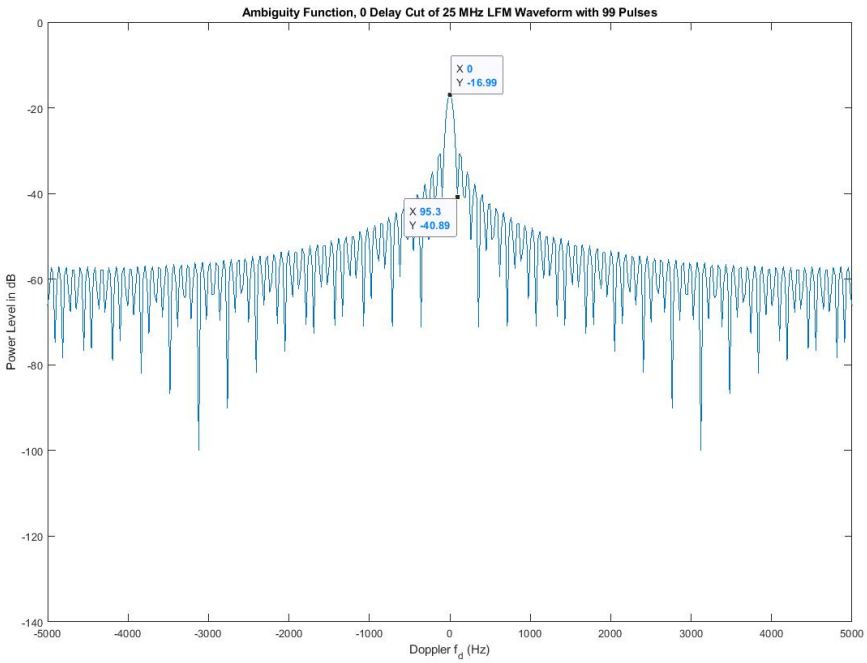

Figure 3.6: Ambiguity Function LFM With Multiple Pulses: 0 Delay Cut

A pure complex noise waveform is generated as shown in figure 3.7 and it is used to compare its performance with other waveforms. Its spectrogram is shown in figure 3.8. In figure 3.9, the ambiguity function of the noise waveform, it is clear that there is no range doppler coupling. Figure 3.10 is similar to that of the LFM waveform with the peak value of the doppler cut at maximum doppler frequency in the bottom graph also being 40 dB below the peak value of the 0 doppler cut in the top graph. Zooming into the doppler cut in figure 3.11 shows that the range resolution occurs at 40.03 ns for both zero doppler cut and maximum doppler frequency cut which is as per the design and the same as the one achieved for the LFM waveform. The doppler resolution in figure 3.12 for the zero delay cut of the noise waveform is 95.3 Hz which is the same as what was achieved for the LFM waveform.

The entire process of analysing the LFM pulse waveform and noise waveform with the same pulse duration was repeated for the FMCW symmetric up chirp waveform and its corresponding random noise waveform. The results achieved for these waveforms are similar to those of the LFM pulse and its corresponding noise waveform, with the exception that the FMCW waveform and its corresponding noise waveform occupy the entire sweep time which is the same as the PRI for the pulse signal. The produced graphs for the FMCW waveform and its corresponding noise waveform are therefore not added since doing so will not add value.

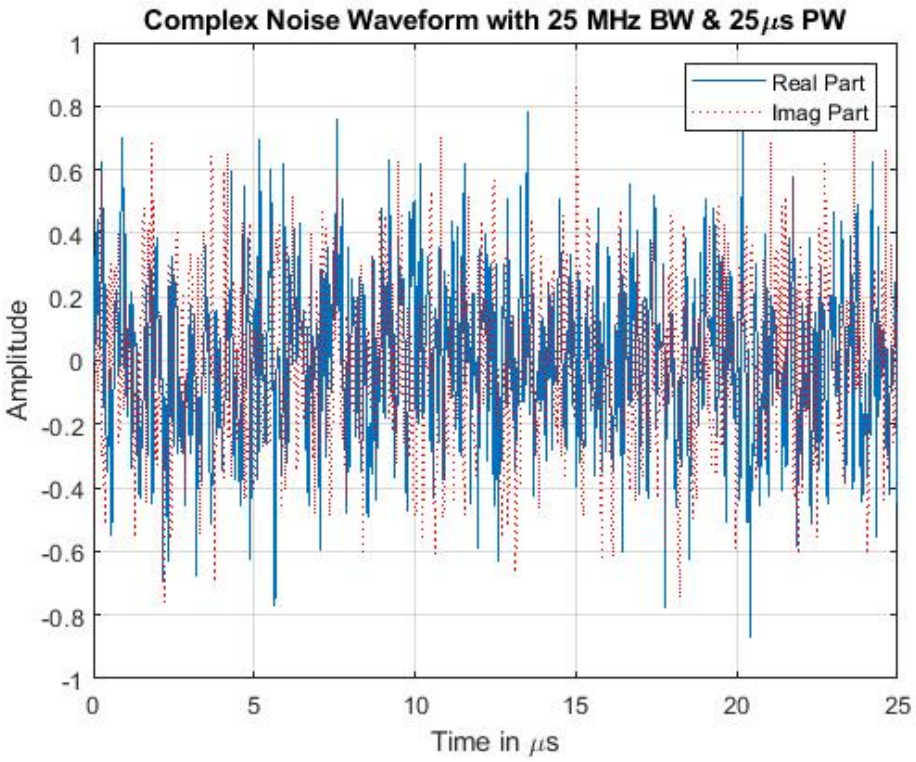

Figure 3.7: Noise Modulated Pulse

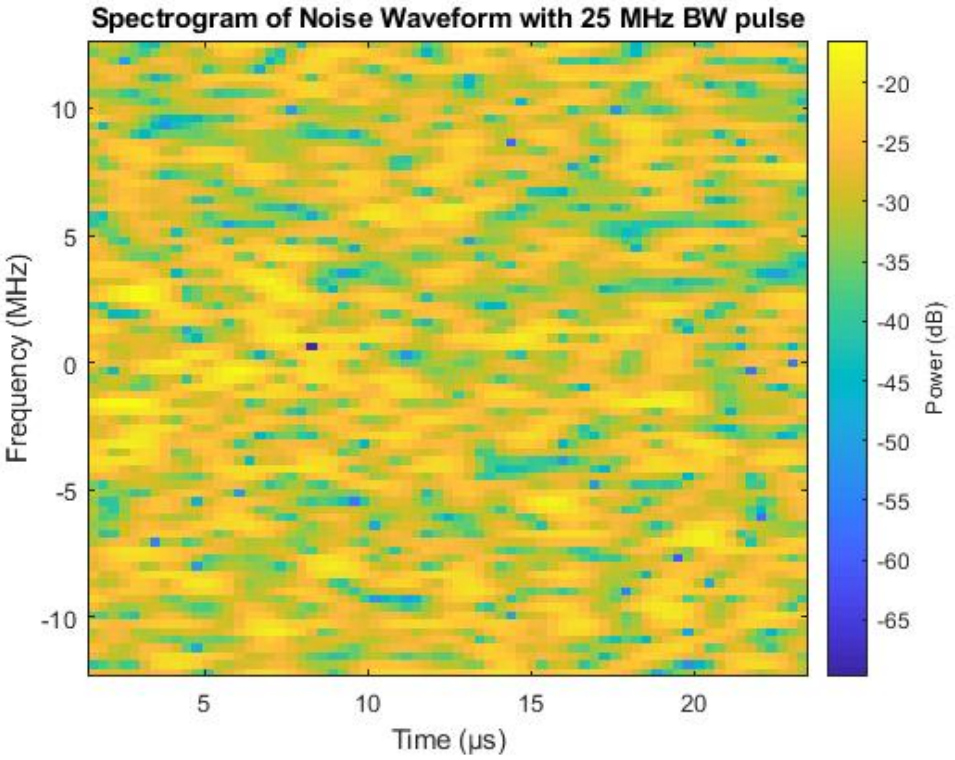

Figure 3.8: Noise Modulated Pulse Spectrogram

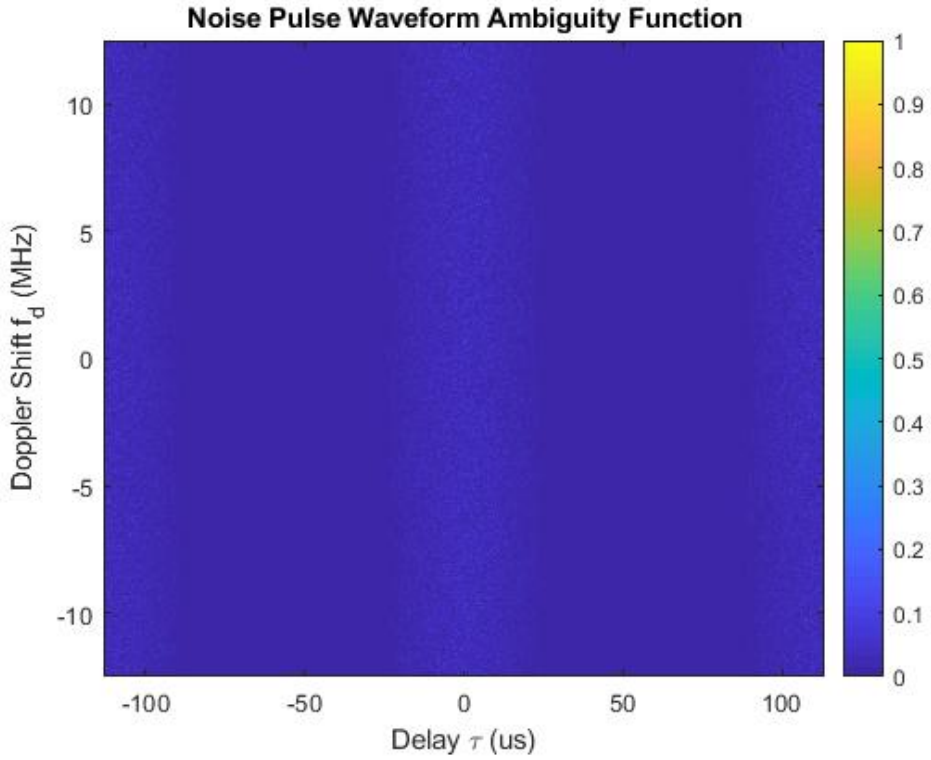

Figure 3.9: Ambiguity Function Of Noise Waveform

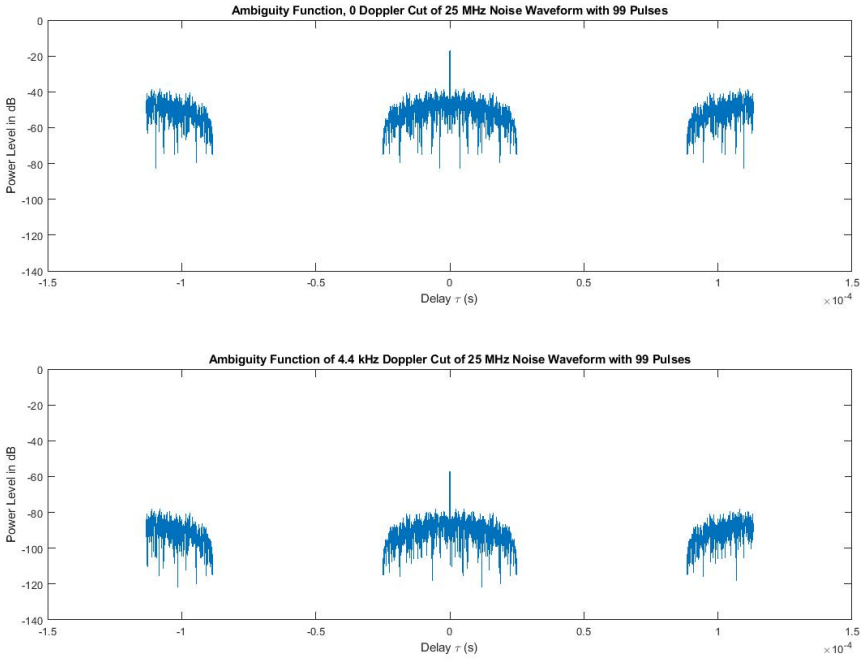

Figure 3.10: Ambiguity Function Of Noise With Multiple Pulses: Doppler Cut

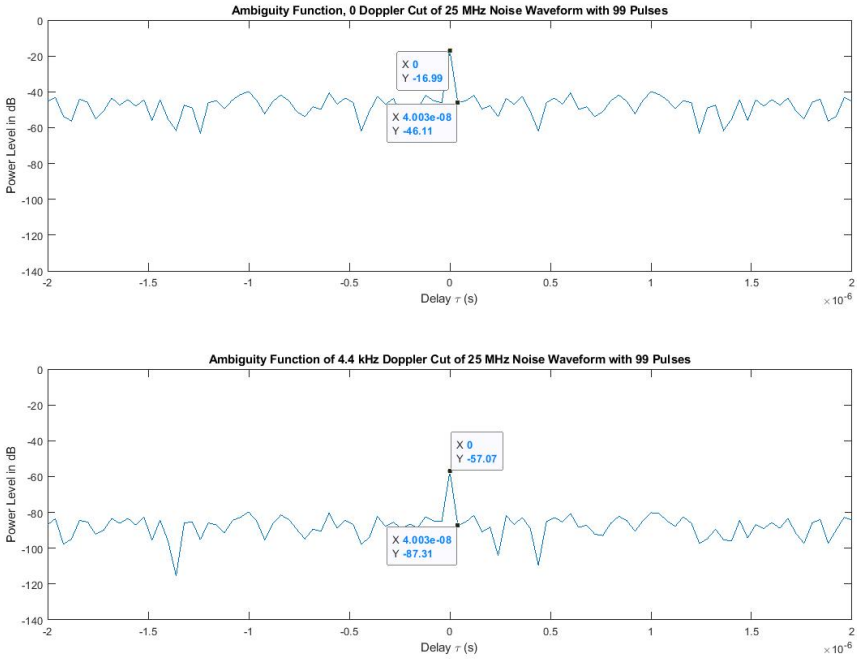

Figure 3.11: Ambiguity Function Of Noise Waveform With Multiple Pulses: Doppler Cut: $2\mu s$ View

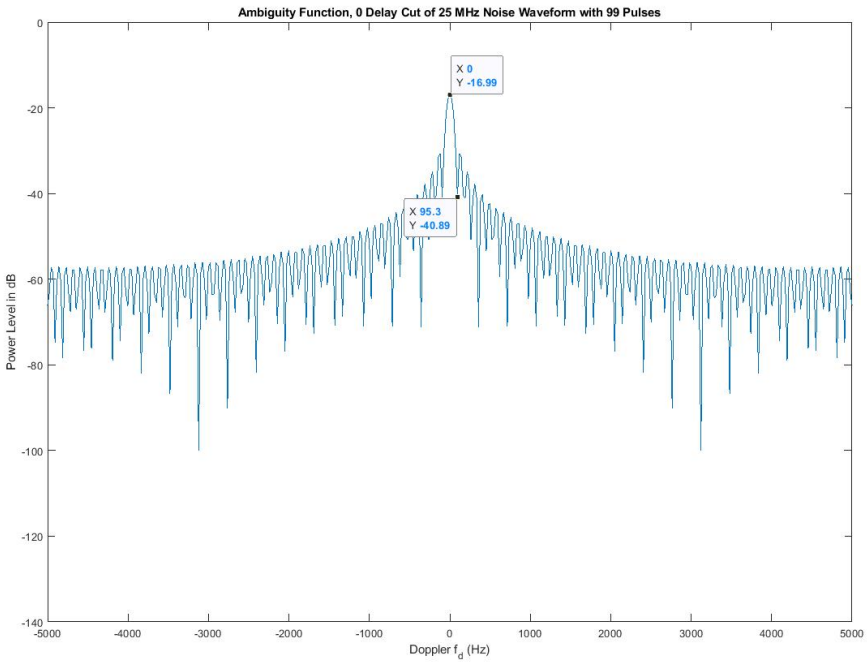

Figure 3.12: Ambiguity Function Of Noise Waveform With Multiple Pulses: 0 Delay Cut

Currently, the user can choose between simulation mode or H/W in the loop mode. In H/W in the loop mode, the user can choose either BladeRF SDR, USRP N210 or USRP B210. In H/W in the loop mode, the user has an option to transmit false targets. This option is relevant when the user wants to confirm that the H/W is working properly by looping back the transmit signal to the received signal via an attenuator. It is the responsibility of the user to make sure the loopback is via an appropriate attenuator otherwise the SDR receiver might be damaged.

If the simulation mode or H/W in the loop mode is not selected, then the S/W uses the chosen SDR to detect targets via the connected antennas. The centre frequency must be linked to the capability of the chosen SDR H/W and the antennas connected to the SDR. The default frequency for this Radar is 2.45 GHz but any frequency can be chosen within the limitations stated above. Normally for VSHORAD, an X Band (8 to 12 GHz) frequency is used because these frequencies do not travel far and a larger bandwidth can be used leading to a fine range resolution. Some of the reasons for choosing the 2.45 GHz are that it is within the capability of the SDRs, antennas and power amplifier available to the researcher. It is also a free-to-air ISM band frequency even though there are restrictions on the output power to be used for this band.

Even though this Radar can operate in pulse mode or modulated continuous wave mode, the terminology of pulse Radar is applied for both modes.

The Graphical User Interface (GUI) only shows the pulse Radar mode terminology and it is up to the user to know the corresponding modulated continuous wave terminology as described in this dissertation when using the Radar in the modulated continuous wave. Where that terminology is used for the first time, an equivalent terminology for modulated continuous wave will be provided whereafter the use of pulse terminology will imply the applicable one in the modulated continuous wave. Pulse bandwidth is the first of these terminologies that are called different names in both modes of the Radar but it is practically the same thing. Pulse bandwidth in the modulated continuous wave is known as sweep bandwidth. The default value is 25 MHz which leads to a range resolution of 6 m. It is up to the user to know the H/W limitation of the chosen SDR when setting this value.

An appropriate sampling frequency for both transmit and receive must be entered. Its value must be twice the highest frequency of the baseband signal. For a positive up chirp signal, the sampling frequency must be twice the bandwidth and for the symmetric up chirp waveform, the sampling frequency must be the same as the bandwidth since the highest frequency is half the bandwidth. The number of samples for transmitting and receiving pulse and PRI samples are computed by the S/W. It is up to the user to make sure the chosen SDR H/W can handle the computed number of pulses.

The LPI requirement of this Radar means the pulse width (or sweep length for modulated continuous wave) has to be as long as possible to reduce the required peak power while keeping the average power the same. When choosing the pulse width the desired duty cycle must be taken into account and it is calculated by the S/W using the values of pulse width and the Pulse Repetition Interval (PRI) (or sweep length for modulated continuous wave). It must be noted that pulse width and PRI are both called sweep length in modulated continuous wave Radar mode. The reason is that in modulated continuous wave mode the Radar transmits continuously and thus the transmit time of the Radar is the same as the time between transmitting sweeps. The user can change the Pulse Repetition Frequency (PRF) (or sweep rate in modulated continuous wave) and the PRI is computed by the S/W. For modulated continuous wave mode the user must choose the pulse width that is the same as the PRI to get a 100% duty cycle. It is possible to have a 100% duty cycle in pulse Radar mode but the maximum unambiguous range will be reduced. In the simulated chapter, this value is practically determined. Time bandwidth product of 277 775 is achieved in pulse Radar mode using the default pulse width and bandwidth values. This value is much greater than 1, and according to Richards [30], this Radar qualifies as a pulse compression Radar.

The user enters the maximum velocity of a target that the Radar must measure. This value is used to compute the minimum PRF required to be able to measure this velocity. The user must make sure the chosen PRF is greater or equal to the computed minimum PRF. The corresponding maximum PRI is computed by the S/W using the minimum PRF.

The default number of pulses of 98 is obtained by first computing the Range resolution quantity based on the speed of light and pulse bandwidth of 2.50×10^7 Hz. Thereafter the integration time of 1.11×10^{-2} s for all pulses is determined based on the time required for the target to leave half of the range cell when it travels at a maximum speed of 270m/s. Finally, the integration time is divided by the PRI of 1.13×10^{-4} s, to get the required number of pulses. The user can overwrite the required number of pulses.

The configurability of the Radar allows the user to enter the Radar Cross Section (RCS) of the target and its maximum detection range. The user must also enter the SDR noise figure, system noise figure and operating temperature of the Radar which are used in the calculation of the required transmit power. The S/W uses the other Radar parameters including the target information to determine the required maximum peak transmit power. The minimum SNR for a P_d of 0.9 and P_{fa} of 1.00×10^{-6} and coherent integration of pulses are computed. To improve the required minimum SNR, the SNR gain from coherently integrating 98 pulses is computed and subtracted from the minimum SNR of a single pulse. From the GUI it is possible to choose non-integration of pulses, non-coherent integration or coherent integration. The minimum required SNR and subsequent peak transmit power are based on the chosen integration option.

To further improve the SNR of the received signal, the matched filter is used to process the received signal but only if the Radar is used in Pulsed mode. The matched filter improves the SNR of a signal at the input regardless of the waveform used by the Radar and is regarded as the optimum filter with regards to SNR since they also improve input SNR by a factor of 2 [13].

Other RF parameters that maybe unique to the chosen SDR H/W can be changed with a thorough knowledge of the SDR capabilities. Some of them are the transmit and receive gains and the master clock rate. Other parameters are hard coded in the S/W such as transmit and receive channels depending on the chosen SDR H/W. The hard-coded parameters are kept to the minimum and in future when time allows they will be made user-configurable.

As stated above, the display parameters can be changed at any time. If any of the graphs (except for the Range Doppler map) is not properly displayed, the user can click the reset axis button to make the graph fit properly in its window. The Range Doppler Map is adjusted by changing the percentage of maximum range and/or doppler to be displayed. These percentages affect their corresponding A-Scope graphs as well. The received pulse to be displayed is also selectable. The GUI has several graph tabs for displaying the baseband LFMW signal, baseband noise signal, baseband transmitted signal, matched filter output signal for pulse mode or dechirp signal for modulated continuous wave mode, range A-Scope, velocity A-Scope, Range Doppler Map (with configurable minimum and maximum signal levels), short windowing signal (pulse length) and long windowing signal (PRI length). Only the Chebyshev window is implemented for now and the user

has an option to choose if windowing is applied or not. The use of the windowing function reduces the sidelobe levels and consequently reduces the effect of target masking of small targets by large targets. Windowing negatively affects range resolution and target detection since the main lobe width is slightly increased and the main lobe peak signal level is slightly reduced.

3.5 Summary

This chapter focused on the design considerations of Configurable LPI VSHORAD Noise Radar. Designing an SDR-based Radar gives the ultimate flexibility such that its mode and parameters can easily be changed. With the same S/W and H/W, the user has an option of running the Radar as a pulse Radar or modulated continuous wave Radar. It is possible to have a pure noise waveform or another waveform modulated with noise. This flexibility makes it possible to test and compare the performance of different types of Radars using one S/W and H/W platform. Without the use of SDR, this is not achievable since the cost is extremely high.

The ability to use different SDRs with the S/W makes it possible to expand the usage of this Radar. So far three SDRs are integrated with the Radar and they can be used to compare the performance of the Radar at different frequencies and different bandwidths. If frequencies that are higher than the capabilities of the integrated SDRs are required, then appropriate SDRs can be integrated by just writing the new drivers to interface with them. The rest of the S/W will be useable as is.

This Radar experimental tool is ready to test the hypothesis of this research. Depending on the target of interest, the user will know in advance the required transmitting power to detect it and choose the appropriate amplifier. Therefore depending on the mission, the appropriate power amplifier is selected to maintain the LPI characteristics of the Radar. The next chapter simulates the performance of the Radar under different scenarios.

Chapter 4
Simulation Of LPI AD Noise Radar

4.1 Introduction

This chapter simulates the LPI AD Noise Radar at S-Band for flying targets that are within 1.70×10^4 m maximum unambiguous range. The simulation goes through several scenarios to evaluate the performance of the Radar. The first scenario is the simulation of six targets that are at different ranges and velocities as shown in table 4.1. The targets are simulated in such a way that others are moving toward the Radar (negative velocities) whilst others are moving away from the Radar (positive velocities). When a target moving towards the Radar reaches 0 m range, its velocity is multiplied by negative 1 and then changes direction and starts moving away from the Radar at 0 m range. For a target that reaches the maximum unambiguous range, its velocity is also multiplied by negative 1 and its direction changes towards the Radar. Therefore all simulated targets are in a perpetual circular loop. For each scenario, the simulation results are compared with the expected results. It must be noted that the power levels for all results in this chapter and the next one for the A-Scope and Range Doppler Map graphs, were not calibrated to be realistic and the focus was just on the difference in signal intensity for targets with strong reflections versus those with weak returns. The signal levels for hardware characterisation in the next chapter, are however accurate.

4.2 Scenarios

The simulation aims to test the hypothesis which states that "LPI AD Noise Radar with high range and doppler resolutions is realisable." Section 2.1 broke down this hypothesis and examined it thoroughly. This section creates scenarios that test the following elements of the hypothesis:

1. Detect airborne targets

2. Test LPI characteristics
3. Test mutual interference and spectrum sharing
4. Test high-range resolution
5. Test high doppler resolution

Each scenario is implemented in continuous wave mode, first with frequency modulated waveform and then with a noise modulated waveform. For all tests, only the symmetric up chirp waveform format is chosen to maximise the signal bandwidth.

4.2.1 Detect Simulated Airborne Targets

At the moment, the targets' list parameters are hard coded in the source code. The next version of the software will allow the user to change them in the Graphical User Interface (GUI). The targets' parameters shown in table 4.1 were entered in the constructor of the target_list_class. These parameters were chosen to ensure that target detection is tested up to 1.70×10^4 m and 2.70×10^2 m/s default parameters. The user can easily change these default parameters in the GUI. The number of targets can be as many as the user wants.

Targets Parameters			
Target	Range [m]	Velocity [m/s]	Sample #
1.	1000	-220	167
2.	3000	60	500
3.	5000	-90	834
4.	12000	-25	2001
5.	13000	240	2168
6.	14000	100	2335

Table 4.1: Simulated Airborne Targets To Be Detected

4.2.1.1 Detect Simulated Airborne Targets: MCW Radar

The number of pulses is overwritten from 99 to 1024 which improves the velocity resolution from 5.46 m/s to 0.53 m/s. Figure 4.1 shows that the initial positions and velocities of the six simulated targets just after the processing is started are the same as they were configured. The Radar is configured to work as MCW Radar that is frequency modulated which is also known as FMCW Radar. Figure 4.2 shows the zoomed-in view of target 1 moving towards the Radar before it loops back. After target 1 has reached the first range bin, figure 4.3 shows that its direction is changed to move away from the Radar and its velocity is negative one times its configured velocity. The Range Doppler map is zoomed in by showing only 20% of the range to show the targets clearly. Figure 4.4 shows the A-Scope display of

the initial targets' positions. It can be concluded that the radar correctly simulates, detects and displays multiple targets in FMCW mode.

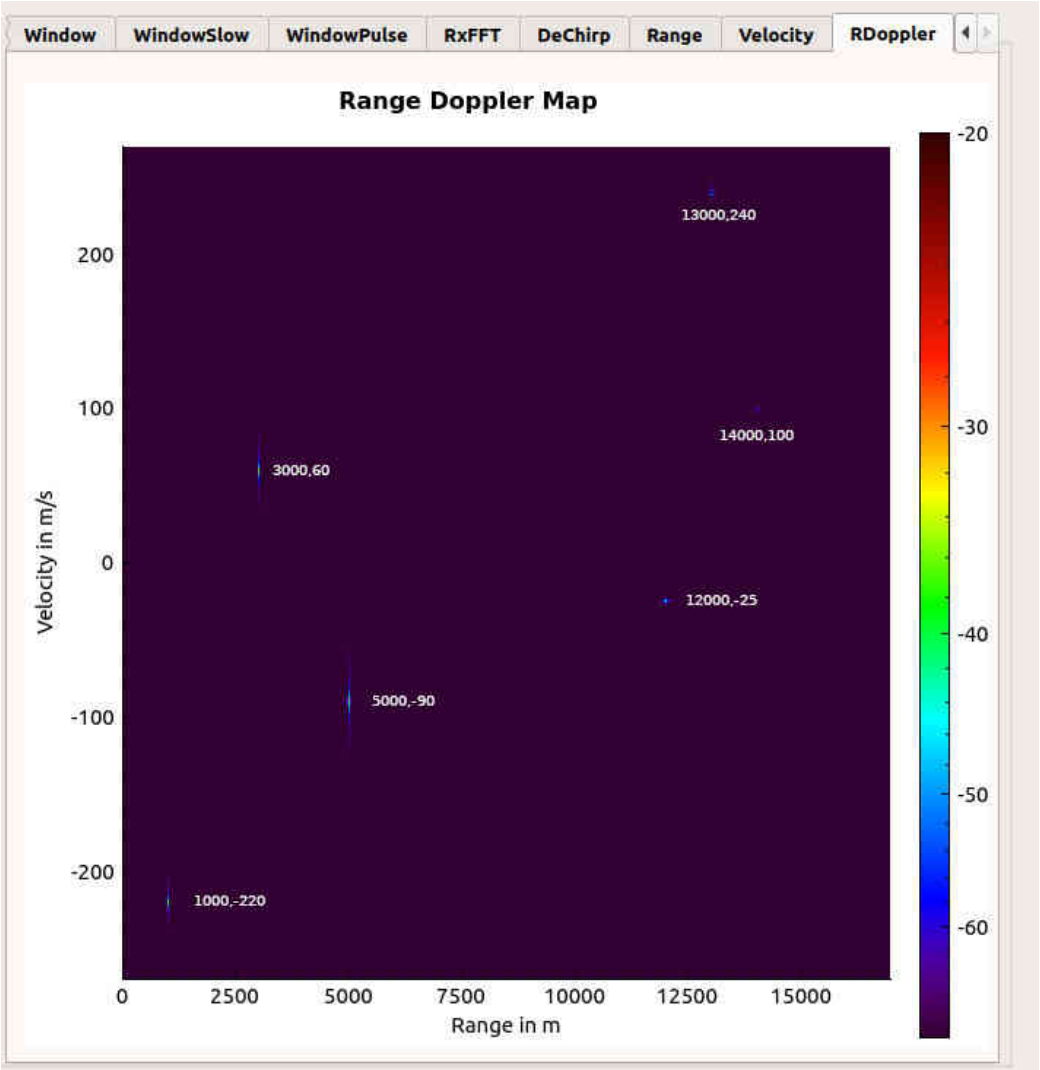

Figure 4.1: All Simulated Targets For FMCW Radar Mode

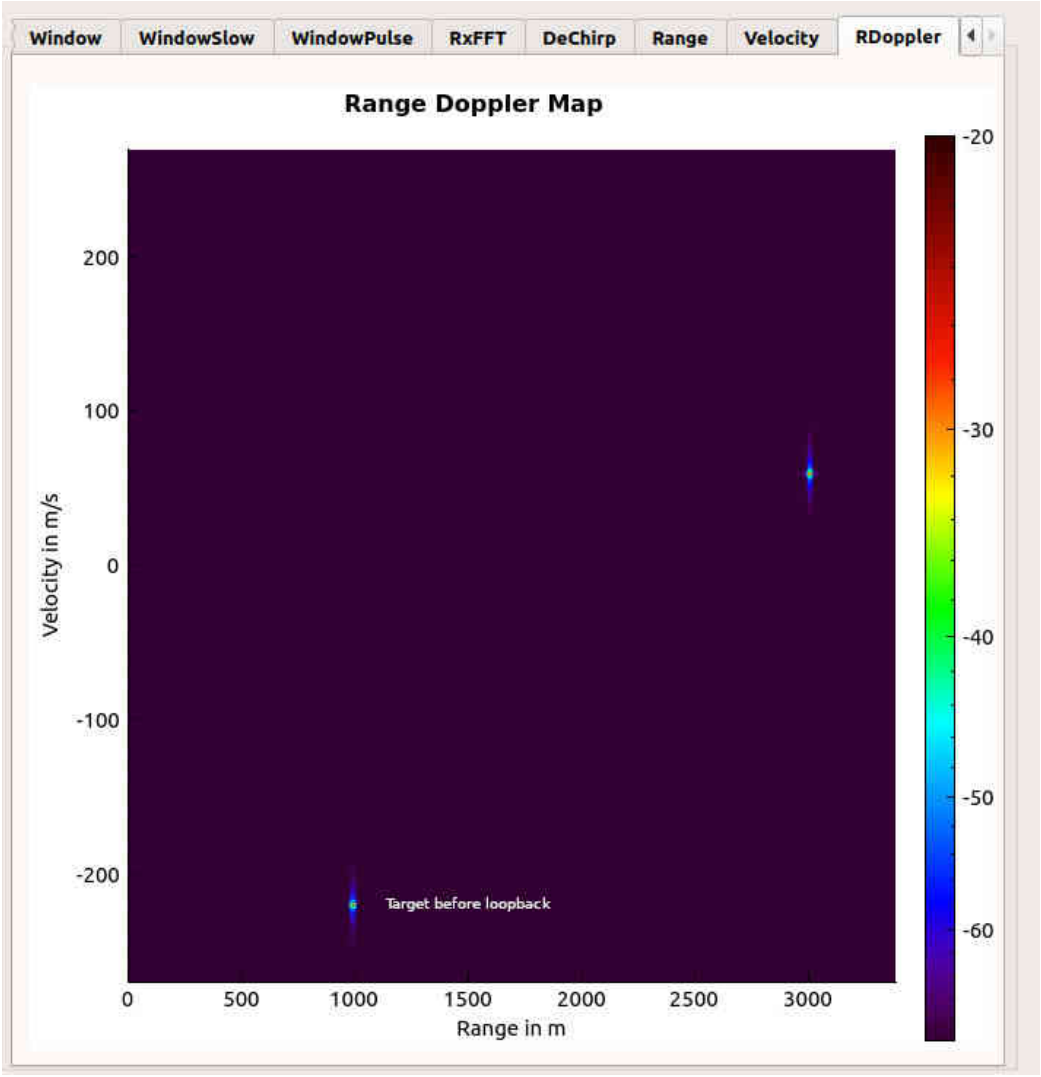

Figure 4.2: Simulated Targets Before Loopback In FMCW Radar Mode

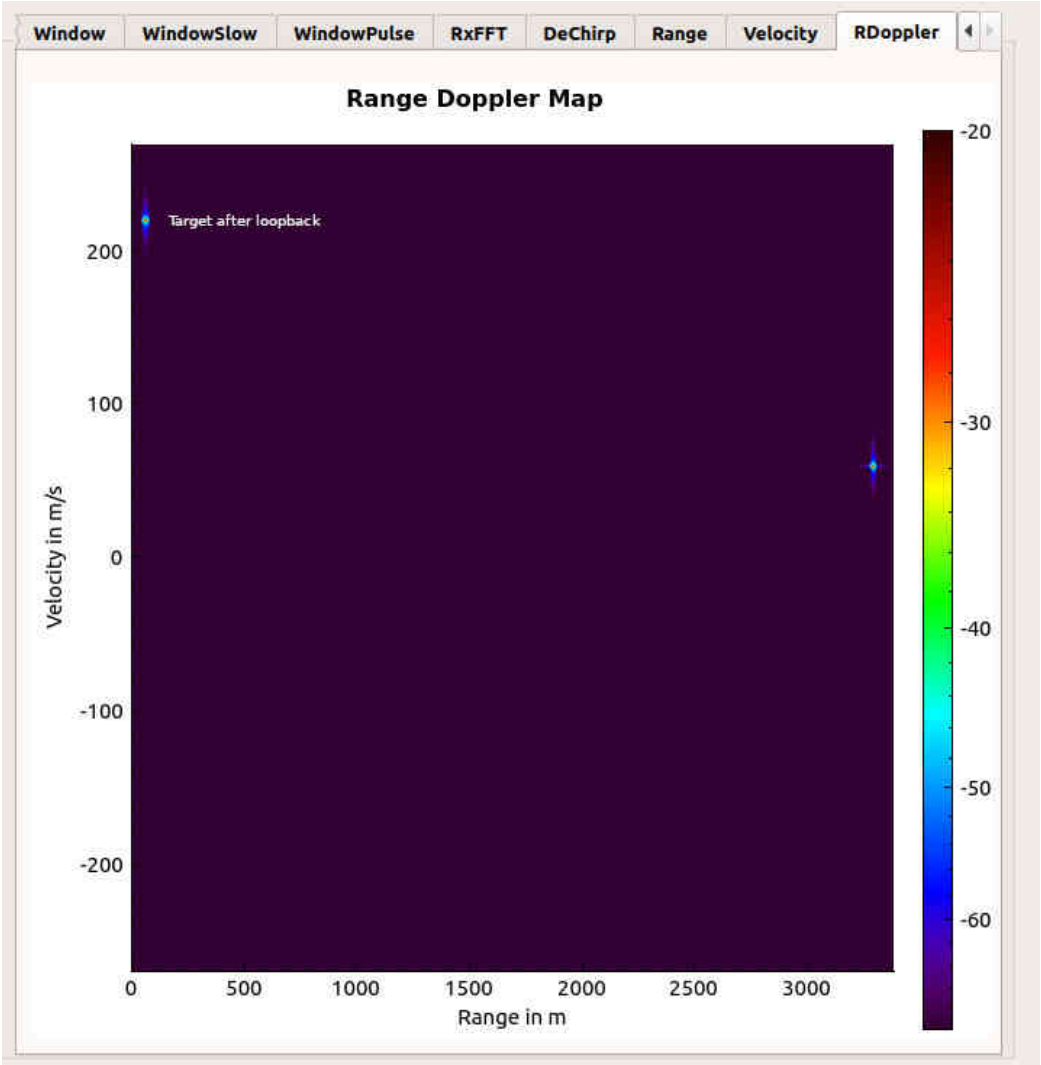

Figure 4.3: Simulated FMCW Radar Targets After Loopback

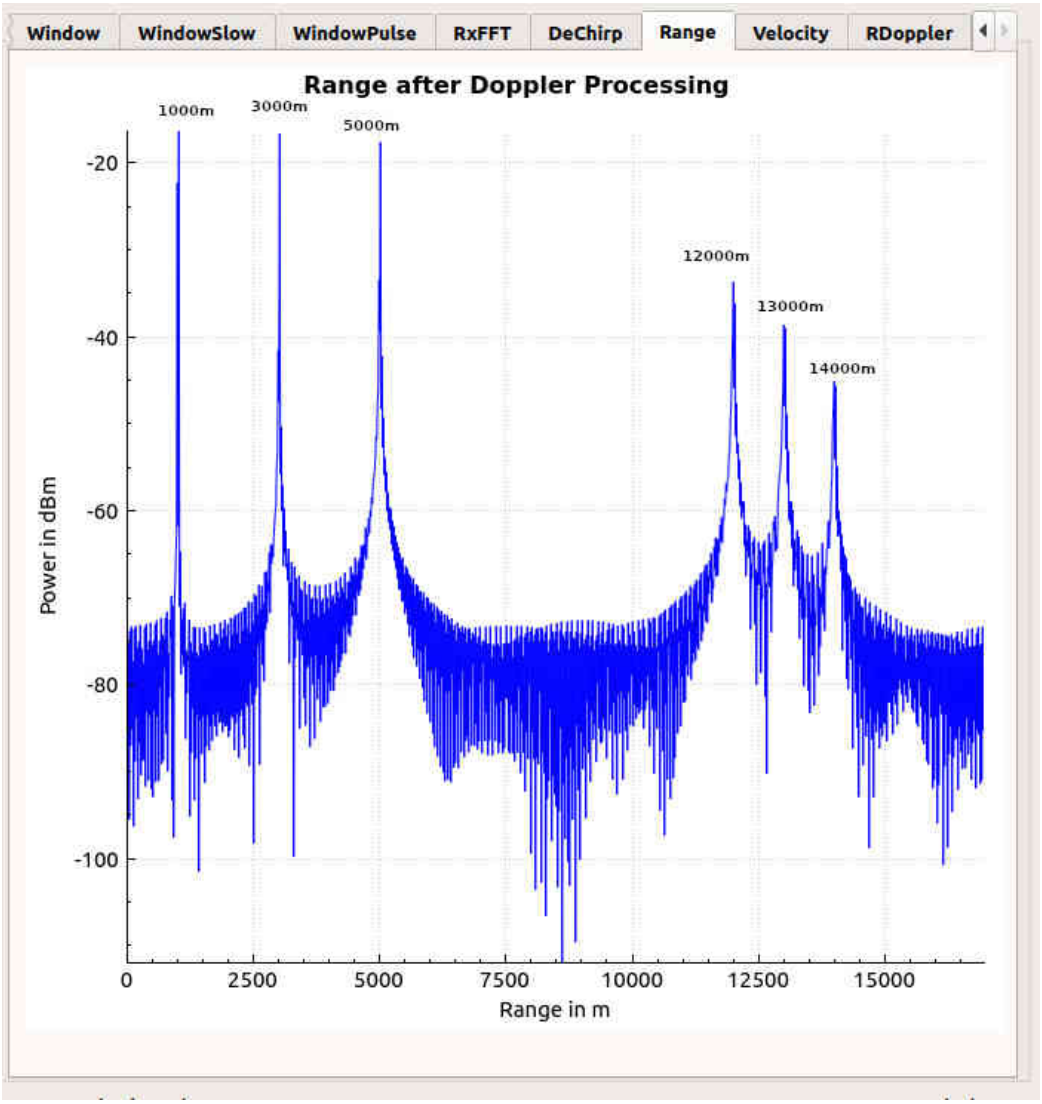

Figure 4.4: Simulated FMCW Radar A Scope

This test is repeated for MCW Radar using Noise modulation. It was discovered that using a noise waveform in CW mode which de-chirps the signal, does not provide range information but does provide velocity information. This is because the pseudo-random noise signal does not have a unique set of frequencies which can be mixed with frequencies returning from the target. The Radar was then configured to work in pulse mode with the pulse length equal to the PRI. This effectively makes it an MCW pulse Radar which provides both range and velocity of the targets by using a matched filter instead of a dechirp signal processing technique. The reason why this works is that matched filter cross correlates the transmitted signal with the signal reflected by the target. From now onwards all tests for Noise MCW Radar mode will follow this approach of a pulse Radar mode with a pulse length that is equal to the PRI.

Figures 4.5, 4.6, 4.7 and 4.8 show the Range Doppler map of the three simulated targets just after processing has started, the Range Doppler map before target 1 is looped back, the Range Doppler map after target 1 has reached range bin 1 and its direction changed to move away from the Radar and finally the A-Scope of the three simulated targets. Remember that the A-Scope is shown in the Dechirp output, but since it is in pulse mode, what is shown is the output of the matched filter. This is in line with the dual use of terminology as described earlier for this project. This experiment confirmed that the Noise MCW Radar detection of targets is the same as its FMCW counterpart even though it had to be realised by using a matched filter of the pulse Radar mode.

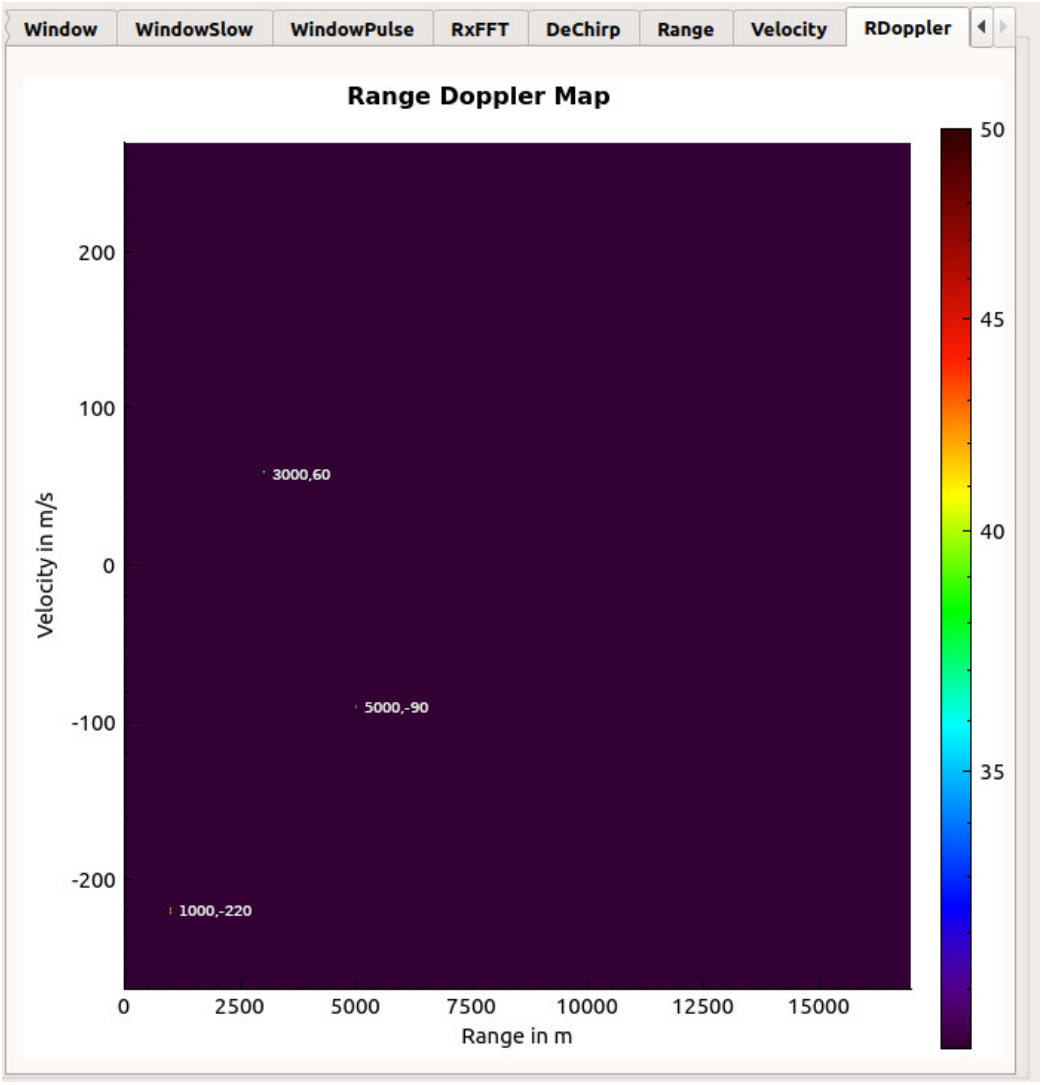

Figure 4.5: Three Of The Simulated Targets For Noise Pulse CW Radar Mode

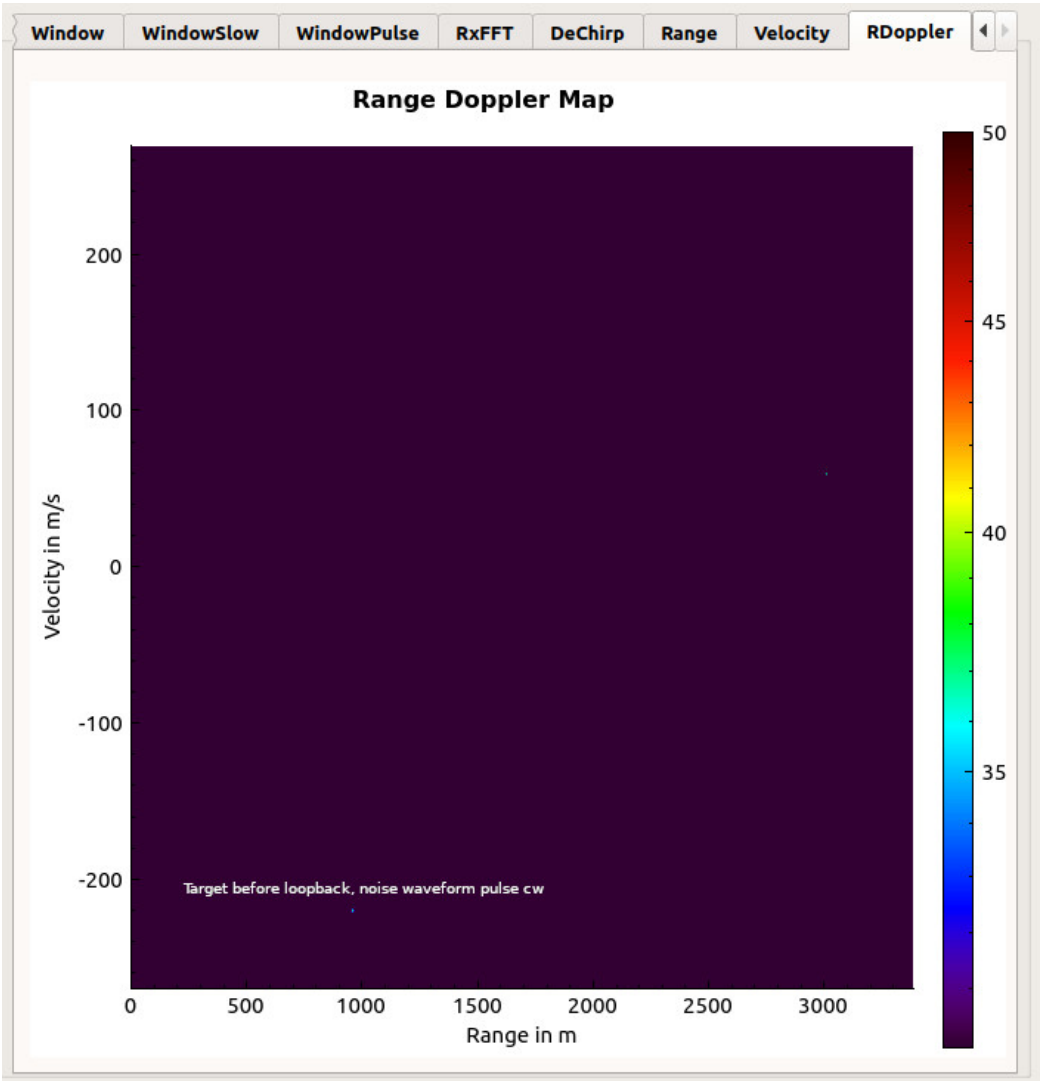

Figure 4.6: Simulated Targets Before Loopback In Noise Pulse CW Radar Mode

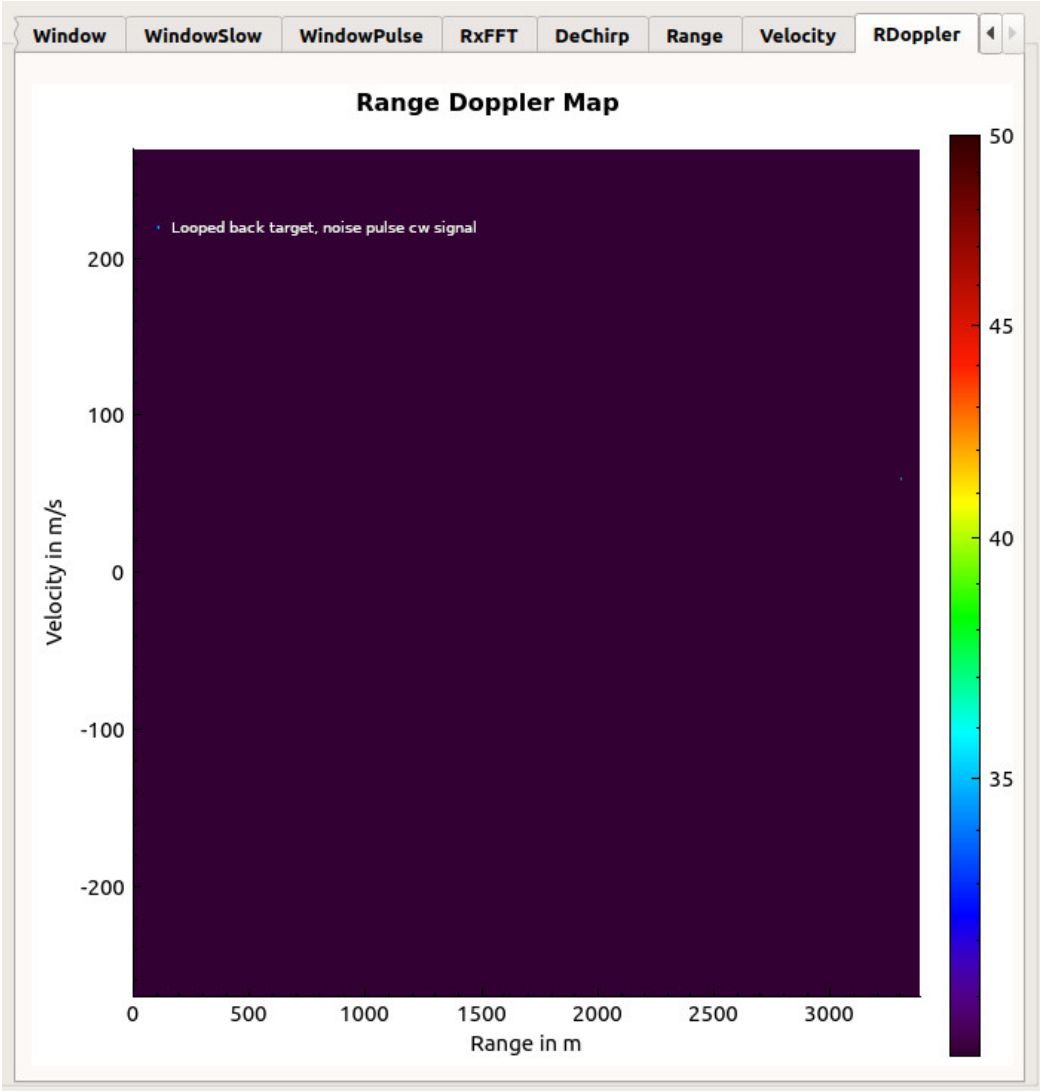

Figure 4.7: Simulated Noise Pulse CW Radar Targets After Loopback

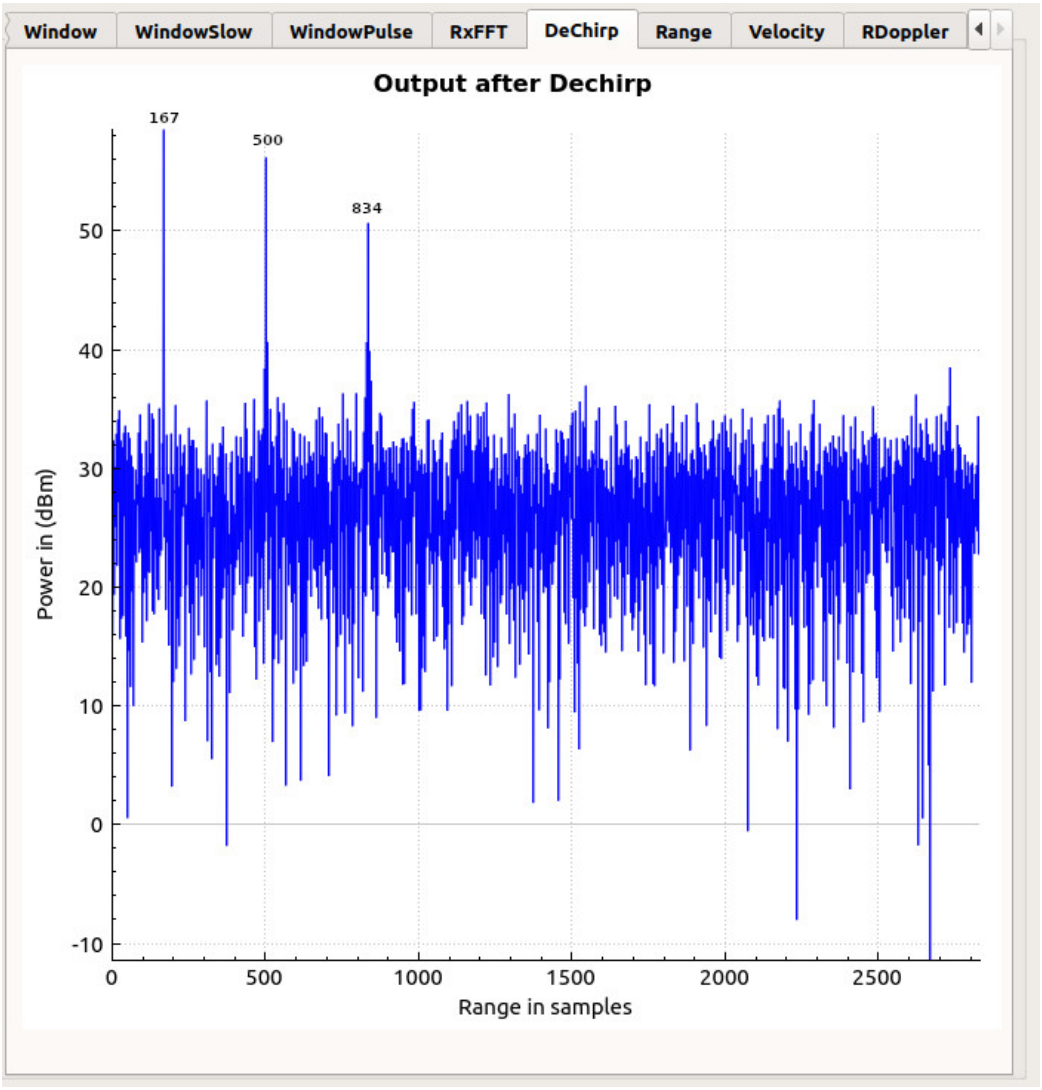

Figure 4.8: Simulated Noise Pulse CW Radar A Scope

4.2.2 Test LPI Characteristics

As mentioned in previous paragraphs, LPI characteristics are divided into LPD and low probability of exploitation (LPE). The two sub-sections below look at these sub-topics for MCW Radar for both frequency and noise modulated waveforms.

4.2.2.1 Test LPI Characteristics: MCW Radar

The fact that MCW Radar transmits for the duration of the sweep time means that for the same target at the same range, it will require much less power compared to a pulse Radar. This is because MCW Radar has a 100% duty cyle in contrast to a typical pulse Radar which has a much lower percentage duty cycle, normally less than 20%. Therefore MCW radar has

LPD characteristics.

The second LPI characteristic to be explored is that of LPE. A signal can only be exploited if it is known or predictable. FMCW Radar does not have LPE characteristics since it is known and predictable and can therefore be easily exploited once it is detected. The noise MCW Radar transmits a random noise signal for each batch of sweeps. This means that the transmitted noise signal is the same from sweep to sweep within a batch but may be different between batches. Since the noise is generated randomly, no one can predict or know what it will look like and thus making the noise MCW completely LPE. Changing the transmitted noise waveform from batch to batch makes it even more difficult to predict this waveform since it only stays the same for a limited number of sweeps within a batch. This discussion shows that noise-modulated MCW Radar has LPE characteristics.

4.2.3 Test Mutual Interference And Spectrum Sharing

The biggest problem of colocated Radars is that of mutual interference. A Radar located next to another Radar with the same non-random waveform will process the other Radar's waveform as if it is it's own and thus increase the number of false alarms. Experiments for testing this problem are done for MCW Radar mode for both frequency and noise modulated waveforms. For a normal FMCW Radar, this problem of mutual interference means that colocated Radars of this type have to use a different set of frequencies or transmit at different times to share the spectrum efficiently. This section will show that noise waveform allows the same Radars to be colocated without the creation of ghost targets and thus lead to an efficient sharing of the spectrum which is a very expensive and limited resource.

4.2.3.1 Test Mutual Interference And Spectrum Sharing: MCW Radar

The Radar is run in FMCW mode and another Radar is simulated to be pointing at the same simulated targets but with a slight delay due to it being at a different range from the main Radar of interest. The real simulated targets are the first three targets listed in table 4.1 whilst the ghost targets are those shown in table 4.2. Figure 4.9 shows that for each of the simulated targets, there is a ghost target at a different range and velocity as a result of the processed received signal from reflections of the other Radar. Therefore mutual interference is a serious problem for FMCW Radar.

The same experiment is repeated for noise-modulated MCW Radar. Figure 4.10 shows that only the simulated targets are shown by the Radar. This shows that noise MCW Radar is immune to mutual interference problems and can thus be colocated with other Radars of the same type and only real targets will be displayed. The reason for this good performance is that noise MCW Radar transmits a different noise waveform compared to another

noise MCW Radar next to it since the noise waveform is generated randomly and the same Radars next to each other will generate a unique waveform which is filtered out by the other Radar.

Ghost Targets Parameters			
Target	Ghost Range [m]	Ghost Velocity [m/s]	Ghost Sample #
1.	1500	-210	250
2.	3500	70	584
3.	5500	-80	917

Table 4.2: Simulated Airborne Ghost Targets

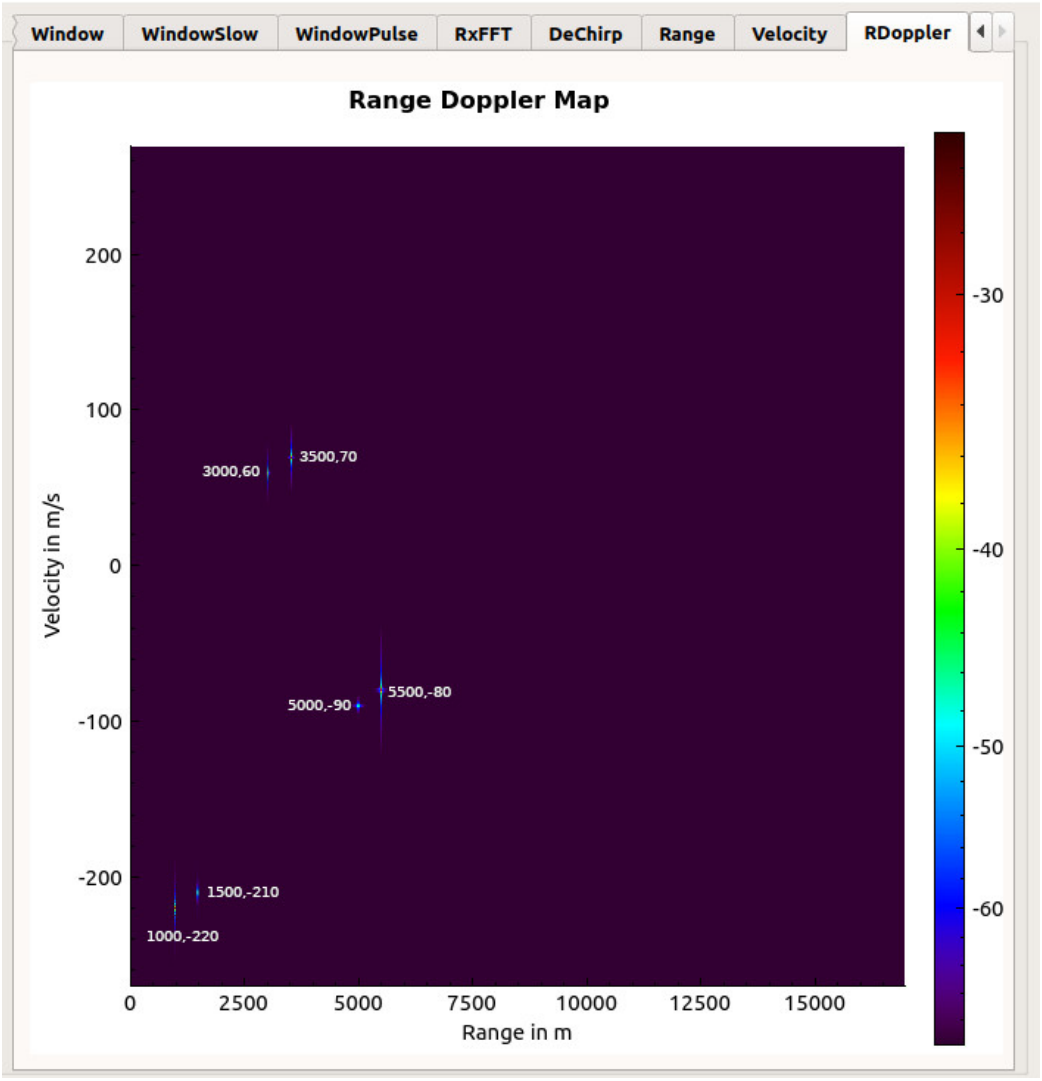

Figure 4.9: Simulated Targets With Injected Ghost Targets In FMCW Radar Mode

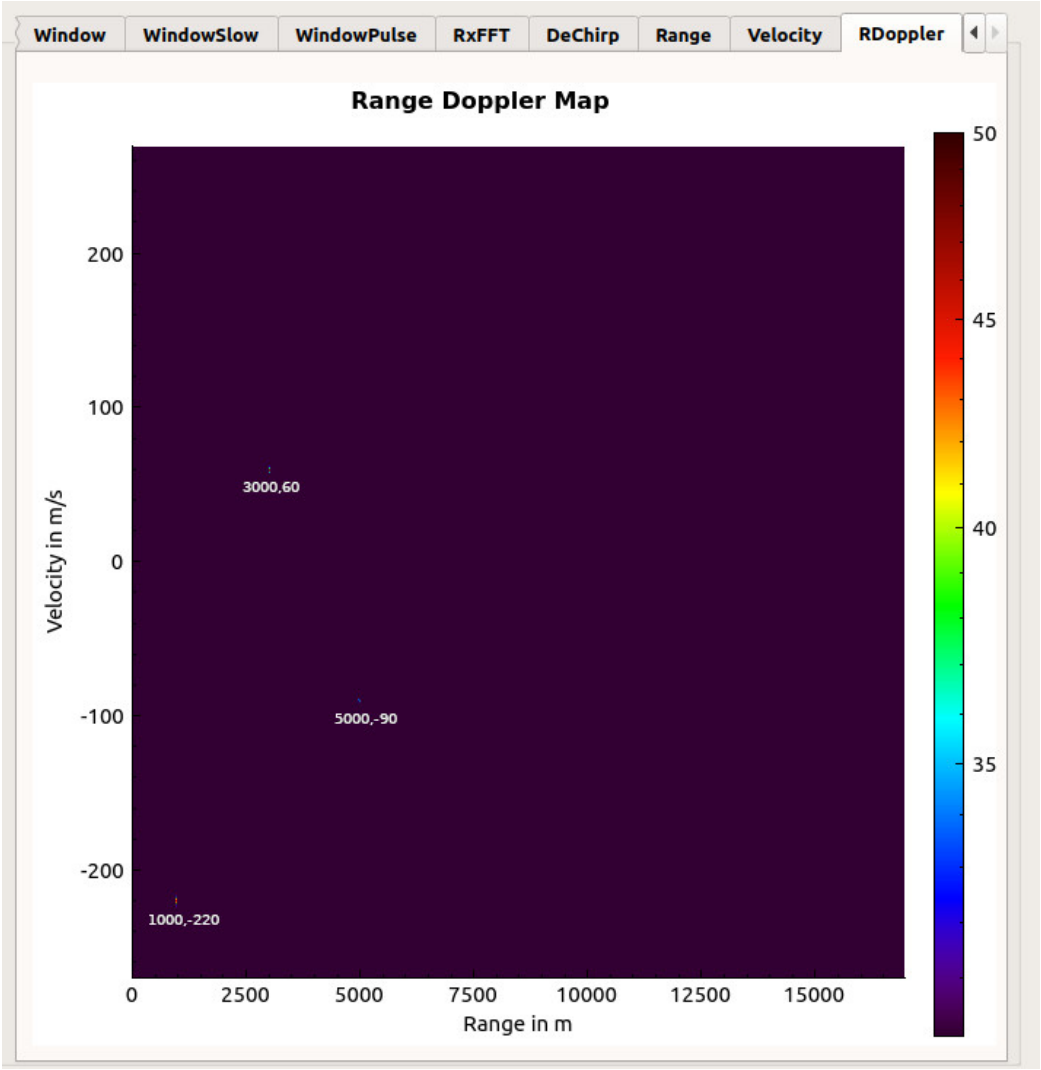

Figure 4.10: Simulated Pulse CW Noise Radar Targets With Injected Ghost Targets Suppressed

4.2.4 Test High Range Resolution

Table 4.3 has a list of two targets that are located apart by 6.00 m range resolution and travelling at the same velocity. The next table 4.4 shows targets that are 12 m apart but with the Radar configured for the same range resolution of 6.00 m. The experiment for range resolution is done for MCW Radar both with frequency modulated and noise modulated waveforms each.

Targets Parameters		
Target	Range [m]	Velocity [m/s]
1.	30	10
2.	36	10

Table 4.3: Simulated Range Resolution 6m Apart

Targets Parameters		
Target	Range [m]	Velocity [m/s]
1.	30	10
2.	42	10

Table 4.4: Simulated Range Resolution 12m Apart

4.2.4.1 Test High Range Resolution: MCW Radar

Figure 4.11 shows that the two targets for FMCW Radar are displayed as two distinct targets at the minimum range resolution. It is clear from this figure that the two targets are not distinguishable as compared to figure 4.12 where the two targets are 12 m apart and the separation of the two targets is unambiguous. Take note that the image of the targets that are 12 m apart was taken after the simulation has run for some time and the separation distance remained constant at 12 m since the two targets are travelling at the same radial velocity. Repeating the same experiment for pulse noise MCW Radar yields similar results which are shown in figure 4.13 for 6 m separation and figure 4.14 for 12 m separation. Therefore the noise Radar achieves the same range resolution as the FMCW Radar.

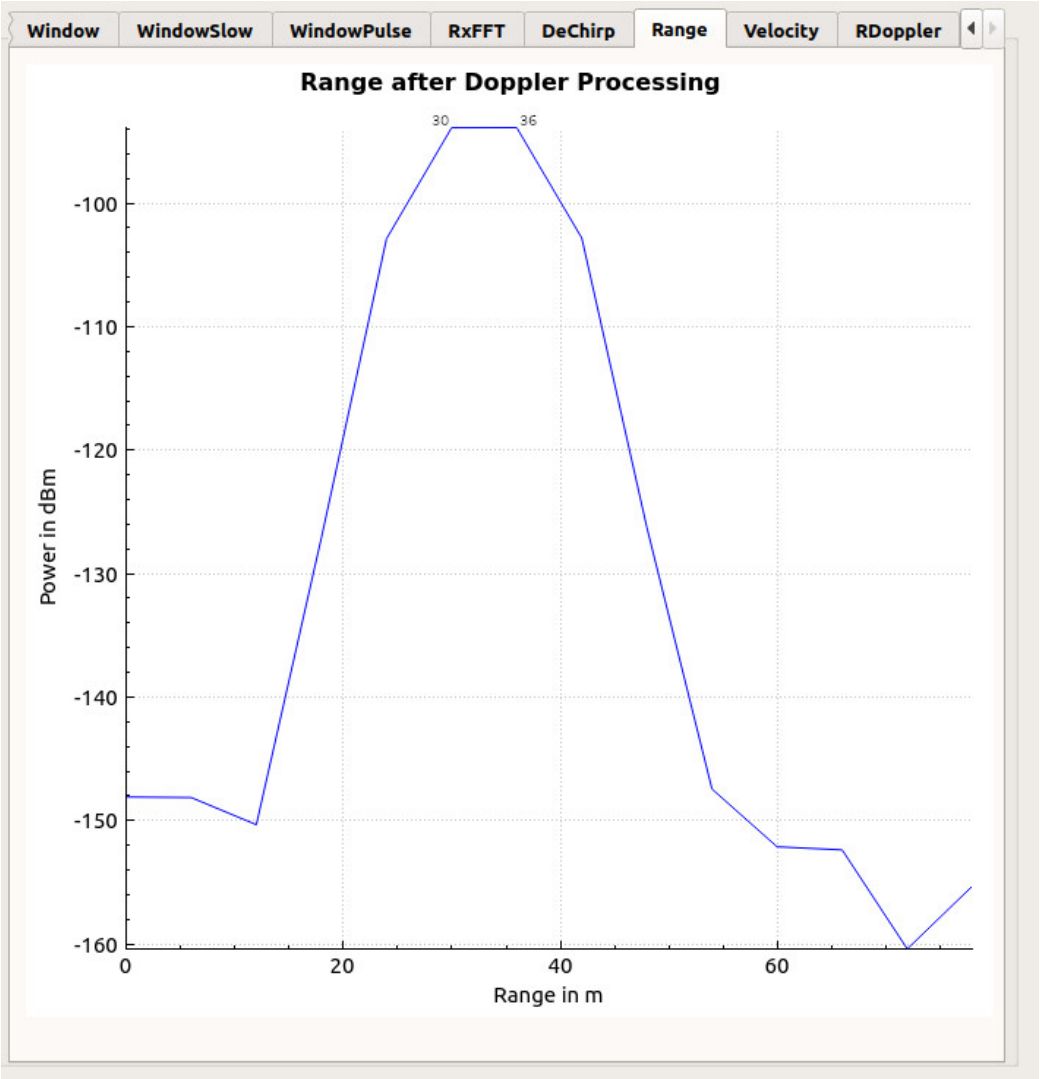

Figure 4.11: Simulated Targets 6m Apart In FMCW Radar Mode

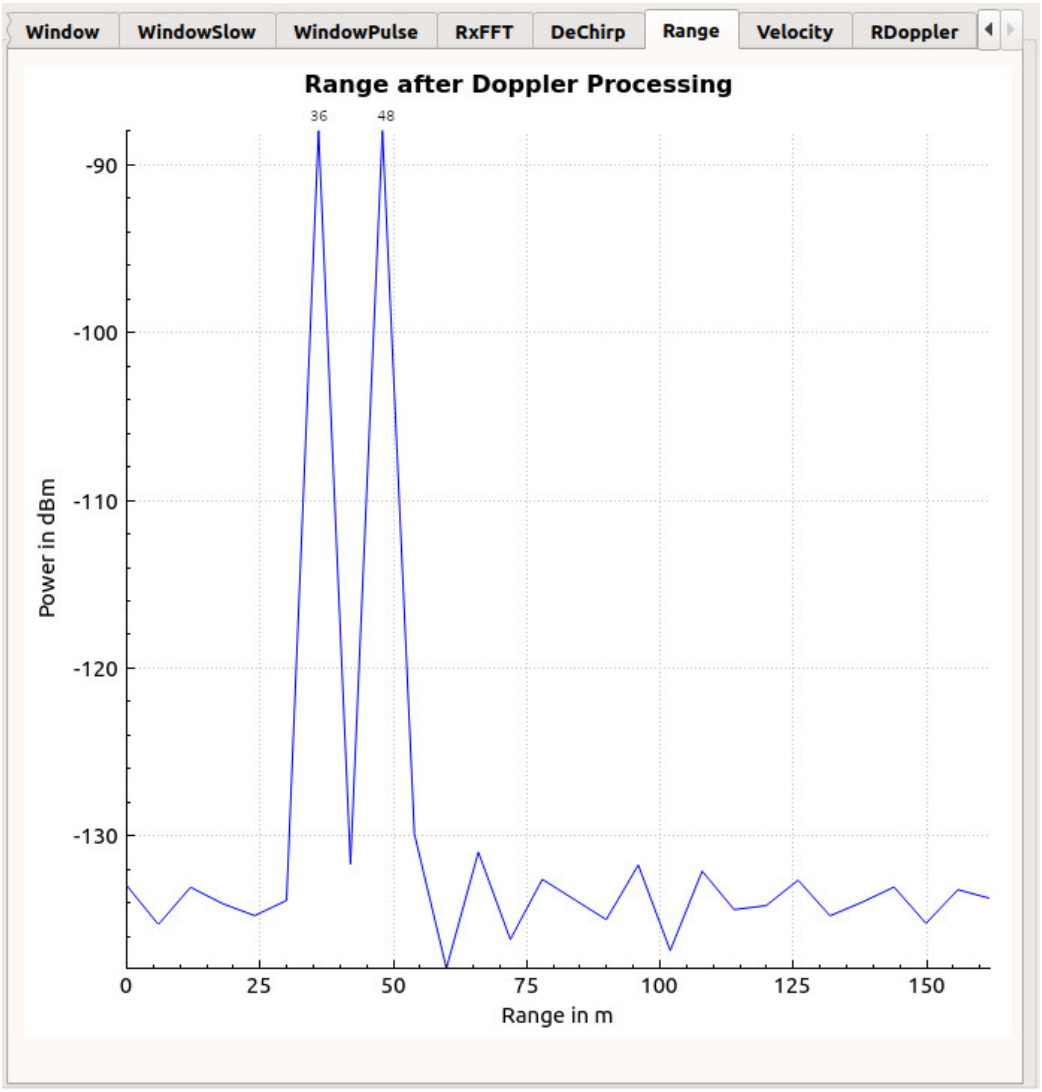

Figure 4.12: Simulated Targets 12m Apart In FMCW Radar Mode

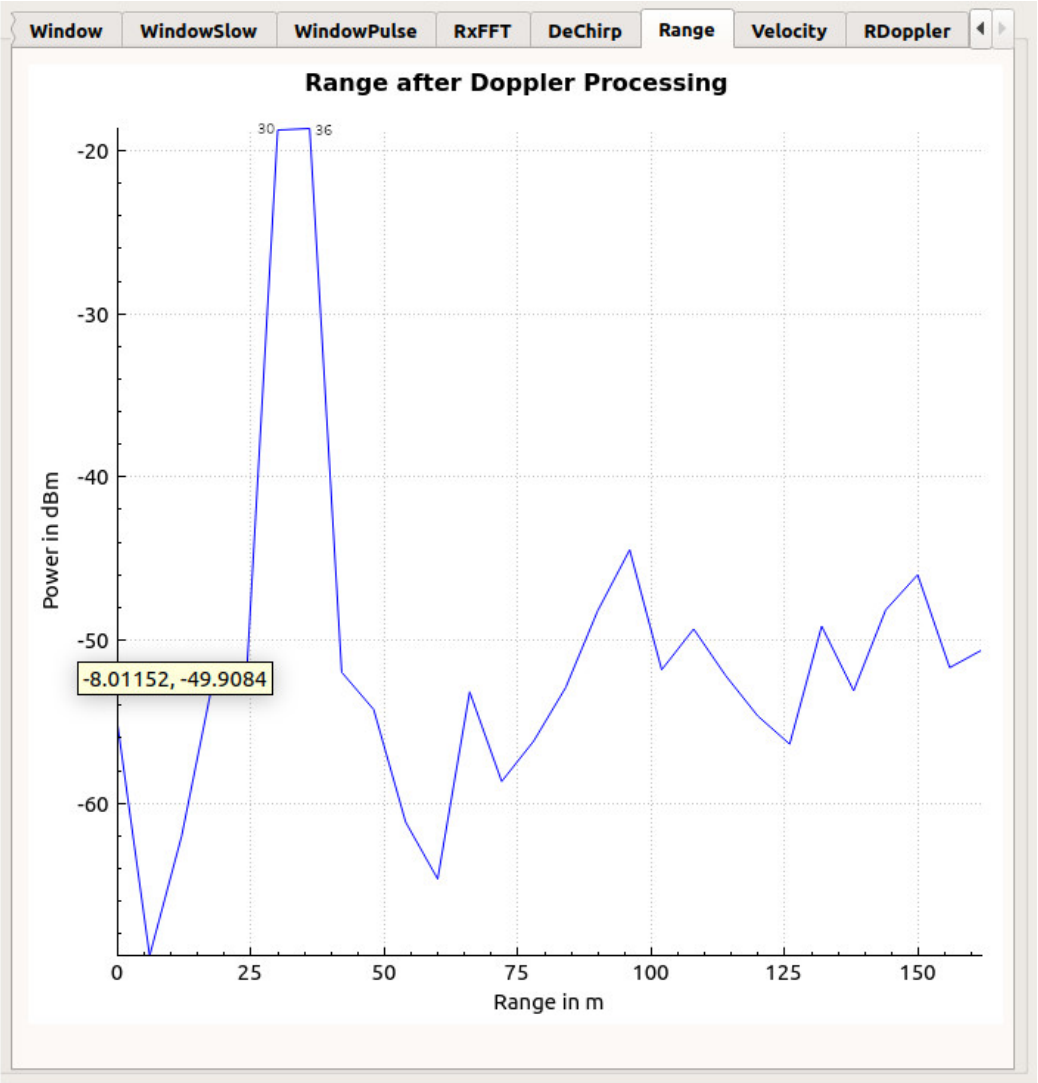

Figure 4.13: Simulated Targets 6m Apart In Pulse Noise CW Radar Mode

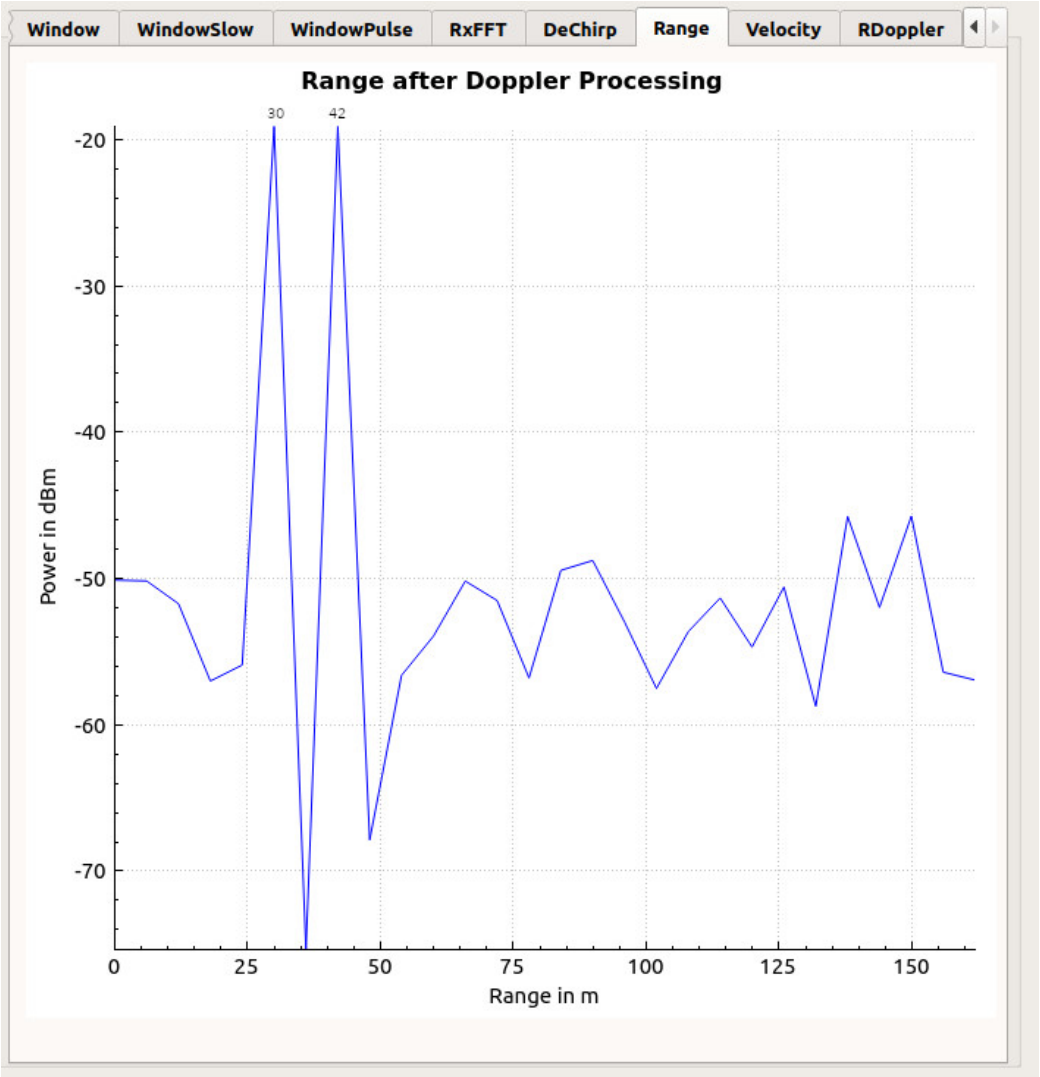

Figure 4.14: Simulated Targets 12m Apart In Pulse Noise CW Radar Mode

4.2.5 Test High Doppler Resolution

The ability to distinguish targets in velocity is important since it is possible to have targets at the same range but with different velocities. Table 4.5 shows two targets at the same range but with different velocities. The velocities in the table are apart by 1.2 m/s which is slightly more than twice the velocity resolution of 0.53 m/s when using 1024 pulses or sweeps. Clear unambiguous separation in velocity was found to occur at twice the velocity resolution of 0.53 m/s at 1.06 m/s and 1.2 m/s velocity separation was found to be much clearer after several experiments were run. The experiment is performed for both MCW and pulse Radar and for each Radar type, the frequency and noise modulation waveforms are used separately to determine their effect on performance. It must be noted that the velocity displayed by the Radar has an offset of 0.447 m/s below the real velocity. This value must

be added to the velocity values shown in the graphs in this section.

Targets Parameters		
Target	Range [m]	Velocity [m/s]
1.	30	10
2.	30	11.2

Table 4.5: Simulated Velocity Resolution

4.2.5.1 Test High Doppler Resolution: MCW Radar

Figure 4.15 clearly shows that for FMCW Radar the two targets at the same range are distinguishable in velocity which are apart by slightly more than twice velocity resolution. The same experiment for noise-modulated MCW Radar also shows the two targets as distinct in the velocity domain in figure 4.16. Adding the velocity offset of 0.447 m/s (as described above) to the velocities of the two targets in the two figures shows that target 1 is travelling at 9.553 m/s plus 0.447 m/s which means its real velocity is 10 m/s and target 2 velocity of 10.659 translates to actual velocity of 11.106 m/s. This means that target 2 computed velocity is lower than the actual velocity by 0.094 m/s which is acceptable.

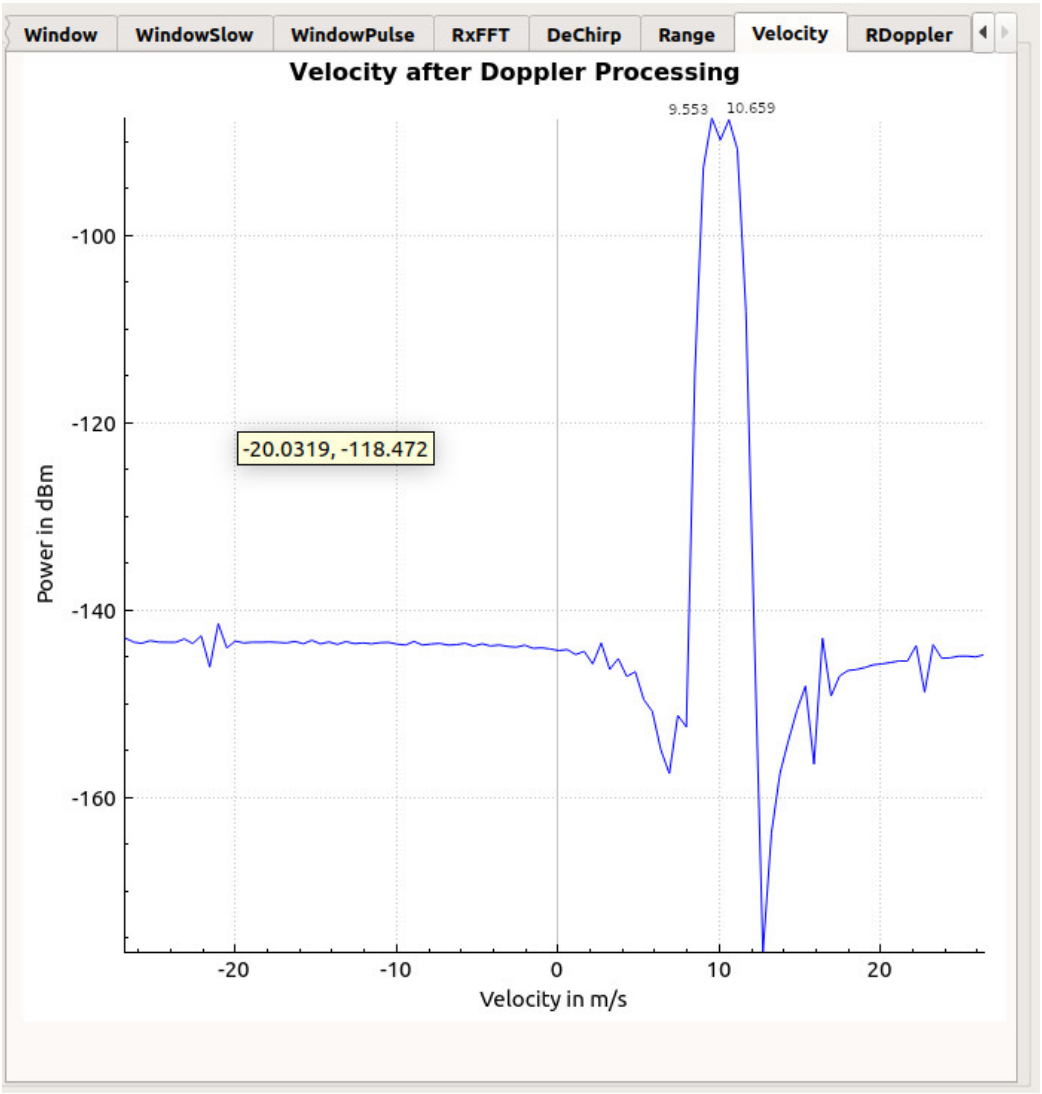

Figure 4.15: Simulated Targets Velocity Resolution In FMCW Radar Mode

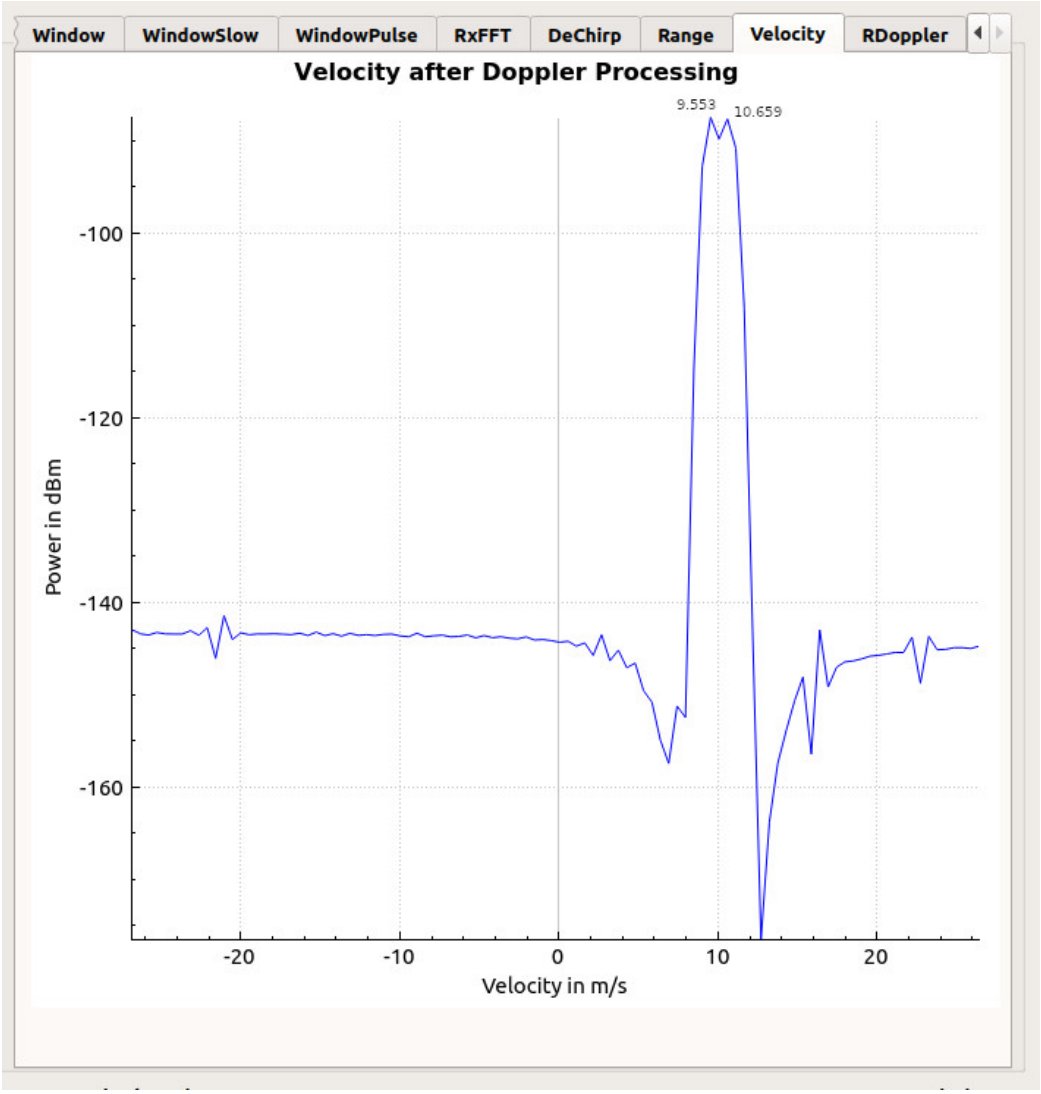

Figure 4.16: Simulated Targets Velocity Resolution In Pulse Noise CW Radar Mode

4.3 Summary

In this chapter, it was decided to operate the Radar in MCW due to the benefit of low peak power and thus improved LPI characteristics. During testing, it was discovered that de-chirping a noise signal does not provide range information. Therefore the Radar was used in Pulse CW mode for noise signals which provided range information for noise waveform since the received signal goes through a matched filter process instead of the dechirp process.

The performance of FMCW Radar was compared with that of Pulse CW Noise Radar for different tests. It was shown that noise Radar can detect targets the same as its FMCW Radar counterparts. Noise Radar

performed exceptionally well when it came to LPE characteristics with no equal in the FMCW Radar type. The noise MCW LPD characteristics are the same as that of the FMCW Radar type. In the mutual interference experiment, only the noise Radar has no ghost targets when colocated with other similar Radars. Frequency modulated Radar failed dismally with the real targets having ghost targets at different ranges and velocities. The noise Radar performance for high range resolution and high doppler resolution experiments was the same as those of the FMCW Radar type. Based on the experiments in this chapter it is clear that a noise MCW Radar provides good LPI characteristics and is free from mutual interference, can detect targets and has both high range resolution and high doppler resolution.

This chapter used simulated targets to test the performance of the Radar. The next chapter will focus on actual field experiments whereby real targets will be detected using the Radar in both FMCW mode and in Pulse CW Noise mode.

Chapter 5
H/W Implementation Of LPI AD Noise Radar

5.1 Introduction

This chapter implements in hardware the LPI AD Noise Radar at S-Band for a flying target that is within a 17 km range. The chosen H/W is the Universal Software Radio Peripheral (USRP) B210 and 25 W Power Amplifier (PA). The H/W experiment was the first setup in a H/W in the loop configuration to confirm that the H/W works as expected. Thereafter, the Radar was setup to detect cars to confirm that it works in a real environment. Further experiments with controlled targets to validate the performance of the Radar, were done by detecting humans and detecting animals. Finally, the Radar was setup to detect aeroplanes flying next to the researcher's house and eventually was used to detect a helicopter drone at a plot not too far from the researcher's house. The next section discusses the hardware (H/W) block diagram and the H/W link budget analysis.

5.2 Hardware Analysis

This section is dedicated to the analysis of the hardware used for this research, starting first with the block diagram of the Radar. An analysis of the hardware modules follows with the first focus on the antennas, the Power Amplifier (PA), USRP B210 and last but not least, the computer.

5.2.1 Hardware Block Diagram

Figure 5.1 shows the H/W block diagram of the LPI Air Defence Noise Radar. In this diagram, the USRP B210 is connected to an 8 physical core computer via Universal Serial Bus (USB) 3.0 interface. A 25W Power Amplifier (PA) is connected to the RFB: TX/RX interface of USRP B210. Transmit antenna is then connected to the output of the PA. The receive antenna is connected directly to the RFA: RX2 interface of USRP B210. The reason

for connecting transmit and receive signals on different RF blocks of USRP B210 (RF B and RF A respectively), is to reduce crosstalk between transmit and receive channels.

5.2.2 Antenna Analysis

Table 5.1 gives a list of various antenna parameters, followed by required values for each of those parameters, then the two columns for Grid antenna and LTE antenna parameter values.

Antenna selection was first informed by the frequency of operation. The frequency of operation is 2.45 GHz as motivated previously in this dissertation. The required frequency range of operation is given as 2300 MHz to 2500 MHz which makes provision for a maximum bandwidth of 200 MHz for future expansion of this Radar's capability. The two types of selected antennas, Grid antenna (Model number KB-2424-GRIDW) and LTE (Long Term Evolution) Antenna (Model number AC-D7027W08 from Asian Creation) meet this requirement as shown in the table. It must be noted that two Grid antennas and two LTE antennas were bought and only one type of antenna is used per experiment. This means that at any point in time, both TX and RX will have the same antenna type, either a Grid antenna or LTE antenna.

The next parameter of importance is the antenna beam shape with the $cosec^2$ beam shape being chosen for its ability to give a constant target detection height over a long range. A constant target detection height (beam height) of 8 km is preferred since the airborne targets around the researcher's area were all flying below this height. The researcher could not find a ready-made $cosec^2$ antenna and settled for the Grid and LTE antennas which have conical beam shapes with the target detection height which varies with radial range.

The deployment of this Radar is sector based with no continuous rotation. The more directional an antenna is, the narrower is its beamwidth and the higher the gain. For surface targets, it is important to have a narrow horizontal beam width to reduce the number of targets that are detected horizontally. Due to a small number of airborne targets flying around the researcher's house at any point in time, the horizontal beamwidth for airborne target detection must be as wide as possible and the vertical beamwidth must give a constant height as mentioned previously and have a high back angle to even increase the target detection height closer to the Radar. From the table currently under focus, it is clear that the Grid antenna is more suitable for surface targets due to its high gain and narrow horizontal and vertical beamwidths. It can however still be useful for controlled airborne targets which can be forced to fly into its narrow beams and its high gain will increase its target detection range. The LTE antenna is suitable for the detection of airborne targets due to its high horizontal and vertical beam widths but has a small target detection range due to its low gain.

Voltage Standing Wave Ratio (V.S.W.R) is a value that determines how matched the connected devices are. A high V.S.W.R implies an impedance mismatch which means most of the transmitted signal will be reflected into the transmitter and thus damage it. A V.S.W.R of less than 1.5 is chosen at an impedance of 50 Ω which means most of the transmitted signal will be transferred into the antenna. Both antennas have the correct impedance and low V.S.W.R but the one of the LTE is slightly higher with a value of 2.0 which is not too bad.

Polarisation is critical in detecting targets based on their shape. Vertical polarisation was chosen since targets of interest for the researcher are longer in the direction of the Radar. Both antennas meet the required polarisation.

The antennas are mounted on a rotator which can carry a maximum weight of 3 kg. This means each of the antennas must weight less than 1.5 kg. From the table, under focus, it is clear that the Grid antenna cannot be mounted on the antenna rotator since its weight is 3.5 kg. However, the LTE antenna is extremely lightweight with each antenna weighing only 200 g.

Even though the chosen PA is 25 W, it is a good idea to have an antenna that can handle higher power ranges to allow for future upgrades of the Radar. The required maximum power than can be handled by the antenna is 50 W and both antenna types meet this requirement.

Last but not least for antenna analysis is the wind velocity that it can tolerate. The maximum wind velocity to have ever been recorded in South Africa is 186 km/h (51.67 m/s) [37]. Based on this value, the required rated wind velocity was set at 60 m/s and both antenna types met this requirement.

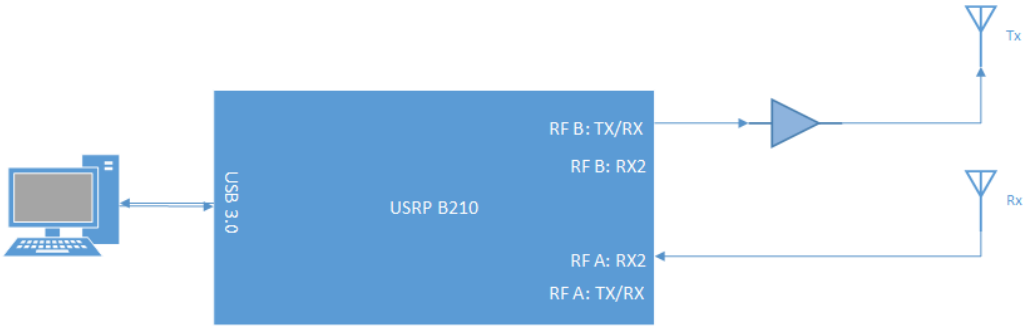

Figure 5.1: H/W Block Diagram Of LPI AD Noise Radar

No.	Category	Required Antenna	Grid Antenna	LTE Antenna
1.	Beam shape	$cosec^2$	conical	conical
2.	Frequency Range (MHz)	2300-2500	2300-2500	698-960/1710-2700
3.	Horizontal Beam Width	10^o / 180^o	10^o	68^o
4.	Vertical Beam Width	70^o back angle	14^o	58^o
5.	Beam height	Constant 8 km	Varies with radial range	Varies with radial range
6.	Polarisation	Vertical	Horizontal & Vertical	Vertical
7.	V.S.W.R	≤ 1.5	≤ 1.5	≤ 2.0
8.	Gain	≥ 30 dBi	24 dBi	5/7 dBi
9.	Radiation	Directional	Directional	Directional
10.	Weight	$\leq 1\ 500$ g	3 500 g	200 g
11.	Maximum Power	≥ 50 W	100 W	50 W
12.	Impedance	50Ω	50Ω	50Ω
13.	Rated Wind Velocity	60 m/s	60 m/s	60 m/s

Table 5.1: Required versus Actual Antenna Characteristics for Airborne Targets

5.2.3 Power Amplifier

In chapter 3 it was shown that 25 W is adequate for the maximum unambiguous range for this Radar. The chosen amplifier is the BBM3K5KEL (SKU 1117) from Empower RF Systems Inc. which has a frequency range of 500 - 2500 MHz at 25 W output power.

5.2.4 USRP B210

The USRP B210 has a frequency range of 70 MHz to 6 GHz. With a bandwidth of 25 MHz for transmitting and receiving concurrently at 32 bits per sample, each one-way link requires at least 800 Mb/s leading to a full duplex link of 1.6 Gb/s which can easily be handled by the USB 3.0 interface that has a maximum throughput of 5 Gb/s.

The Agilent N5182A MXG Vector Signal Generator with a frequency range of 100 kHz to 6 GHz, together with the SDR Console software version 3.1 build 2320 was used to characterise USRP B210. SDR Console soft-

ware makes provision for predetermined bandwidth for B210 and the closest bandwidth to 25 MHz was 28 MHz. A 28 MHz bandwidth LFM signal was generated in Matlab version R2021b. The generated 3 172 complex double samples were converted into signed integer two columns I and Q matrix whose values were scaled to be within the range of -32 768 to 32 767 as per the requirement of the N5182A. This matrix was then saved into a text file and uploaded into the N5182A using the Keysight N7622C Signal Studio Toolkit 2022 version 3.0.0.0. This toolkit handles all the conversion from the little-endian byte format of the Intel processor computer to the big-endian byte format required by the N5182A and saves it in binary format inside the N5182A.

N5182A was tuned to transmit a signal of 2.45 Gz at a signal level of -16 dBm. The RF output of N5182A was connected to the B210 RFA: RX2 port. SDR Console was configured to use B210 and tuned to 2.45 GHz with a bandwidth of 28 MHz. The RF output of N5182A was enabled but its modulation feature was kept disabled. A screenshot of the received signal is shown in figure 5.2. From this figure, the measured noise floor (MeasuredNoiseFloordBm) is -92.00 dBm.

The receiver sensitivity or Minimum Detectable Signal (MDS) is determined by adding the measured noise floor of -92.00 dBm to the computed minimum SNR from chapter 3 of 21.18 dB, to get -70.82 dBm. The measured noise floor is obtained from figure 5.2 and it is clear that three of the noise floor markers round up to -92.00 dBm.

Real Noise Figure (RNF) is the next parameter which must be computed. At room temperature, computed thermal noise for 1 Hz bandwidth is given by k$T_0 = 1.38 \times 10^{-23} * 290.00 * 1000 = -173.98 \frac{dBm}{Hz}$. Since the B210 is tuned to a bandwidth of 28 MHz via SDR Console, its bandwidth in dB ($SDRC_{BWdB}$) is 74.47 dB. Real Noise Figure can thus be computed as follows: RNF = MeasuredNoiseFloordBm - kT_{0dBm} - $SDRC_{BWdB}$ = 7.51 dB. This value is inline with the specified B210 Noise Figure which is indicated as better than 8 dB.

Only a maximum of -15 dBm is allowed into any of the B210 Rx ports. To allow a small margin of safety, the N5182A output signal level was set to -16 dBm so that it is 1 dB below the maximum allowed signal level. Figure 5.2 shows the carrier signal level to be -16.70 dBm and the strongest spurious signal level of around -90.00 dBm. Subtracting -90.00 dBm from -16.70 dBm results in 73.30 dBc Spurious Free Dynamic Range (SFDR) which is very close to the specified B210 SFDR of 78 dBc.

The downloaded waveform was selected for output inside the N5182A with modulation and RF output enabled. The screenshot of the received signal inside the B210 is shown in figure 5.3. This shows that the B210 is capable of receiving a signal with 28 MHz bandwidth.

This sub-section showed that the measured performance characteristics of USRP B210 are very close to the specified values.

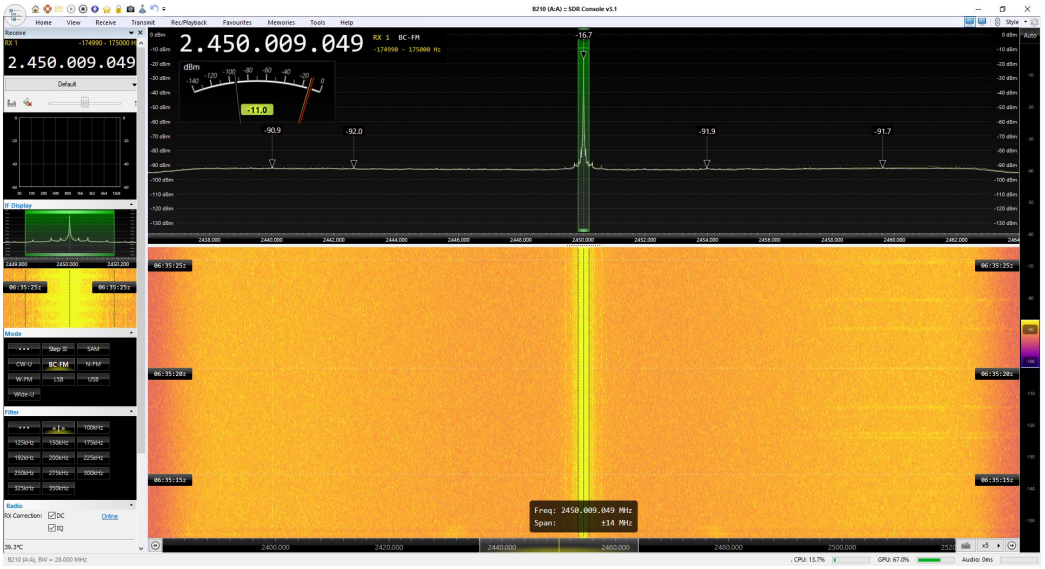

Figure 5.2: USRP B210 Noise Floor For 28MHz Bandwidth With Carrier Signal Only At -16 DBm

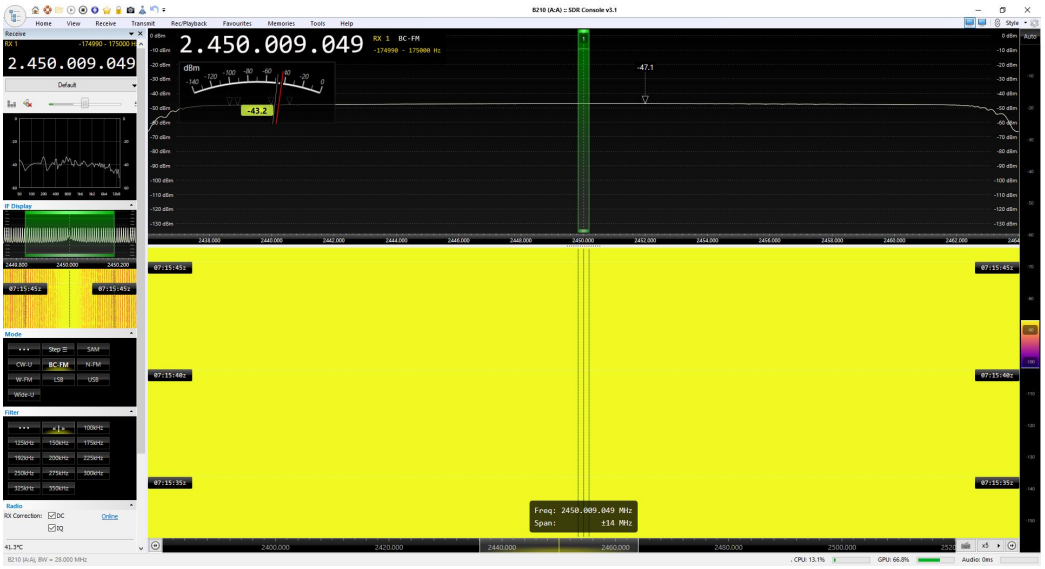

Figure 5.3: USRP B210 28MHz Bandwidth Signal At -16 DBm

5.2.5 Computer

The computer used was packaged together by the researcher. The critical feature was to have Random Access Memory (RAM) of at least 16 GB. Since a maximum of thirteen threads are used concurrently in the software, ideally sixteen cores are required to make sure each of these threads runs on its core. Due to budget constraints, a Central Processing Unit (CPU) of 8

cores and 16 threads was utilised. In future, some of the processing will be moved to the Graphical Processing Unit (GPU).

5.3 Hardware In The Loop Simulation

The previous chapter simulated the LPI AD Noise Radar without any hardware in the loop. This was good to confirm that all the software related to the Radar works as expected. The software that works in a pure simulation environment without any H/W will not necessarily work when integrated with H/W. Some of the issues that the researcher had to deal with were timing between the B210 and the PC to make sure samples are transmitted and received in full as and when required, and how many samples can the B210 handle in full-duplex without crashing and cross-talk. H/W in the loop simulation is critical before deploying the Radar to make sure the H/W and S/W still work well together since it will be a waste of time to discover that the Radar is not working after the Radar is already setup at the test site.

5.3.1 Test Setup For H/W In The Loop Simulation

The same software used for pure simulation in the previous chapter is used for H/W in the loop simulation, with the change being that the B210 H/W is selected and the option to simulate targets via the SDR is selected as well. The first three targets from table 4.1 are simulated and transmitted via the selected TX/RX port of B210. The phase and range of each simulated target are changed for every pulse in line with its velocity before the signal is transmitted. The Radar is tested in FMCW mode followed by the Pulse CW Noise Radar mode. This is in line with the experiment done in the previous chapter whereby the performance of FMCW Radar was compared with that of Pulse CW Noise Radar.

The received signal goes through the same signal processing chain that a signal received via the antenna from a real target will go through. The entire process of transmitting and receiving the signal is the same one used for detecting real targets and the only difference is that targets are induced and their range and motion changed in the transmit signal. Therefore, after this experiment, the only delta between the H/W in the loop simulation and the Radar configured to detect real targets are the cables connecting the SDR to the PA and antennas, the PA, the antennas and finally how the antennas are positioned both vertically and horizontally.

To test mutual interference, the S/W was run under the same H/W setup with the first ghost target from table 4.2 injected into the received signal and with no other simulated targets. This test was run for FMCW Radar mode and repeated for Pulse CW Noise Radar mode. The results were compared with theoretical expectations and those from the previous chapter.

Figure 5.4 shows the H/W in the loop setup with a 30 dB attenuator

connected between the TX/RX of channel A and RX2 of channel B. The reason for using RX2 of channel B and not of channel A is to reduce the crosstalk between TX and RX paths. The gain on the receiver was also set to zero which also led to a further reduction in crosstalk.

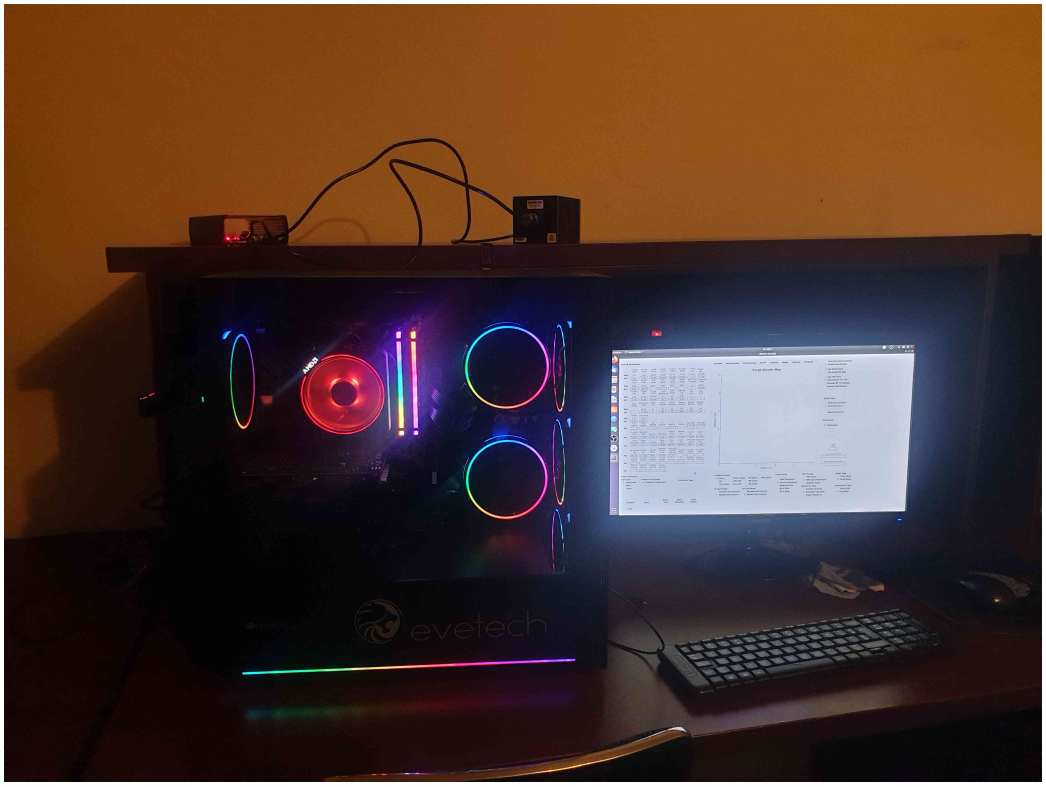

Figure 5.4: H/W In The Loop Setup

5.3.2 Experimental Results And Analysis For H/W In The Loop Simulation

Figure 5.5 shows the Range Doppler map of FMCW Radar target detection for H/W in the loop simulation. The outcome shows that the FMCW Radar works as expected even when the signal goes through the SDR H/W. Figure 5.7 shows similar results for the Range Doppler map of Pulse CW Noise Radar. It has thus been proven that the integrated S/W and H/W for FMCW Radar and Pulse CW Noise Radar work as expected. For both tests, the simulated target is detected at a range of 1000m with a velocity of -220 m/s which is inline with the first target in table 4.1.

The results of mutual interference are shown in figures 5.6 and 5.8 for FMCW Radar mode and Pulse CW Noise Radar mode respectively. As expected from the theory and simulated results of the previous chapter, the ghost target at a range of 1500m with a velocity of -210 m/s is visible for FMCW Radar mode and it is suppressed for Pulse CW Noise Radar mode. The target parameters of the ghost target detected in FMCW Radar mode

are the same as those shown in table 4.2. Once again it has been shown that Noise Radar suppresses ghost targets whereas FMCW Radar displays ghost targets and thus increases its false alarm rate.

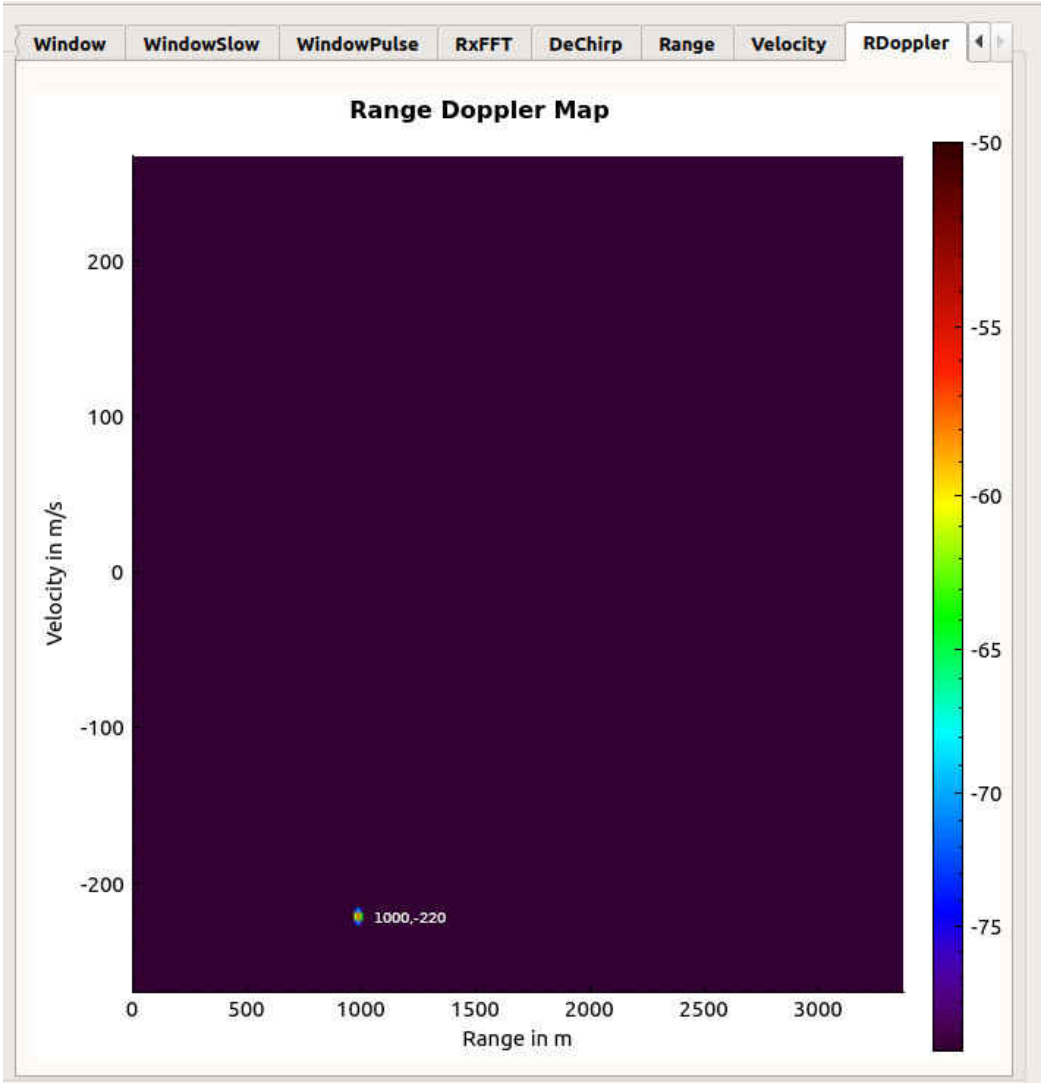

Figure 5.5: H/W In The Loop FMCW Target Detection

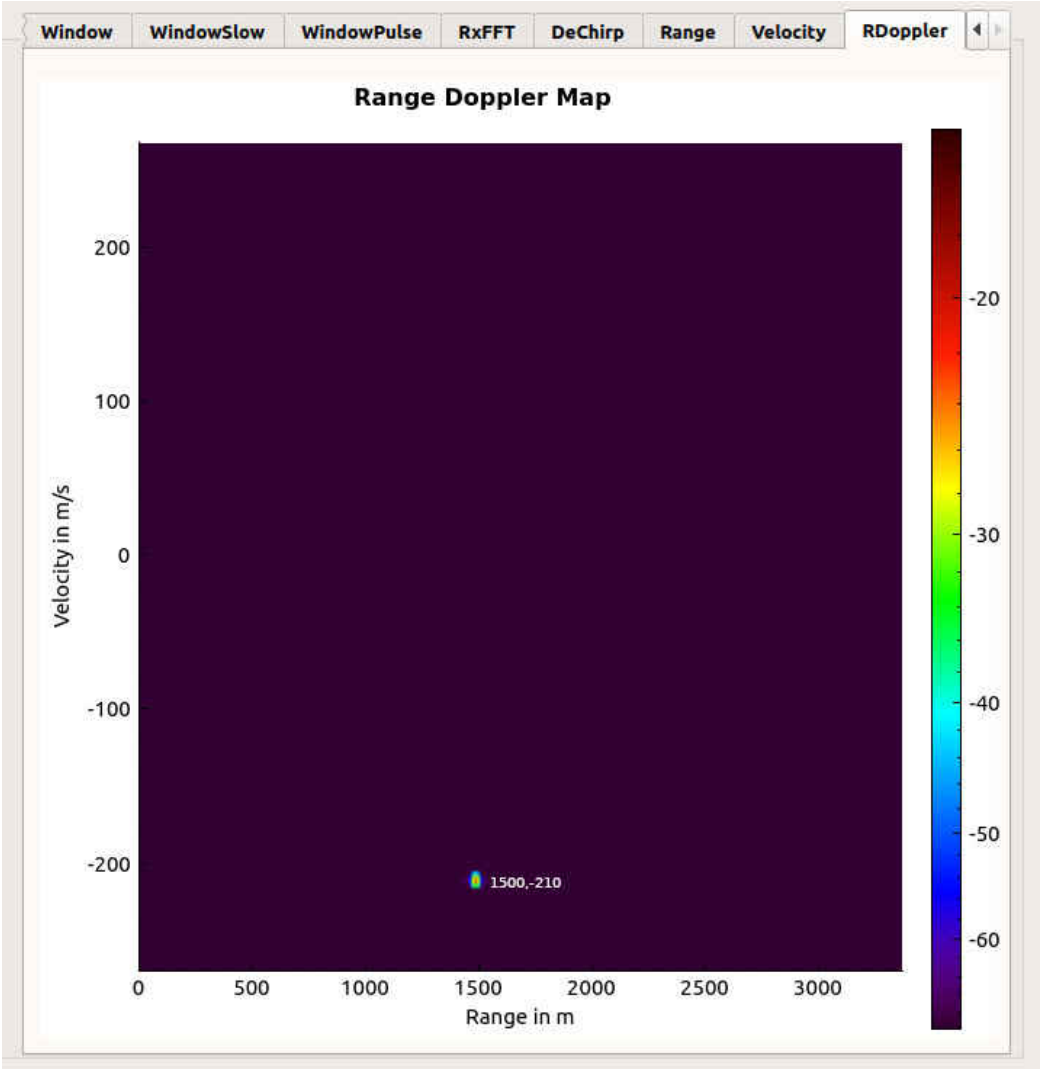

Figure 5.6: H/W In The Loop FMCW Target Detection With Ghost Target Only

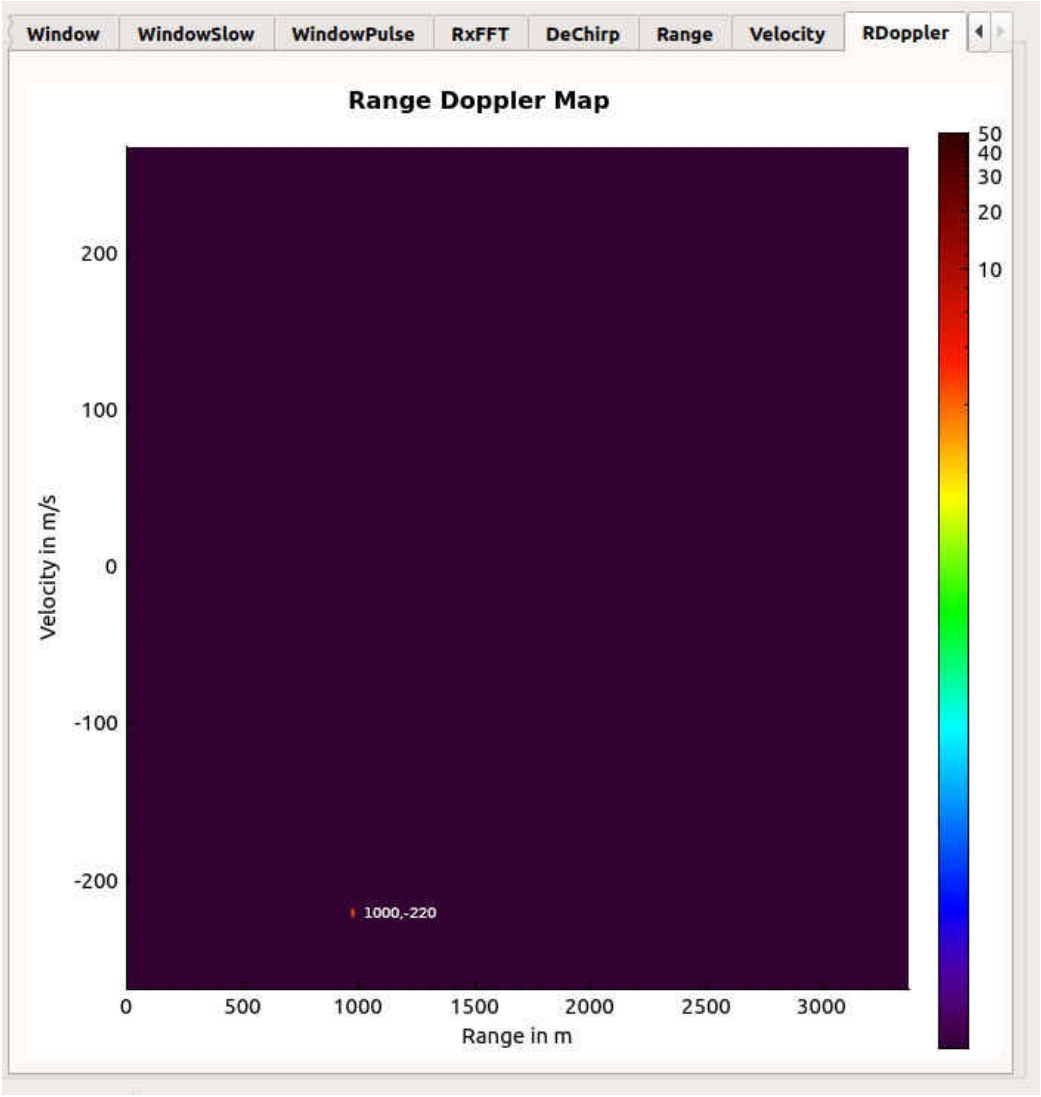

Figure 5.7: H/W In The Loop Pulse CW Noise Target Detection

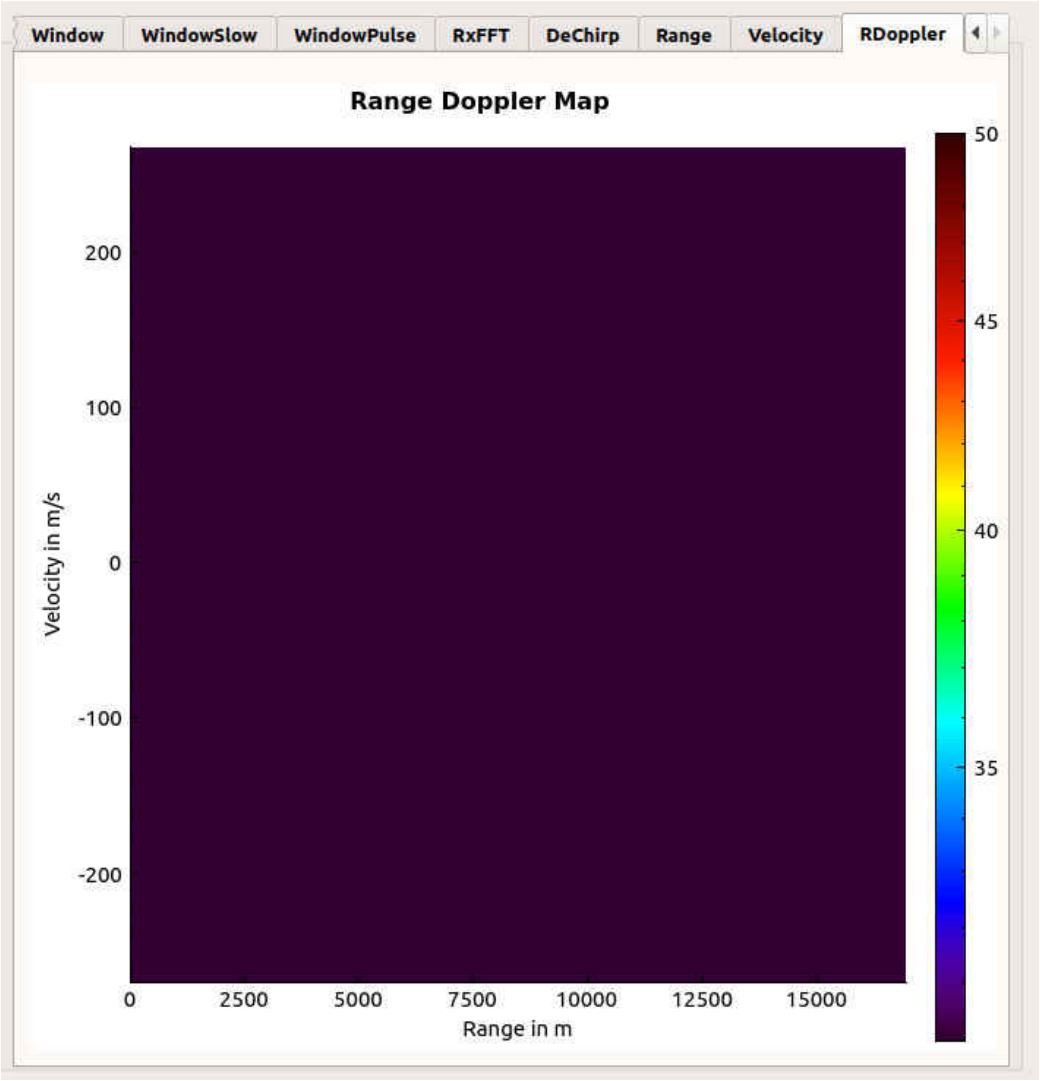

Figure 5.8: H/W In The Loop Pulse CW Noise Target Detection With Ghost Target Only Suppressed

5.4 Detection Of Cars

The previous section tested the SDR that was integrated with S/W but the antennas were not connected and there was no detection of real targets. In this section, the Radar is used to detect cars which are almost always available in the area behind the researcher's house which makes it easier to confirm the functioning of the Radar. There is a surveillance camera illuminating the same area pointed to by the Radar and thus serves as a confirmation sensor. The purpose of this experiment is to confirm that the Radar can detect surface targets and provide realistic ranges and velocities of these targets for both FMCW and Pulse CW Noise Radar mode.

5.4.1 Test Setup For The Detection Of Cars

The cars to be detected are passing on the main road behind the researcher's house and the road happens to be busy 24 hours a day which makes it easy to perform the tests any time of the day. The researcher performed the experiments in the early hours of the morning when the cars are fewer and it is easier to determine which cars are detected. Two grid antennas are mounted on a T mast as shown in figure 5.9 and they are 5 m above the ground and their antenna feeds are 2 m apart horizontally. TX and RX cables of 10 m each with 0.2 dB loss per meter resulting in 2 dB loss for each 10-meter cable are used. These TX and RX cables are connected to the output of the 25 W PA and RX 2 port of B210 respectively as shown in figure 5.10. For the surface Line Of Site (LOS) of about 300 m at this location, the 25 W PA is overkill but the researcher decided to use it in any case so that when deploying to detect airborne targets there are very minimal changes to the setup.

At first, the Radar was configured with default values and thereafter optimised for the targets of interest. The optimisation involved changing the velocity axis to 15% of the maximum velocity of 270 m/s which resulted in a displayed maximum velocity of 40.5 m/s which is equivalent to 145.8 km/h. No car is expected to exceed 145.8 km/h on this road since the speed limit is 80 km/h and there is a traffic light which forces the cars to slow down when approaching it. The range axis was also scaled to display only 2.5% of the maximum unambiguous range of 16.98 km which resulted in a displayed maximum range of 424.5 m. It must be noted that changing the scaling only affects what is displayed and not the actual maximums. In this case, regardless of the chosen scaling factor, the maximum unambiguous velocity and maximum unambiguous range are still 270 m/s and 16.98 km respectively in line with the chosen PRF and PRI. The number of pulses was changed to 1024 to improve the velocity resolution to a value of 0.53 m/s. The Radar was again run in FMCW mode and Pulse CW Noise mode and the results were compared. Since the Radar is detecting real moving targets, it is not possible to compare the same targets with each other but a general comparison of different targets was done to get an idea of the performance of each Radar mode.

Taking the experiment further to test for mutual interference, the first Ghost target from table 4.2 was injected into the received signal for both FMCW Radar mode and Pulse CW Noise Radar mode. The results were analysed and compared with the expected results.

Figure 5.9: Antenna Setup For Car Detection

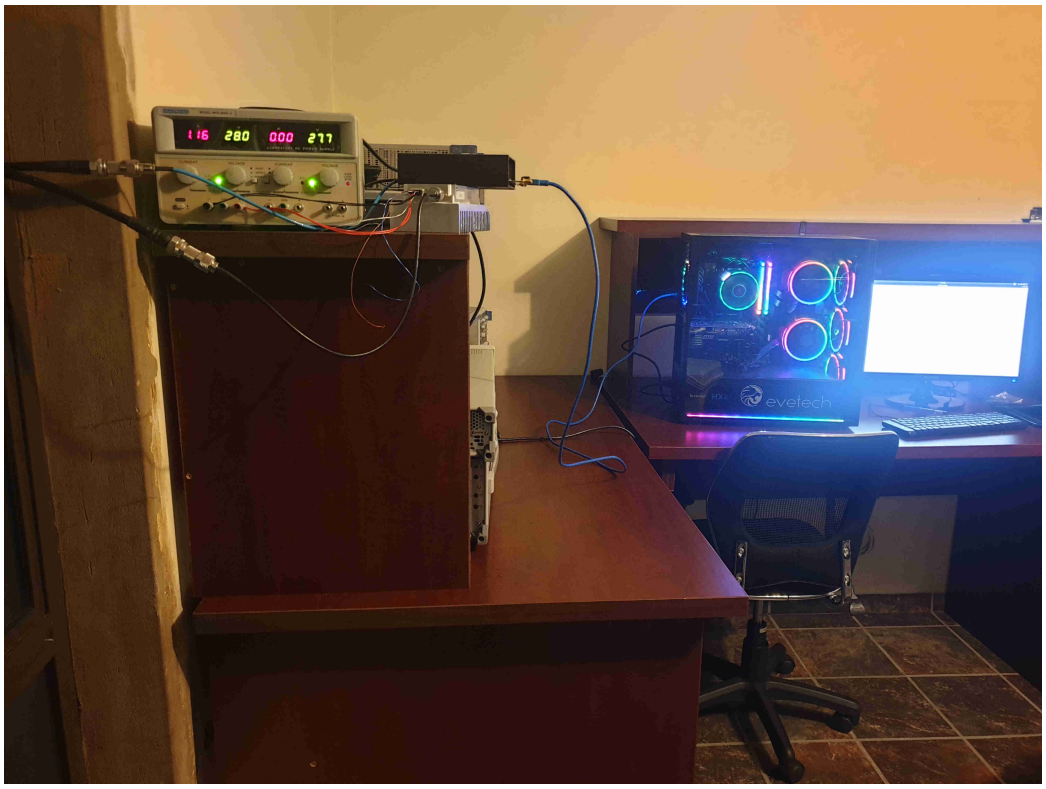

Figure 5.10: SDR Setup For Target Detection

5.4.2 Experimental Results And Analysis For The Detection Of Cars

The Radar was run for several hours split between FMCW Radar mode and Pulse CW Noise Radar mode. At different times the performance of the Radar was compared with the surveillance camera display to confirm that what the Radar displayed is in line with what was shown from the surveillance camera. Figure 5.11 shows a Range Doppler map of a target moving towards the Radar at a velocity of about -18 m/s or -64.8 km/h for FMCW Radar mode. The same results for Pulse CW Noise Radar mode are shown in figure 5.13 with three cars moving away from the Radar.

Since the injected ghost target is at a range of 1 500 m and has a velocity of -220 m/s, the range axis scaling was changed to 10 %, leading to a displayed maximum range of 1 698 m and the velocity axis scaling was changed to 100 % and thus displaying the maximum velocity of 270 m/s. The results of mutual interference are shown in figure 5.12 for FMCW Radar mode and figure 5.14 for Pulse CW Noise Radar mode. For FMCW Radar mode the ghost target can be seen at a range of 1 500 m with a velocity of -220 m/s together with two cars moving away from the Radar, whereas for Pulse CW Noise Radar mode only the real targets are visible being one car moving away from the Radar. Once again it has been proven that Noise Radar is

immune to mutual interference problems and can share the spectrum with other Noise Radars using the same frequency and thus leading to efficient use of the electromagnetic spectrum.

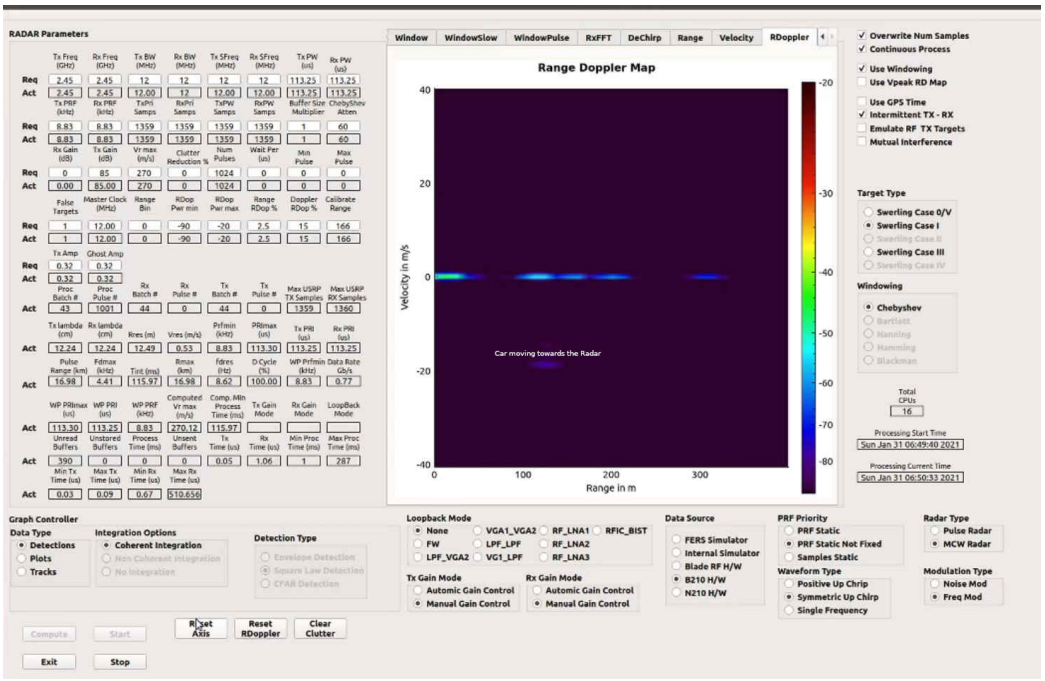

Figure 5.11: FMCW Radar Mode Car Detection

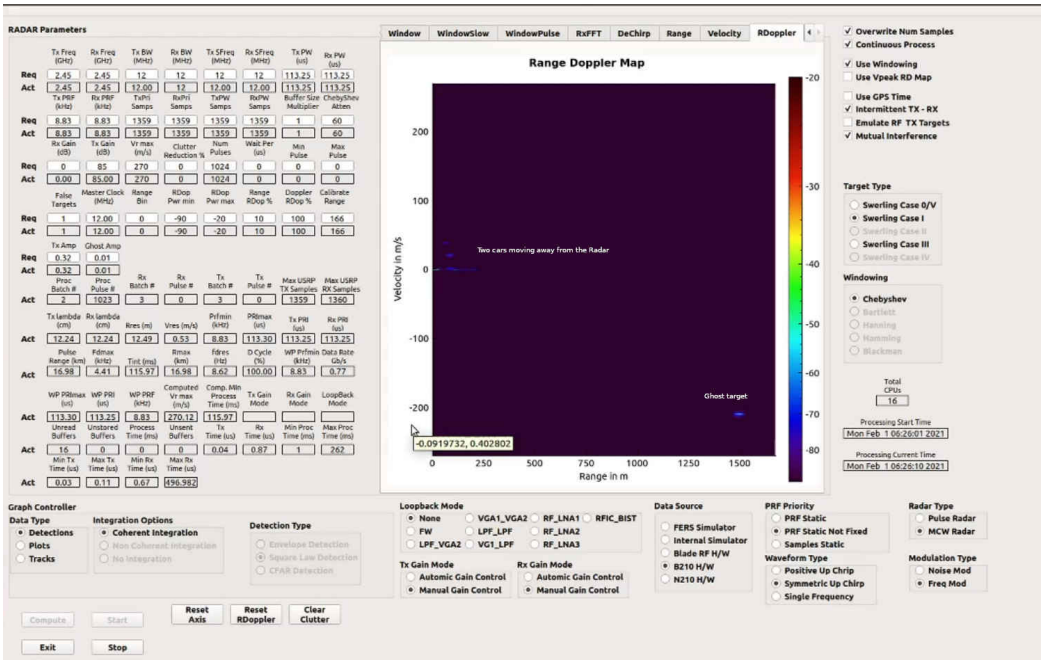

Figure 5.12: FMCW Radar Mode Car Detection With Ghost Target

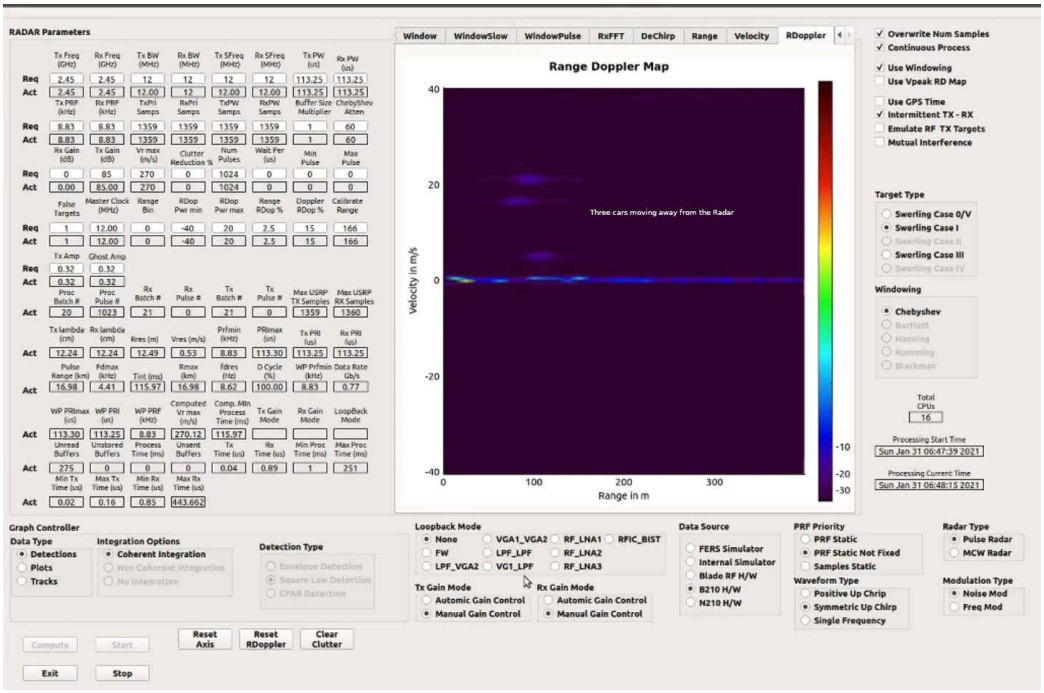

Figure 5.13: Pulse CW Noise Radar Mode Car Detection

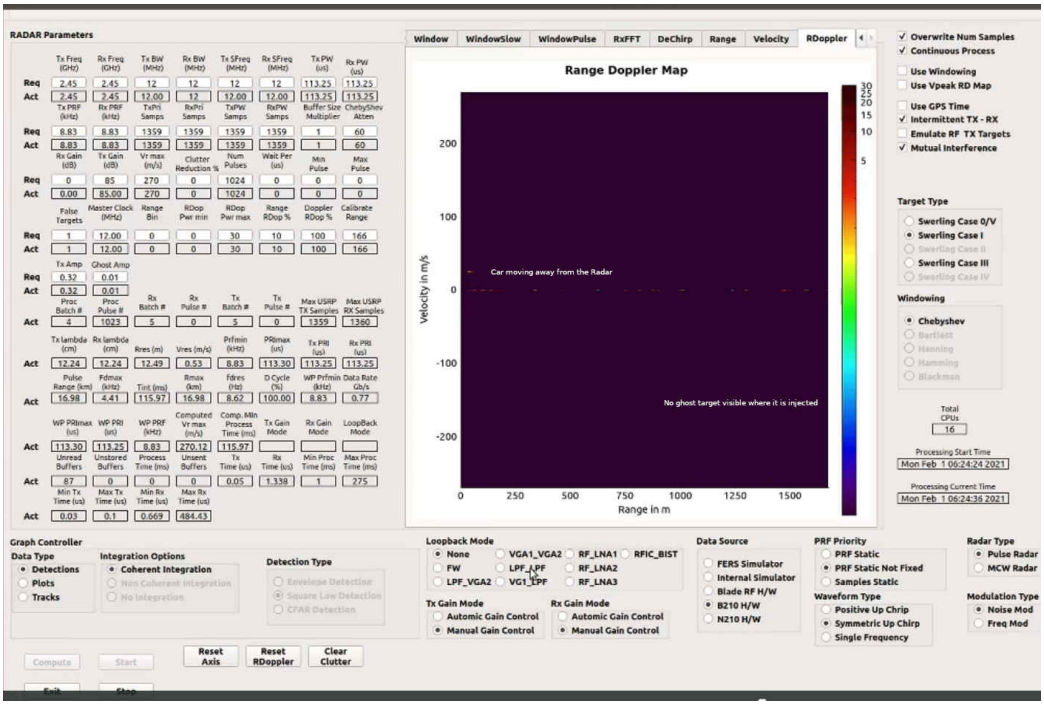

Figure 5.14: Pulse CW Noise Radar Mode Car Detection With Ghost Target Not Visible

It has thus been shown that the performance of the two Radar modes for real targets is as expected and inline with the results obtained for the

simulation experiment. The time spent doing the simulation was extremely valuable since it ensured that most of the bugs were fixed before the Radar was deployed to detect real surface targets. The H/W in the loop simulation also ensured that all the H/W and S/W integration issues are resolved before the detection of real targets is performed.

5.5 Detection Of Airborne Targets

This section deals with the main experiments for LPI Air Defence Noise Radar. It directly speaks to the main topic of this research by detecting airborne targets using Noise Radar and thus proving that Noise Radar can be used as LPI Air Defence Radar. The previous experiments of simulation, H/W in the loop simulation and detection of surface targets were necessary to make sure most performance issues are resolved before detecting airborne targets since they are not always available and it will thus be time-consuming to debug a Radar with targets that are not persistently available.

The researcher's house is surrounded by three airports, one to the north at a radial range of 18 km, the other one in the southwest direction with a radial range of 37 km and the last one in the southern direction with a radial range of 36 km. The Radar is setup in the same location that was used for the detection of cars behind the researcher's house with the antennas facing southwest and the elevation angle chosen such that airborne targets with a radial range of 5 km and a height range of 2.6 km to 4.4 km can be detected. These values were arrived at after analysing the airborne traffic around the researcher's house using FlightRadar 24.

The airborne targets are detected in FMCW Radar mode and again in Pulse CW Noise Radar mode and the results are compared with those from FlightRadar 24. The experiments are again repeated with ghost targets injected in the received signal for the two Radar modes and the results are compared with those from FlightRadar 24.

5.5.1 Test Setup For The Detection Of Airborne Targets - Phase 1

Figure 5.15 shows the antenna setup for the detection of airborne targets. The same grid antennas which were used for the detection of surface targets are used here and they have 14^o vertical beam width and 10^o horizontal beam width and a gain of 24 dBi. Several hours were spent analysing airborne traffic around the researcher's house to determine the typical radial range, absolute velocity and target height at the range of interest. It was discovered that once in a while there are airborne targets that fly at a radial range of 5 km from the researcher's Radar, South West of the researcher's Radar with an azimuth angle of 254^o and with a height range of 2.6 km to 5.2 km. Notice that the antenna beam height allows the Radar to reach a

maximum height of 4.4 km at this range instead of the required 5.2 km. This problem will be elaborated on further in this research. Figure 5.18 shows the antenna azimuth direction for the detection of airborne targets, whereas figure 5.16 shows the diagram used to calculate the antenna elevation angle for the detection of airborne targets.

From figure 5.16, it is clear that the diagram consists of three triangles, two of which are right-angled. The calculations are done using the sine equation for right-angled triangles which is $sin(\theta) = \frac{O}{H}$ and the arc tan equation for right-angled triangles which is $\theta = atan\frac{O}{A}$. Since the adjacent (A) value is known which is 5 km, and the opposite (O) value is known which is 2.616 km and is the minimum airborne target height at a radial range of 5 km, the antenna elevation angle is computed using the arc tan equation and it comes to a value of 27.62^o. Figure 5.17 shows the actual antenna elevation angle after deployment. The top triangle in figure 5.16 has an angle of 14^o which is the antenna elevation beam width. The opposite angle of the largest right-angle triangle in figure 5.16 is obtained by adding the antenna elevation angle and the antenna beam width which is: $27.62^o + 14.00^o = 41.62^o$. Using the cosine equation for right-angled triangles which is $cos(\theta) = \frac{A}{H}$, the hypotenuse of the large triangle is obtained which is 6.66888 km. The maximum detectable target height (O), is obtained by using the sine equation for a right-angled triangle since the opposite angle and the hypotenuse value of the large right-angled triangle are known. The maximum detectable target height comes to 4.443 km. Subtracting the minimum detectable target height from the maximum detectable target height leads to a value of 1.826 km, which is the antenna beam height.

The connection of the SDR, PA and PC is the same as shown in figure 5.10 for the detection of surface targets. The default parameters are mostly left as is which allows the Radar to detect targets up to 17 km and with a maximum velocity of 270 m/s. Airborne targets are not close to each other and the transmit and receive band widths were both reduced to 2 MHz and thus resulting in a range resolution of 74.95 m. The receiver and transmitter sampling frequencies were aligned to their respective reduced band widths of 2 MHz. Since the time on target is determined based on the time required for the target with the highest speed to leave half the range bin, increasing the range bin to 74.95 m resulted in the integration time increasing to 138.79 ms and thus to 1 229 number of pulses without the number of pulses being overwritten by the operator as was the case for surface target detection where the operator manually increased the number of pulses to 1024. This resulted in a velocity resolution of 0.44 m/s. The experiment for the detection of airborne targets is done for FMCW Radar mode and repeated for Pulse CW Noise Radar mode. OBS Studio S/W is used to record the detection of targets. The Radar is run for several hours to detect several targets.

During the period of experimentation, some of the experiments include the test for mutual interference and spectrum sharing. In this test, as it was done for surface targets, the first ghost target from table 4.2 is injected into

the received signal for both FMCW Radar mode and Pulse CW Noise Radar mode. The results are also recorded using OBS Studio and compared with those from FlightRadar 24 for the same time the targets were detected.

Figure 5.15: Antenna Deployed For Airborne Targets Detection

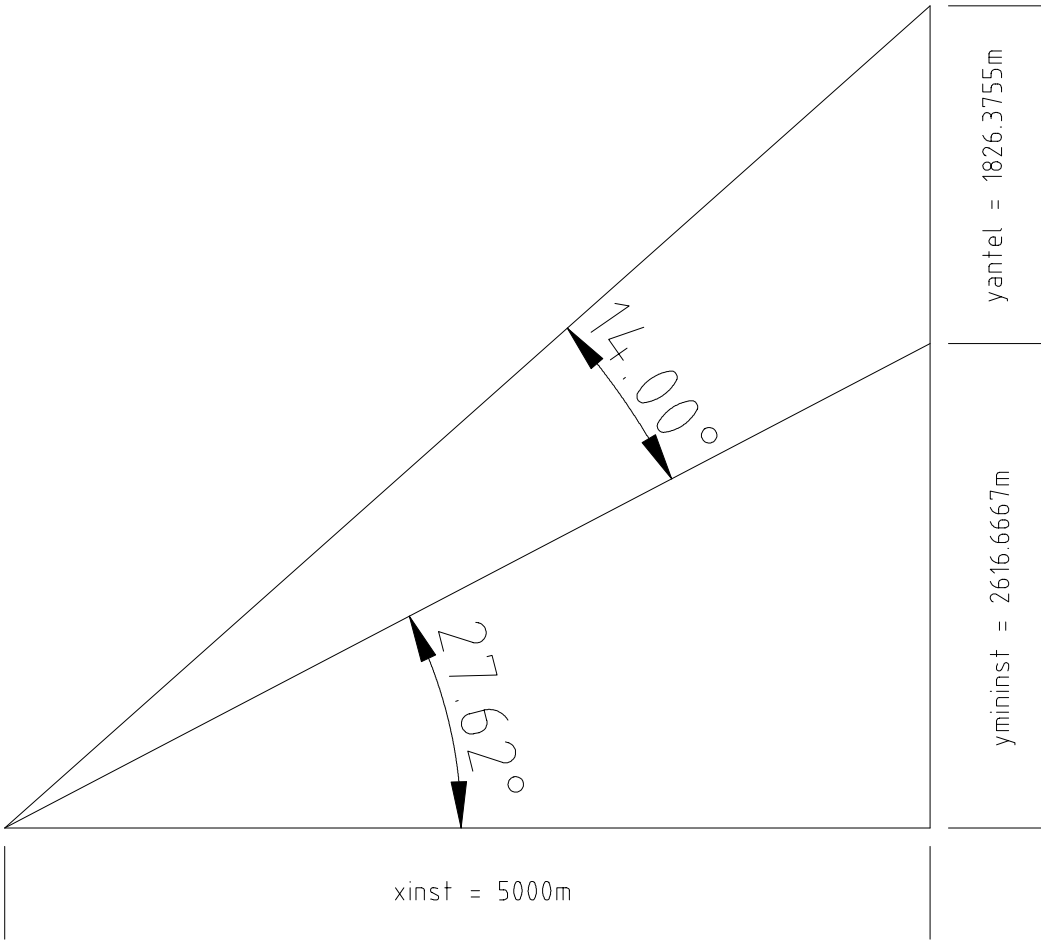

Figure 5.16: Airborne Antenna Position Diagram

Figure 5.17: Antenna Elevation Angle For Airborne Targets Detection

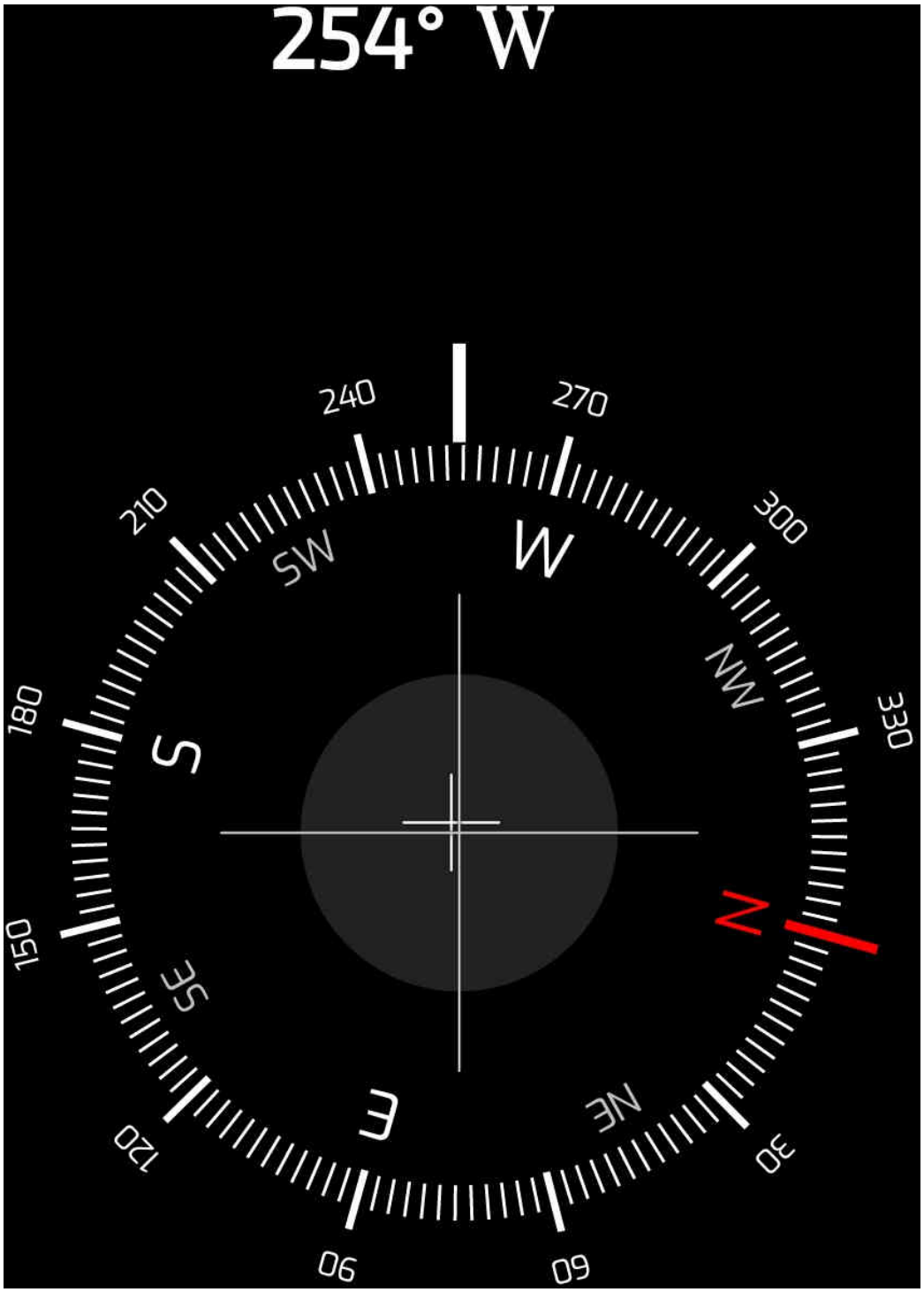

Figure 5.18: Azimuth Antena Position For Airborne Targets Detection

5.5.2 Test Setup For The Detection Of Airborne Targets - Phase 2

The detection of airborne targets in phase 1 did not yield desired results as explained below. Even though the ideal antenna for the detection of airborne targets is a $cosec^2$ antenna as described in the phase 1 results below, the researcher decided to get antennas with larger elevation and azimuth beam widths to increase the coverage volume and thus improve the probability of intercepting the airborne targets. The antennas that were used are Asian Creation antennas with model number AC-D7027W08, a frequency range of 698-960 / 1710 - 2700 MHz. They have vertical beam width and horizontal beam width of 58^o and 68^o respectively and a gain of 10 dB in the frequency range of 1710 - 2700 MHz. The 10 dB antenna gain reduces the maximum detectable range for a $3m^2$ target from 18.840 km with a 24 dB antenna gain to 3.75 km in FMCW Radar mode with 1024 integrated sweeps.

The two antennas were mounted on an improvised antenna tower, made from a 1.5 m x 1.5 m x 6.4 m scaffold as shown in figure 5.19. The advantage of this tower is that it is very spacious and easily climbable without requiring any special climbing skills and if necessary, the RF cable losses can be drastically reduced by working on top of the tower right next to the antennas. These antennas are mounted horizontally 2 m apart on a T mast of 1 m length as shown in figure 5.20. In this picture, the antennas are not yet adjusted in elevation to point at airborne targets. An opened LTE antenna is shown in figure 5.21. The T mast is connected to the antenna positioner, RCA model number VH226E (visible at the bottom of the picture) which allows the antenna to rotate 360^o in azimuth. The azimuthal rotation allows the researcher to point the antennas in the direction of the incoming aeroplanes from any direction around his house without having to climb the antenna tower and rotate it manually. Figure 5.22 shows the antenna rotator before installation. In the middle of the picture is a wireless camera that is used to confirm that the Radar is detecting the correct targets. The camera is EZVIZ C3W and it is not expected to detect airborne targets kms away but it was used for confirmation that the Radar is working fine when it detected cars for hundreds of meters.

Figure 5.19: Antenna Tower Deployed For Airborne Targets Detection Phase 2

Figure 5.20: Antennas, T Mast, Camera And Rotator Deployed For Airborne Targets Detection Phase 2

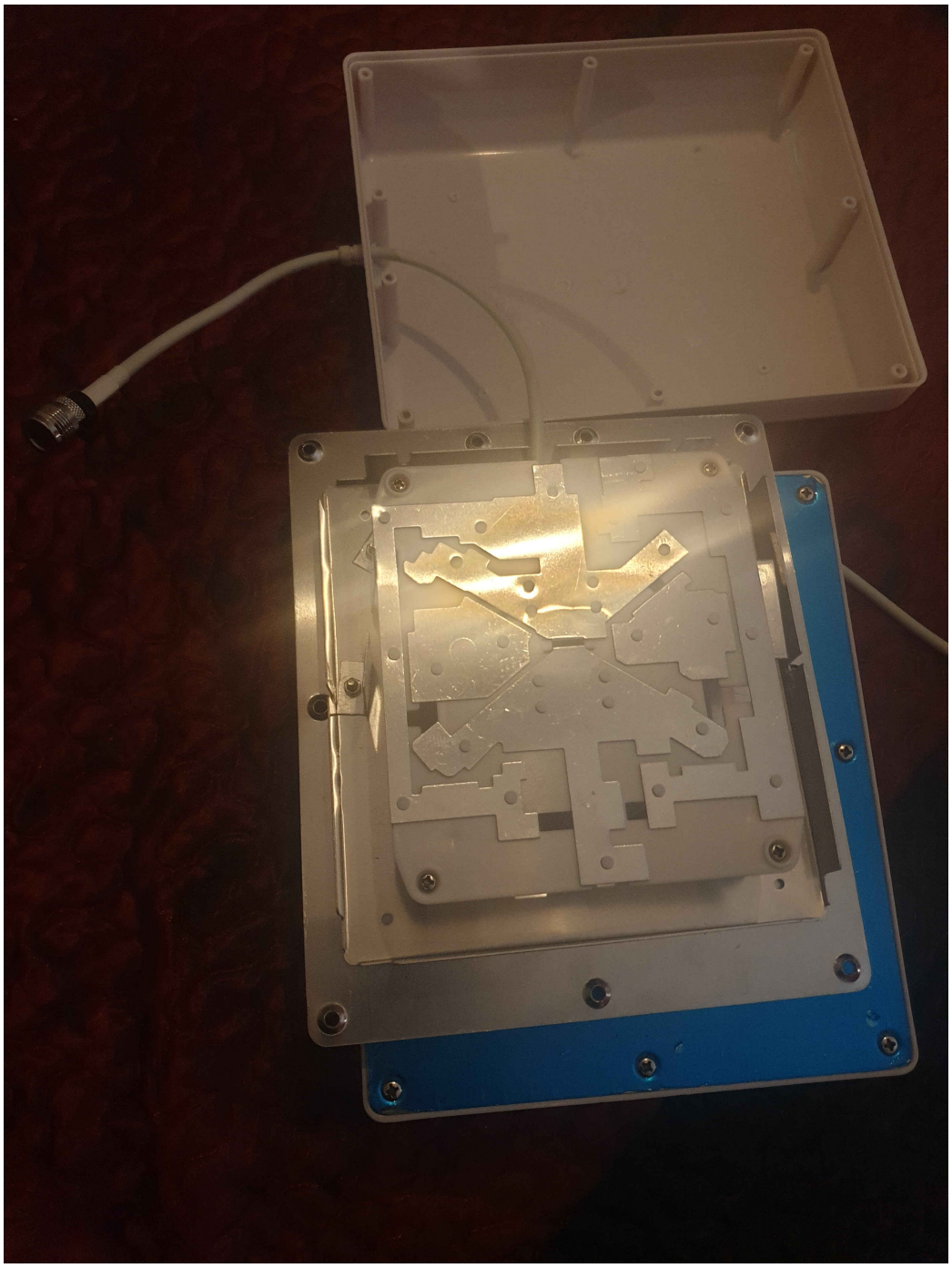

Figure 5.21: Opened LTE Antenna

Figure 5.22: Antenna Rotator Before Installation

Figure 5.23 shows the maximum detectable target height of 13.896 km and a corresponding minimum detectable target height of 1 km at a radial range of 2.5 km for a 3 m^2 target detection with the integration of 196 sweeps. This shows that all targets flying at or above 1km height at the maximum detectable target range of 2.5 km will be detected, which is a serious improvement from the phase 1 experiment. The minimum target height of 1 km was chosen because all the observed aeroplanes from FlightRadar 24 flying at the range of 2.5 km around the researcher's house were flying above 1 km height. The required antenna elevation was computed to be 21.8^o and it is visible in the diagram. At the radial range of 1.7 km, the minimum detectable target height is 680 m and the maximum detectable target height is 9.450 km. The new setup has drastically improved the probability of detecting airborne targets around the researcher's house.

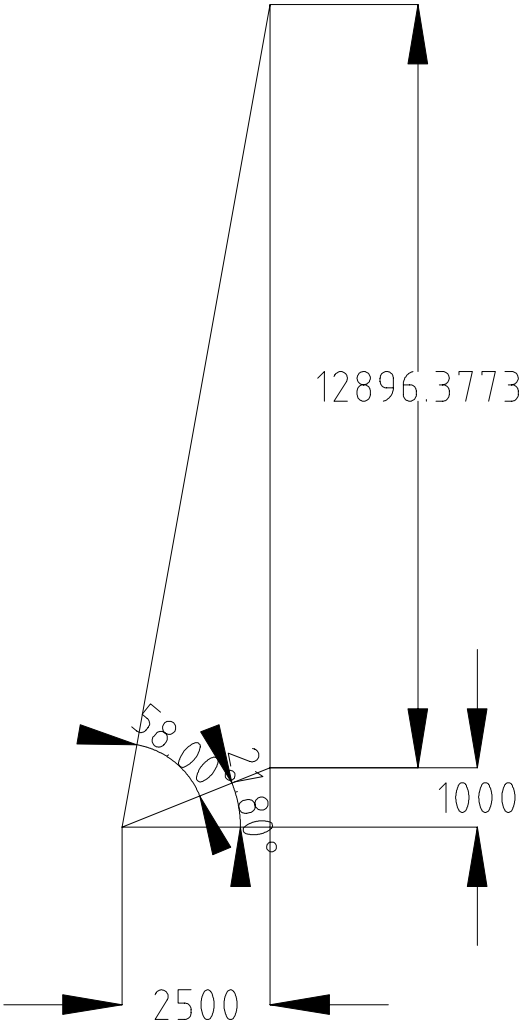

Figure 5.23: Antenna Elevation For Airborne Targets Detection Phase 2 In Meters

The experiment for the detection of airborne targets is done for FMCW Radar mode and repeated for Pulse CW Noise Radar mode. OBS Studio S/W is used to record the detection of targets. The Radar is run for several

hours to detect several targets. During the period of experimentation, some of the experiments include the test for mutual interference and spectrum sharing. In this test, as it was done for phase 1 of airborne targets, the first ghost target from table 4.2 is injected into the received signal for both FMCW Radar mode and Pulse CW Noise Radar mode. The results are also recorded using OBS Studio and compared with those from FlightRadar 24 for the same time the targets were detected.

5.5.3 Test Setup For The Detection Of Airborne Targets - Phase 3

The detection of airborne targets in phase 2 also did not yield desired results as explained below. The researcher then decided to have a more controlled test of airborne targets by using drones. A colleague of the researcher wanted to demonstrate a prototype helicopter drone with a 29cc engine, 1400cc fuel tank and 1200cc/hour average fuel consumption. The reason for choosing the helicopter drone is that its range and height can be controlled by the pilot until the Radar detects it.

The Radar was setup with no amplifier connected, antennas 2 meters apart, using a USRPB210 with a range resolution of 47.89 m since the USRP B210 was detected as a USB 2.0 device instead of a USB 3.0 device. The transmit gain was set to 89.3 dB whilst the receive gain was set to 40 dB. The two grid antennas previously used for the detection of cars were used and their elevation was set to 0^o. Figure 5.25 shows the entire H/W setup. In the same picture, stones used to keep the antennas and screens stable can be seen since it was a very windy day. The maximum windspeed for the day was 30 m/s.

Figure 5.24: Helicopter Drone For Airborne Targets Detection Phase 3

Figure 5.25: Radar Setup For Airborne Targets Detection Phase 3

The experiment for the detection of airborne targets is done for FMCW Radar mode and repeated for Pulse CW Noise Radar mode. OBS Studio S/W is used to record the detection of targets. During the period of experimentation, it was also planned to include the test for mutual interference and spectrum sharing. In this test, it was planned that the first ghost target from table 4.2 is injected into the received signal for both FMCW Radar mode and Pulse CW Noise Radar mode.

5.5.4 Experimental Results And Analysis For The Detection Of Airborne Targets - Phase 1

The Radar was run for several hours to detect airborne targets. Due to the conical antenna beam pattern of the used grid antennas, the height of the targets to be detected for each range of interest must be determined and the elevation angle of the antenna adjusted accordingly. For this research, the elevation angle was chosen to detect targets at a radial range of 5 km with a height of between 2.6 km and 4.4. km. This in itself poses a problem since targets flying above 4.4 km and below 2.6 km at a range of 5 km will not be detected. At radial ranges shorter than 5 km, the maximum detectable target height and the minimum detectable target height decrease. For targets flying at radial ranges larger than 5 km, the maximum detectable target height and minimum detectable target height increase. Therefore this

antenna beam pattern makes it difficult to detect airborne targets especially since targets flying at the range of interest within the required height range is very seldom. For several days many targets were flying between the Radar and the radial range of interest and when they do fly at the radial range of interest, they would be at a height that is not detectable by the Radar and when flying at the correct radial range and height range, if some Radar setting is incorrect, the researcher has to wait a long time before the same opportunity presents itself again. This makes it very difficult to experiment.

The best antenna beam pattern that is used for the detection of airborne targets is the cosecant squared (CSC^2) beam pattern which is shown in figure 5.26 [33]. This beam pattern practically provides a constant height throughout its range coverage continuously from surface to maximum height. The researcher is currently looking for an antenna with a CSC^2 beam pattern, gain of at least 24 dBi, 8 km beam height and frequency range that is between 500 MHz and 2.5 GHz inline with the PA that the researcher is currently using. Once this antenna is obtained, the experiment will be repeated and multiple airborne targets can be detected up to 17 km radial range with a maximum height of 8 km and any minimum height depending on the line of sight. Phase 2 results below provide the outcome of another attempt of detecting airborne targets using this Radar.

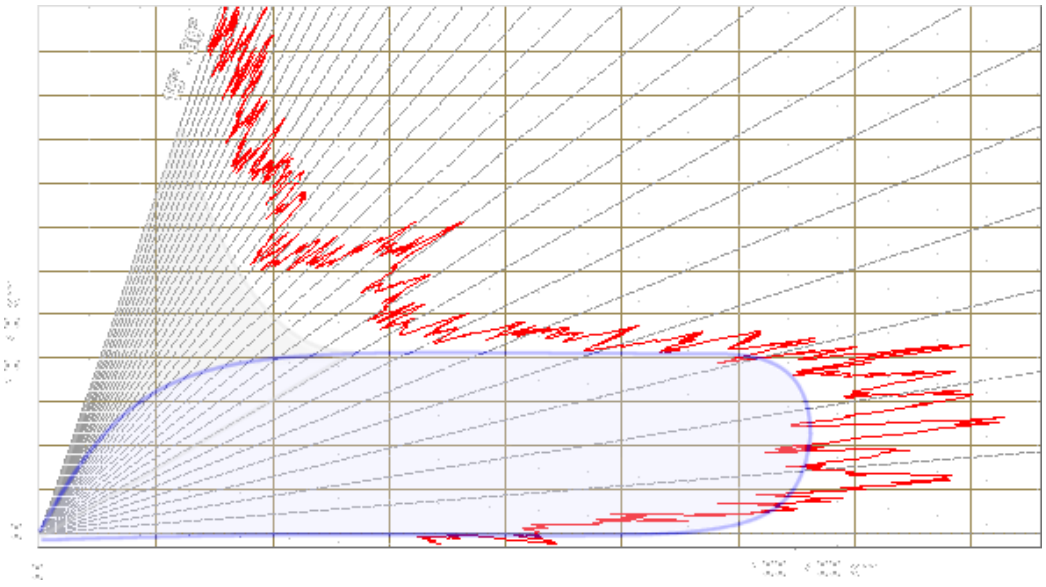

Figure 5.26: Cosecant Squared Beam Pattern

5.5.5 Experimental Results And Analysis For The Detection Of Airborne Targets - Phase 2

Phase 2 of the detection of airborne targets experiment also did not go well even though the antennas with wide elevation beam width were used. It is difficult to determine the cause of the problem in time for submission of

this dissertation since the aeroplanes and helicopters around the researcher's house pass very seldom, at different heights, ranges and times. The researcher, however, undertakes to solve this problem after the dissertation has been submitted. Since the detection of airborne targets is critical for this research, the researcher executed phase 3 of this experiment whose successful results are discussed below.

5.5.6 Experimental Results And Analysis For The Detection Of Airborne Targets - Phase 3

After having failed twice to detect airborne targets, the researcher decided to execute a more controlled experiment by using a helicopter drone with a pilot who could be told where and how high to fly it. This proved to be successful even though the pilot sometimes flew higher than the Radar setup could detect the drone and sometimes flew out of the horizontal beamwidth of the Radar. As much as this flying out of the boundaries of the Radar is undesired, it however proved that the Radar detected the drone only when it was within its performance boundaries and thus confirming that all targets that were detected are real targets.

The first experiment that was done was the detection of airborne targets in FMCW Radar mode. Since the Radar is stationery and not rotating, the main parameters to be compared are the target range and velocity. The mast that the antennas are attached to is used to point antennas in a certain direction and does not continuously rotate. Therefore, the Radar is always operating in starring mode with the benefit of being able to change the starring sector when required. Figure 5.27 shows the drone moving towards the Radar captured using a cellular phone camera. In this picture, the Radar is configured for FMCW Radar mode and the target is shown moving towards the Radar in the Range Doppler map while the helicopter drone is pointing away from the Radar. This could be because the helicopter drone changed direction and was captured by the camera before the Range Doppler display was updated or the helicopter drone flew in reverse. Figure 5.28 shows the Range Doppler map of the detected airborne target flying towards the Radar.

The experiment for the detection of airborne targets was repeated for the Radar operating in Pulse CW Noise Radar mode. The same physical setup is used and the only difference is the mode the Radar is operating in. In figure 5.29 the helicopter drone is captured using the cellular phone camera flying away from the Radar and in the same picture, the range and velocity of the helicopter drone are visible on the Range Doppler map. The Range Doppler map of the same target captured using OBS studio is shown in figure 5.30. From this figure, it is clear that the Radar is configured to operate in Noise Radar mode. This experiment shows that Noise Radar can be used in the Air Defence role for the detection of airborne targets.

Due to time constraints, there was no time to do the mutual interference

experiment since it was late in the afternoon and the drone pilot wanted to pack up.

Figure 5.27: Helicopter Drone Flying Towards The Radar In FMCW Radar Mode CellPhone Picture

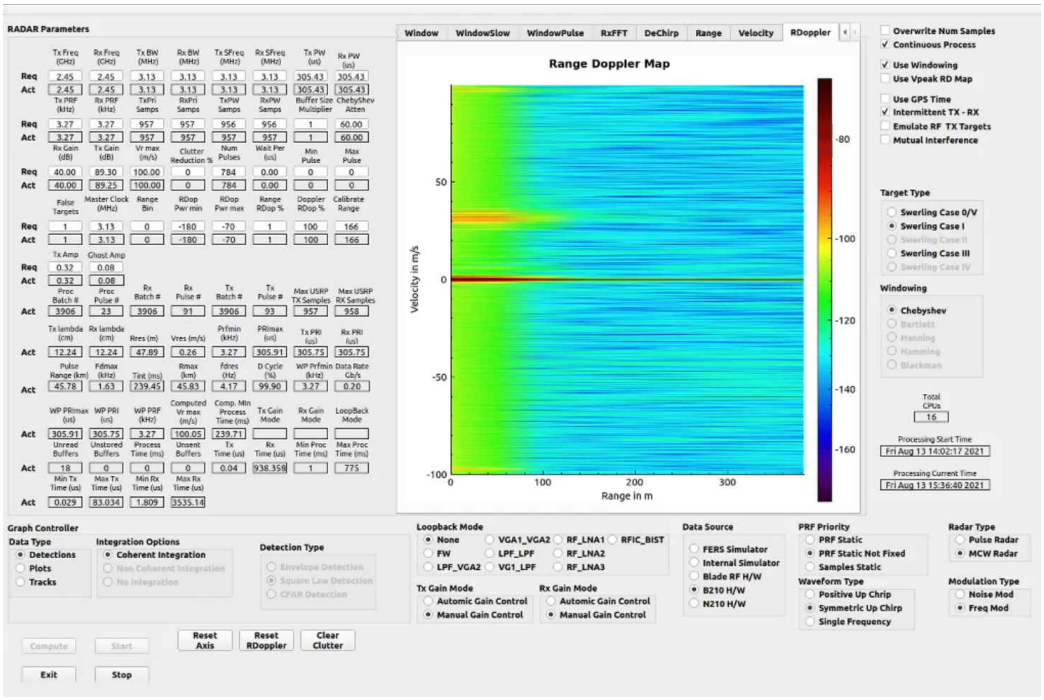

Figure 5.28: Helicopter Drone Flying Away From The Radar In FMCW Radar Mode

Figure 5.29: Helicopter Drone Flying Away From The Radar In Noise Radar Mode CellPhone Picture

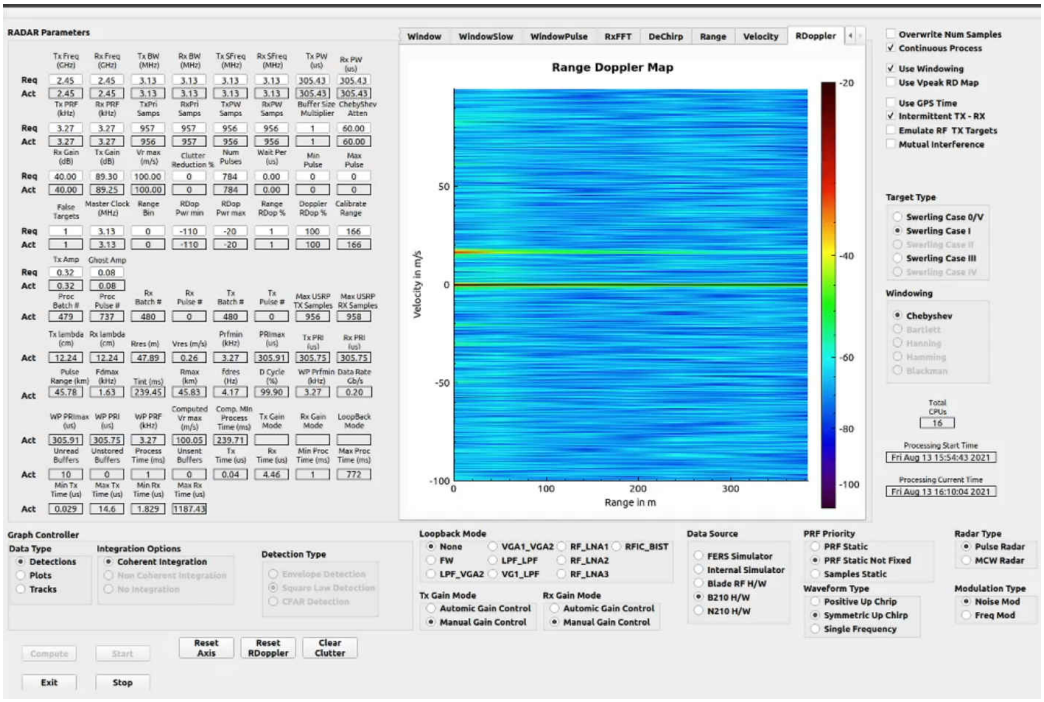

Figure 5.30: Helicopter Drone Flying Away From The Radar In Noise Radar Mode

5.6 Detection Of Animals

South Africa is faced with the problem of stock theft and the poaching of Rhinos in its national parks. This experiment will determine if this Radar can detect animals while deployed at the border for its VSHORAD role. One of the key issues to consider about animals is that they tend to move very slow unless they are chasing something or running away from something. It is therefore easy for a Radar to mistake them for clutter because of their slow velocities.

5.6.1 Test Setup For The Detection Of Animals

The Radar was deployed at a farm past a small town of Northam in Limpopo province of South Africa which is 200 km from the researcher's house. The area of deployment consists of cows and goats within a maximum radial range of 300 m. Two grid antennas were deployed each on its own 1.8 m mast and the antennas were separated by a distance of at least 2 m. In the first two experiments for the detection of airborne targets, it was important to elevate the antenna to maximise the maximum target detection height at the range of interest. To detect surface targets such as humans, the antenna elevation must be zero. In figure 5.31 it is clear that the antenna elevation beam will hit the surface at 14.660 m with the antenna deployed

at 0^o elevation angle.

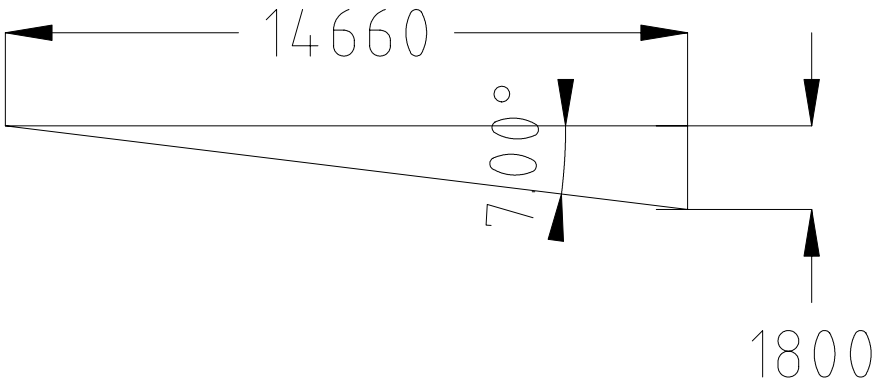

Figure 5.31: Minimum Surface Detection Range In Meters

The experiment was to be done for FMCW Radar mode and Pulse CW Radar mode. Thereafter it was to be repeated for mutual interference and spectrum sharing test by injecting the first ghost target from table 4.2 into the received signal for both FMCW Radar mode and Pulse CW Radar mode. The results are recorded using OBS studio and analysed afterwards.

5.6.2 Experimental Results And Analysis For The Detection Of Animals

It took 30 minutes to deploy the Radar on Saturday after arriving at the farm. USRP B210 could not be detected using the uhd_find_devices command. The rest of Saturday afternoon was spent trying to discover why the USRP B210 was not responding. The problem was partially solved on Sunday afternoon when the researcher tried another USB 3.0 cable. With this new cable, running usb_find_devices detected the USRP B210 but running uhd_usrp_probe detected the USRP B210 as a USB 2.0 device instead of a USB 3.0 device. Fortunately, the configurability of the Radar came in handy by reducing the full duplex data rate to 400 Mb/s, which resulted in a range resolution of 47.89 m instead of the preferred range resolution of 6 m which requires a full duplex data rate of 1.8 Gb/s. Due to time constraints, since it was already late on Sunday and the researcher had to drive back for 200

km, the Radar was tested only in FMCW mode and false targets were not injected.

From the OBS Studio recording, figures 5.32 and 5.33 show a cow moving away from the Radar and multiple cows moving towards the Radar respectively. The utilisation of a course range resolution of 47.89 m is visible by the target detections that are spread too wide across the screen in the range dimension. While the Radar was running, the researcher used his cellphone to capture the video of the Radar screen and the targets concurrently. Figure 5.34 shows a screenshot of the Radar display from the cell phone with the cow out of view of the cell phone. In figure 5.35 a stationery cow is visible in front of the Radar but the Radar display shows no target since it is not moving. The two grid antennas are also visible in the picture with one clearly visible and the right-hand one only partially visible. From figure 5.36 three cows are visible moving away from the Radar and the Radar display shows them moving away as well.

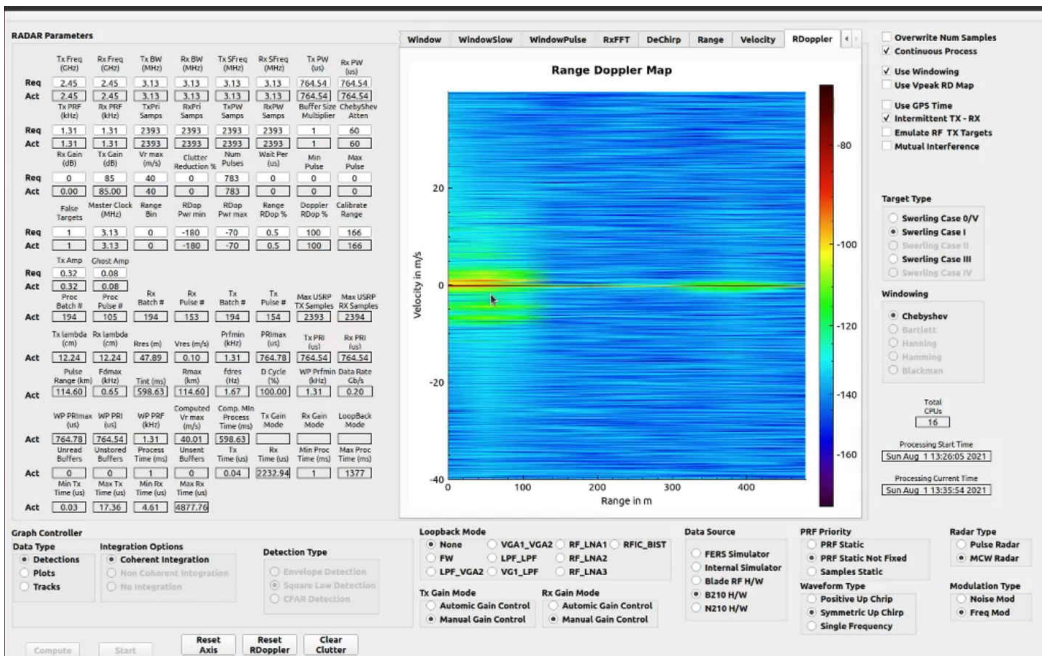

Figure 5.32: Cow Moving Away From The Radar

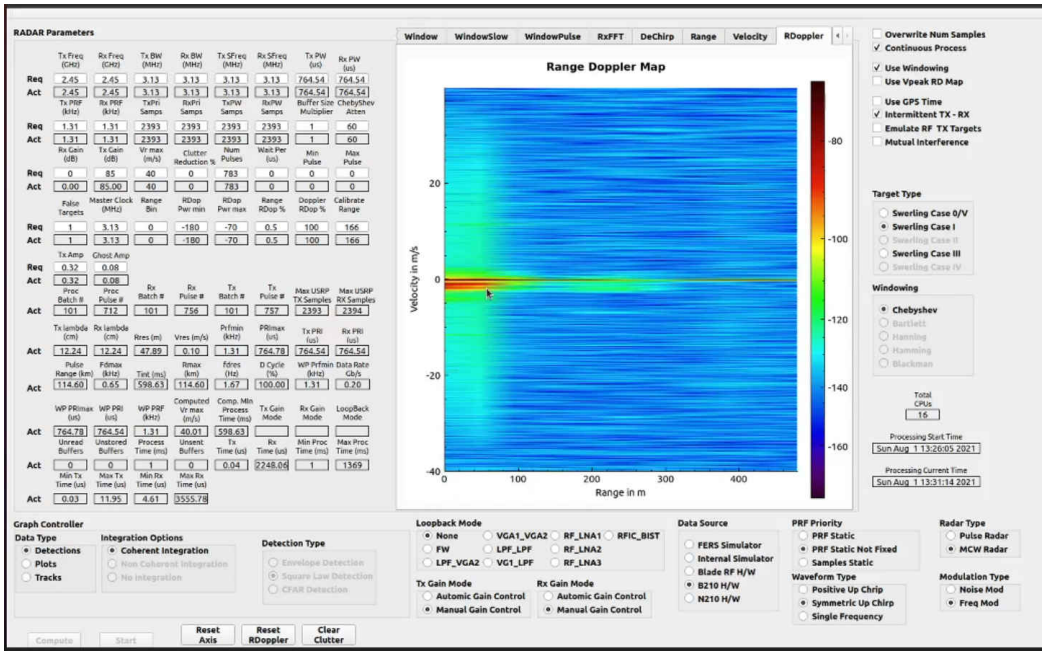

Figure 5.33: Multiple Cows Moving Towards The Radar

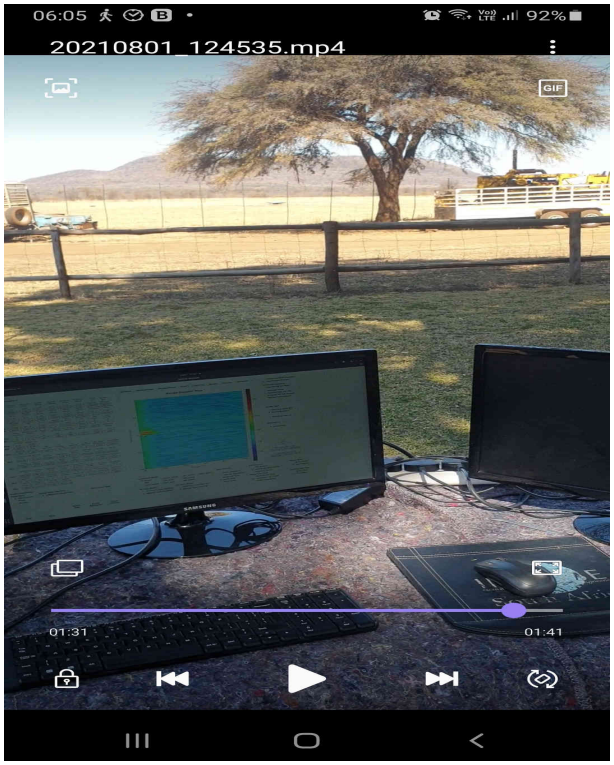

Figure 5.34: Cow Moving Away From The Radar: Cellphone ScreenShot

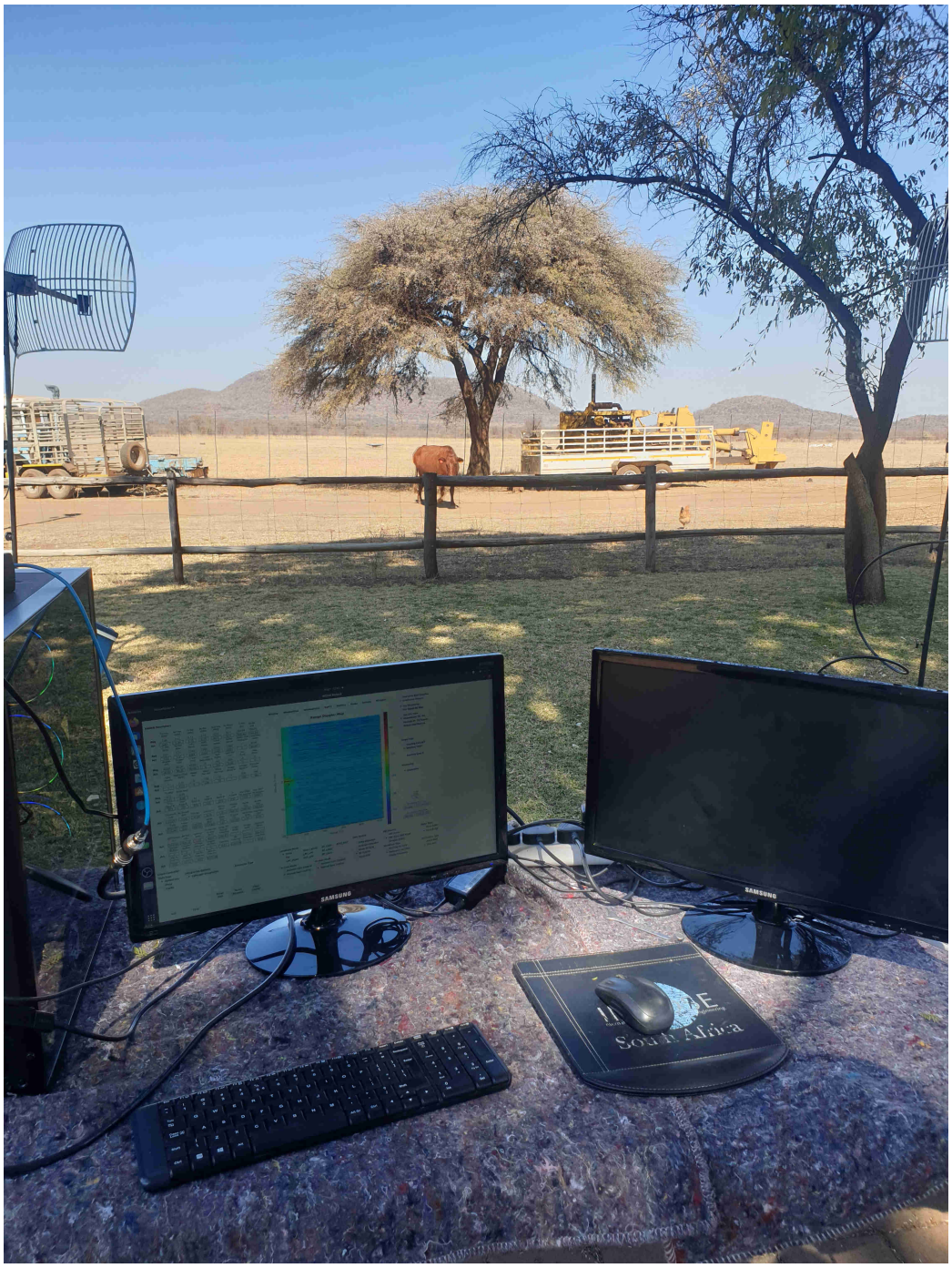

Figure 5.35: Stationery Cow: Cellphone ScreenShot

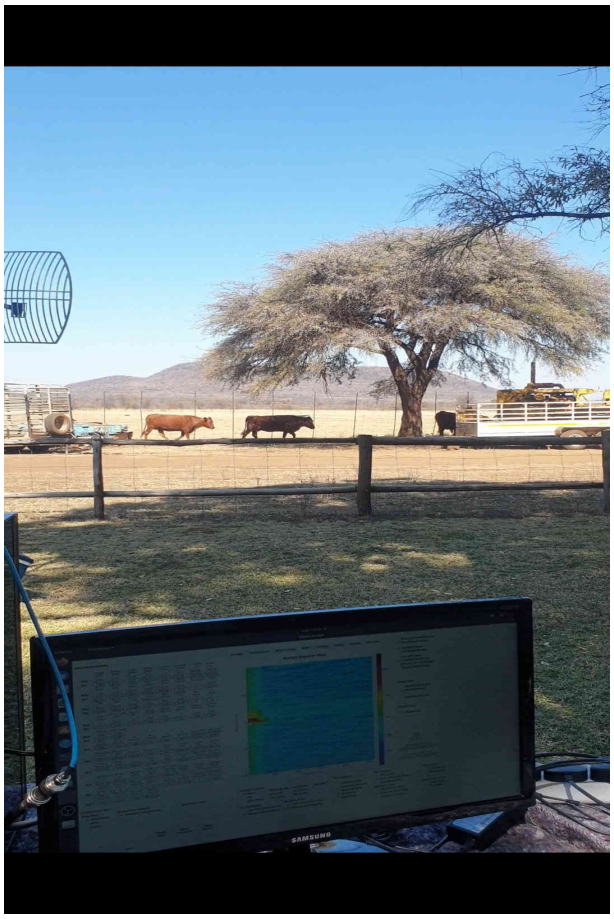

Figure 5.36: Three Cows Moving Away From The Radar: Cellphone Screen-Shot

5.7 Detection Of Humans

The next experiment was for the detection of humans. The usefulness of this experiment is to show that this VSHORAD Radar when deployed along the border, can be used to detect surface targets as well, especially illegal immigrants or terrorists. This will eliminate the need for a second Radar and thus reduce the overall operational cost of border patrollers.

5.7.1 Test Setup For The Detection Of Humans

The same setup for the detection of animals was used for the detection of humans with the researcher's colleague acting as the human target of interest. The target was planned to move away from the Radar up to a distance of about 250 m and then walk and run around that distance.

Like in previous experiments, the detection of humans was planned to be done for FMCW Radar mode and repeated for Pulse CW Noise Radar mode. OBS Studio S/W was used to record the detection of targets. The

next experiment was to include the test for mutual interference and spectrum sharing. In this test, as it was done for previous experiments, the first ghost target from table 4.2 was to be injected into the received signal for both FMCW Radar mode and Pulse CW Noise Radar mode. The results were to be recorded using OBS Studio and analysed.

5.7.2 Experimental Results And Analysis For The Detection Of Humans

All problems that led to using a course range resolution of 47.89 m for the detection of animals and being unable to inject false targets affected this test for the detection of humans since it was the same test setup done on the same day. However, the detection of humans using noise waveform was done on 13 August 2021 at a plot in Bronkhorstspruit, Pretoria, South Africa. In figure 5.37 a human is detected walking towards the Radar within a range of 47.89 m, the Radar in noise Radar mode and no amplifier connected. Another human target was detected walking towards the Radar at a range of around 250 m as shown in figure 5.38 and was again detected running towards the Radar at the same distance as shown in figure 5.39 with the amplifier connected and the Radar in FMCW mode. This Radar has again proven that it can be used for the detection of different types of targets in both FMCW and Noise Radar mode.

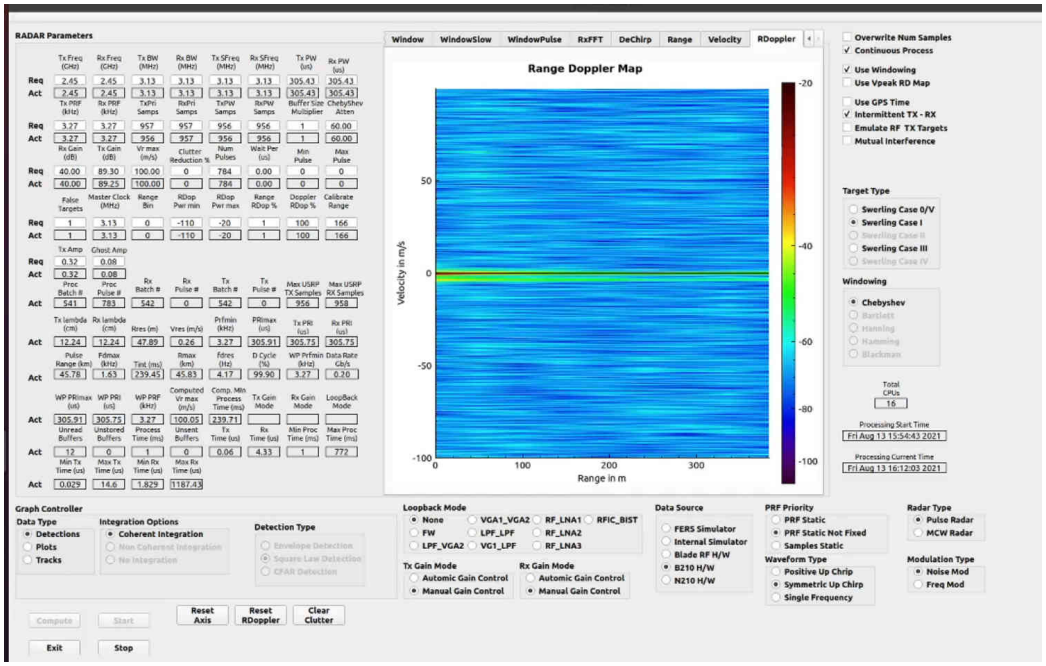

Figure 5.37: Human Walking Towards The Radar In Noise Radar Mode

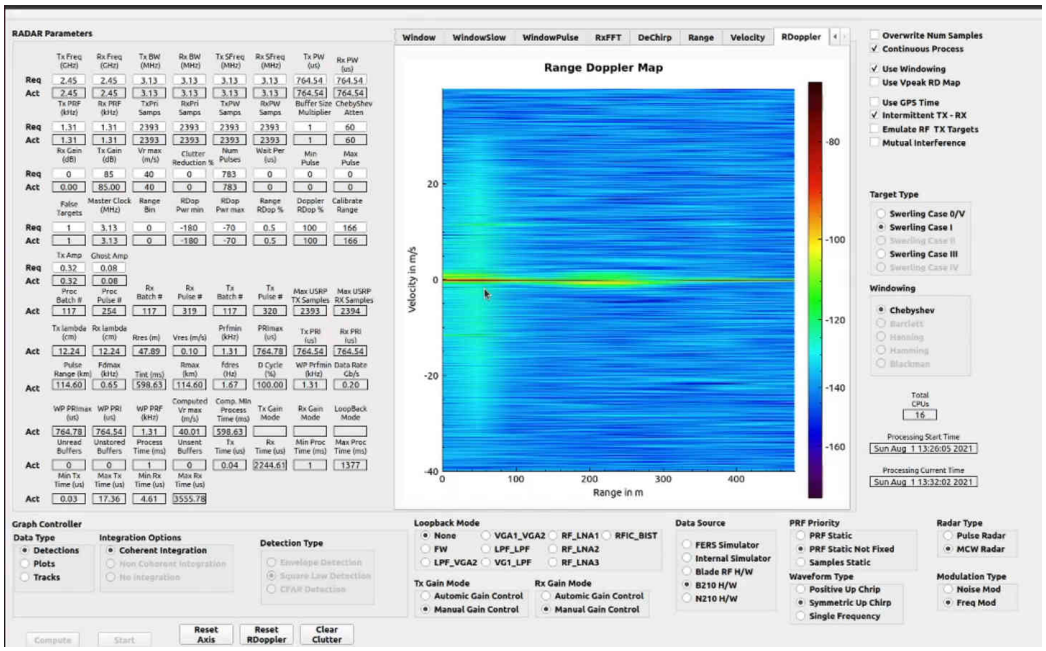

Figure 5.38: Human Walking Towards The Radar

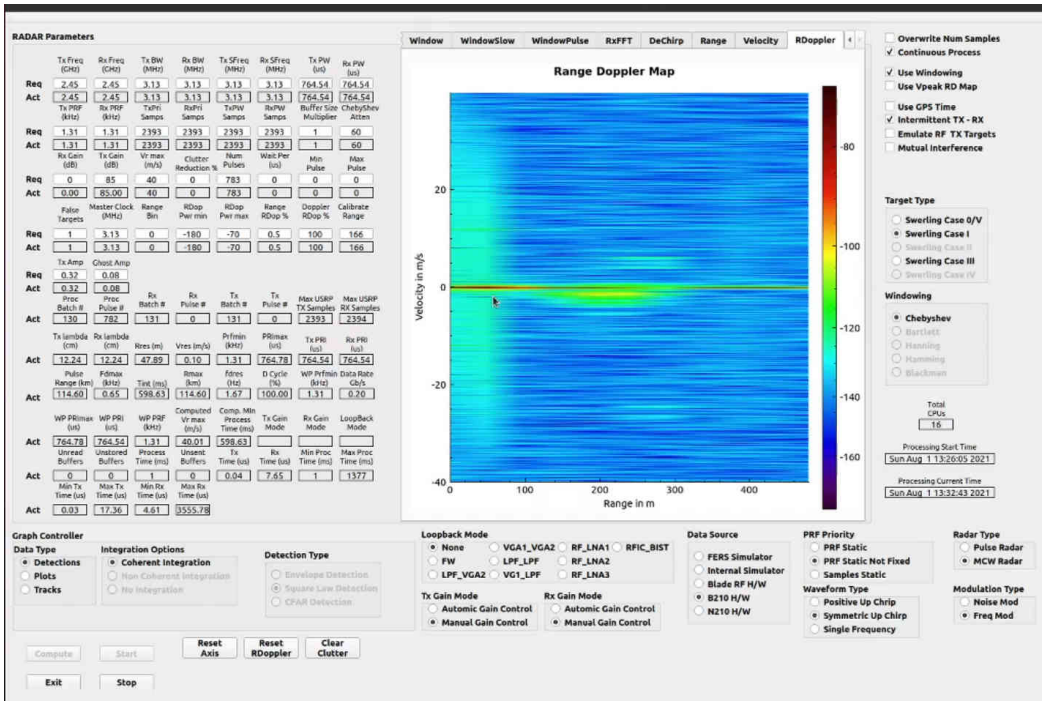

Figure 5.39: Human Running Towards The Radar

5.8 Summary

This chapter focused on integrating H/W such as SDR, antennas, cables and PA with the S/W that was used for simulation in the previous chapter. The first experiment was for H/W in the loop simulation whereby the USRP B210 SDR was used to transmit and receive simulated targets and the Radar performed as expected for FMCW Radar mode and Pulse CW Radar mode.

The experiments for the detection cars also went well and the results were as expected. The surveillance camera was used as a confirmation sensor for the detection of cars and it was possible to view all types of targets in the Radar display and confirm their presence in the surveillance camera output. Detection of airborne targets experiment could not be completed twice using targets of opportunity and was only successful after a controlled experiment using the helicopter drone operated by the researcher's colleague. Ghost targets for FMCW radar mode were not visible in the confirmation sensor for the detection of cars in the FMCW Radar mode since the confirmation sensor only shows real targets and ghost targets are not real. The experiment of injecting ghost targets in the received signal for Pulse CW Noise Radar mode proved the robustness of Noise Radar against the problem of mutual interference and confirmed that Noise Radar can efficiently share the EM spectrum with other Radars. In detecting humans and animals at a farm 200 km away from the researcher's house, it was proven that the Radar can be easily deployed and used to detect different types of targets. The next chapter is the conclusion of this research. The versatility of this Radar has been proven beyond doubt.

Chapter 6
Conclusion, Limitations And Future Work

This dissertation started with the user requirement of developing an LPI Air Defence Noise Radar. The hypothesis to be tested was derived as "LPI AD Noise Radar with high-range and Doppler resolutions is realisable." Furthermore, the hypothesis was tested by doing experiments which tested the following:

1. Detect airborne targets
2. Test LPI characteristics
3. Test mutual interference and spectrum sharing
4. Test high-range resolution
5. Test high doppler resolution

Going through different literature, it was discovered that even though research in Noise Radar has been done since the 1950s, this type of Radar has not been adopted for military use. The hypothesis was therefore chosen to determine the feasibility of using Noise Radar in the military environment. Air Defence is one of the critical capabilities of any military since airborne attacks can cause serious damage with extremely low risk for the attacker. It is therefore of utmost importance to detect airborne threats such as fighter aircraft, helicopters, Unmanned Aerial Vehicles (UAVs), drones and missiles launched from airborne targets from the furthest distance possible to have enough time to react against the threat. Pulse Radar is normally used for long-distance threats to avoid the problem of a high-power transmit signal going into the receive channel of the Radar since a pulse Radar does not receive when it transmits. FMCW Radar is normally used for the detection of targets in the short range due to its low power requirements, therefore, even though some of the transmitted signals go into the receive channel, its low power characteristics do not damage the receive channel. Frequency modulation is normally used for both Pulse and CW Radars, with the frequency modulated pulse waveform known as LFM waveform and the frequency modulated

continuous waveform known as FMCW waveform. All frequency modulated waveform Radars suffer a problem of mutual interference and inefficient sharing of the EM spectrum which literature indicated that these problems are resolved in Noise Radar. This research, therefore, took the approach of comparing the performance of a frequency modulated waveform Radar against a Noise modulated waveform Radar to test the hypothesis.

The first step was to develop a tool that will be used to test the hypothesis. This was achieved through the development of a configurable Radar that could operate in pure simulation mode and also as a real Radar with H/W integrated with the S/W. The same S/W was used for simulation and for real Radar mode with integrated H/W with only minor deltas for features that are unique to simulation and integrated H/W. Most of the Radar parameters such as PRF, PRI, Pulse BandWidth, Pulse length, Center Frequency, connected SDR type, Radar Type (Pulse or CW), Modulation Type (FM or Noise) etc are configurable, which makes it easy to repeat different types of experiments without changing the source code. It was explained in the research that even though the terminology used is mainly that of pulse Radar, the same terminologies have their equivalents in FMCW Radar such as PRI which is the same as Sweep Time in FMCW, PRF which is the same as Sweep Rate in FMCW etc.

Once the Radar tool was confirmed to be stable and working as expected, the entire elements of the hypothesis were tested using the Radar tool in simulation mode. It was shown that all simulated targets were detected in FMCW Radar mode and Pulse CW Radar mode. Pulse CW Noise Radar mode was explained to be a Noise modulated Radar mode that uses matched filter signal processing technique instead of a de-chirp signal processing technique.

Both FMCW Radar mode and Pulse CW Noise Radar mode were shown to have LPD characteristics due to their low Effective Radiated Power (ERP) as a result of transmitting continuously. However, when it came to LPE characteristics, Pulse CW Noise Radar mode outperformed the FMCW Radar mode due to the fact the noise waveform is unique for each deployed Radar and it is also unique for each batch of pulses in any deployed Noise Radar. This means that it is difficult to predict the waveform of a Noise Radar and thus making it extremely difficult to exploit it. Since LPI is a combination of LPD and LPE characteristics, therefore Noise Radar has more LPI characteristics than FMCW Radar.

Mutual interference and spectrum sharing were shown to be a huge problem for FMCW Radar whilst Noise Radar was shown to be immune to the problem of mutual interference and shares the EM spectrum efficiently with other Radars. In FMCW Radar mode, ghost targets were visible together with real targets, whereas for Pulse CW Noise Radar mode these ghost targets were suppressed and only real targets were visible. This is a very important benefit for Noise Radar since, during Air Defence, Radars are normally deployed in such a way that their coverage overlap, which means

for each of the Noise Radars with overlapping coverage, only real targets will be shown and the operator will not be overwhelmed with too many false targets. It, therefore, implies that only a small portion of the EM spectrum is needed for Noise Radars used in the Air Defence role with overlapping coverage. Therefore it was proven that Noise Radar is immune to mutual interference problems and used the EM spectrum efficiently.

When multiple targets are attacking, a Radar needs to have high range and doppler resolutions so that targets that are very close in range and doppler can be detected as distinct targets. The configurability of the Radar allows it to be configured for various range and doppler resolutions. The range resolution is configured by changing the bandwidth of the Radar, with a higher bandwidth leading to a high range resolution. Doppler resolution is determined by the number of pulses that are integrated and the higher the number of pulses the higher the doppler resolution. The operator can overwrite the number of pulses to choose the preferred doppler resolution. The experiments showed that both FMCW Radar mode and Pulse CW Noise Radar mode were able to distinguish targets that were close in range and doppler as per the configured range and doppler resolutions respectively.

The simulation experiments have proven all elements of the hypothesis which shows that an LPI Noise Radar with high range and doppler resolutions is realisable. The H/W in the loop experiments focused only on some of the elements of the hypothesis which are the detection of targets, mutual interference and spectrum sharing. H/W in the loop experiments started with H/W in loop simulations followed by detection of cars. The results were the same as those obtained from pure simulation experiments and it was once again shown that Noise Radar can detect targets similar to FMCW Radar, Noise Radar is immune to the problem of mutual interference and can thus share the spectrum efficiently with other Radars. The detection of airborne targets using H/W could not be completed with the first two experiments that focused on targets of opportunity, however, the researcher was third time lucky when he successfully detected a helicopter drone in both FMCW and Noise Radar modes. The Radar also successfully detected humans in both FMCW and Noise Radar modes. Even though the experiment for the detection of animals was done only in FMCW Radar mode, it can be concluded with reasonable confidence that the Radar will detect animals in Noise Radar mode as well since it was successfully used to detect objects of the same size, smaller size and larger size as animals.

This research has thus proven that Noise Radar can be used as an LPI Air Defence Radar. It has the benefit of sharing the EM spectrum efficiently with other Radars and it does not have the problem of ghost targets. Its high LPI characteristics mean that it is not easily detectable by Electronic Warfare (EW) systems and it is not easily exploitable by EW systems due to the continuous changing and unique nature of its waveform. Targets that are very close in range and/or in doppler are easily detected as distinct targets due to the high range and doppler resolutions that are possible with Noise

Radar. It was also proven that Radar can detect both airborne and surface targets. The military should therefore consider adopting Noise Radar for their Air Defence missions.

In addition to some of the limitations and future work previously mentioned, the current Radar has the following limitations: sector-based, Range doppler map and A-Scope displays, Central Processing Unit based and cross-talk problem. A continuous rotator will be added in the future to provide 360^o coverage using a Plan Position Indicator (PPI) display. In future, processing will be shared between the 8 CPU cores and the Graphical Processing Unit (GPU) to improve the Radar performance. The cross-talk problem will be addressed by the implementation of self-interference cancellation techniques.

Bibliography

[1] R. Narayanan. (2012, September 11). *Ultra-wide-band noise radar systems* [Online]. Available: http://spie.org/newsroom/4429-ultra-wide-band-noise-radar-systems?ArticleID=x90215

[2] A. Barrow. (2016, March 15). *Army developing more adaptable, secure Radar technology* [Online]. Available: http://www.army.mil/article/164251/

[3] K. A. Lukin, "Noise Radar Technology," *Telecommun. and Radio Eng.,* vol. 55, no. 12, pp. 8-16, 2001.

[4] T. Thayaparan and C. Wernik, "Noise Radar Technology Basics," Defence R&D Canada, Ontario, Rep. TM 2006-266, 2006.

[5] K. A. Lukin et al., "Use of Noise Radar in High PRF Mode for Far Range Surveillance," *International Young Scientists Forum On Applied Physics,* Dnipropetrovsk, Ukraine, 2015, pp. 1-2.

[6] K.A. Lukin et al., "Advances in Noise Radar Design," Laboratory for Nonlinear Dynamics of Electron. Syst. Inst. for Radiophysics and Electronics, Kharkiv, Ukraine, Rep. n.a., n.d.

[7] K.A. Lukin and R.A. Narayanan, "Historical Overview and Current Research on Noise Radar," Laboratory for Nonlinear Dynamics of Electron. Syst. Usikov Inst. for Radiophysics and Electronics of NASU, Kharkiv, Ukraine, Rep. n.a., n.d.

[8] M. Malanowski and K. Kulpa, "Detection of Moving Targets With Continuous-Wave Noise Radar: Theory and Measurements," *IEEE Trans. Geosci. Remote Sens.*, vol. 50, pp. 3502-3509, Sept. 2012.

[9] K.A. Lukin et al., "High Resolution and High Dynamic Range Noise Radar," *in Microwave, Radar and Remote Sensing Symposium,* Kyiv, Ukraine, 2011, pp. 247-250.

[10] K. Kulpa, "Introduction," in *Signal Processing in Noise Waveform Radar.* Norwood, MA: Artech House, 2013, ch. 1, pp. 1-5.

[11] K. Kulpa, "Noise Radar," in *Signal Processing in Noise Waveform Radar.* Norwood, MA: Artech House, 2013, ch. 3, pp. 45-69.

[12] B.R. Mahafza and A.Z. Elsherbeni, "Introduction to Radar Basics," in *Matlab Simulations for Radar Systems Design.* Boca Raton, Florida: CRC Press, 2004, ch. 1, sec. Appendix 1A Pulse Radar, pp. 76-84 **N.B. Page numbers are not written in the book and are obtained from the pdf status bar.**

[13] B.R. Mahafza and A.Z. Elsherbeni, "Radar Waveforms," in *Matlab Simulations for Radar Systems Design.* Boca Raton, Florida: CRC Press, 2004, ch. 3, sec. 3.1 - 3.10, pp. 157-192. **N.B. Page numbers are not written in the book and are obtained from the pdf status bar.**

[14] M. A. Govoni et al., "Range-Doppler Resolution of the Linear-FM Noise Radar Waveform," *IEEE Trans. Aerosp. Electron. Syst.*, vol. 49, pp. 658-664, Jan. 2013.

[15] B.R. Mahafza and A.Z. Elsherbeni, "Radar Waveforms," in *Matlab Simulations for Radar Systems Design.* Boca Raton, Florida: CRC Press, 2004, ch. 5, sec. 5.1 - 5.4, pp. 250-276. **N.B. Page numbers not written in the book are obtained from the pdf status bar.**

[16] M. Malanowski and K. Kulpa, "Detection of Moving Targets With Continuous-Wave Noise Radar: Theory and Measurements," *IEEE Trans. Geosci. Remote Sens.*, vol. 50, pp. 3502-3509, Sept. 2012.

[17] O. Adrian, "Future Surface Radar Technology: From Air Defence to Air and Missile Defence," Thales Air Systems: Surface Radar, Hameau de Roussigny, Limours, France, Rep. 1-4244-0284-0/07, 2007. **N.B. This is the IEEE Xplore report number and date.**

[18] SAAB. (Accessed: 2020, Sept. 06). *RBS 70 NG* [Online]. Available: https://saab.com/globalassets/commercial/land/weapon-systems/ground-based-air-defence-missile-systems/rbs-70-ng/rbs-70-ng-product-sheet.pdf

[19] IAI. (Accessed: 2020, Sept. 06). *ELM-2026B Very Short Air Defense Radar (VSHORAD)* [Online]. Available: https://www.iai.co.il/p/elm-2026b

[20] SRC. (2019, Dec. 16). *AN/TPQ-49 MULTI-MISSION RADAR* [Online]. Available: https://www.srcinc.com/pdf/Radars-and-Sensors-ANTPQ49.pdf

[21] SAAB. (Accessed: 2020, Sept. 06). *ADVANCED RADAR WARNING SYSTEM* [Online]. Available: https://saab.com/globalassets/commercial/air/electronic-warfare/radar-warning-receivers/bow/bow-product-sheet.pdf

[22] Indra. (Accessed: 2020, Sept. 06). *ALR-400 RADAR WARNING RECEIVER* [Online]. Available: https://www.indracompany.com/sites/default/files/indra_alr-400_rwr.pdf

[23] Leonardo MW. (2019, Sept.). *SEER ADVANCED RADAR WARNING RECEIVER* [Online]. Available: https://www.leonardo.us/hubfs/Product%20Brochures/SEER%20Digital%20RWR%20(mm07739)%20LQ.pdf

[24] P.F. Jarpa, "Quantifying the difference in low probability of intercept radar waveforms using quadrature mirror filtering," M.S. thesis, Dept. Elect. & Comp. Eng., Naval Post Grad. School, Monterey, Calif., 2002.

[25] M. A. Govoni et al., "Low Probability of Intercept of an Advanced Noise Radar Waveform with Linear-FM," *IEEE Trans. Aerosp. Electron. Syst.*, vol. 49, no. 2, pp. 1351-1356, April 2013.

[26] M.M. Hashemi and M.M. Nayebi, "Performance evaluation of random PRF signals in LPD Radars," in *IEEE International Radar Conference*, 2000, pp. 134-139.

[27] F. Wang et al., "Target Tracking While Jamming by Airborne Radar for Low Probability of Detection," *Sensors*, vol. 18, no. 2903, pp. 1-16, Spet. 2018.

[28] D.C. Schleher, "LPI Radar: Fact or Fiction," *IEEE Aerosp. & Electron. Syst. Mag.*, pp. 3 - 6, May 2006.

[29] Electronics-Notes. (Accessed: 2020, September 11). *Electronic & Radio Frequency Noise* [Online]. Available: https://www.electronics-notes.com/articles/basic_concepts/electronic-rf-noise/radio-frequency-noise-basics.php

[30] M.A. Richards, "Radar Waveforms," in *Fundamentals of Radar Signal Processing,* 2nd ed. New York: McGraw-Hill, 2014, ch. 4.

[31] K. Patel et al., "Linear Frequency Modulation Waveform Synthesis," in 2012 IEEE Students' Conference on Electrical, Electronics and Computer Science, 2012 © IEEE. doi: 10.1109/SCEECS.2012.6184744

[32] K. Kulpa, *Signal Processing in Noise Waveform Radar*. Norwood, MA: Artech House, 2013.

[33] Radartutorial (2021, February 16). *Antenna with Cosecant Squared Pattern* [Online]. Available: https://www.radartutorial.eu/06.antennas/Cosecant%20Squared%20Pattern.en.html

[34] Militaryaerospace.com. (2021, May 13). *What are the ISM Bands, What Are They Used For?* [Online]. Available: https://www.militaryaerospace.com/directory/blog/14059677/what-are-the-ism-bands-and-what-are-they-used-for

[35] Weibelradars.com. (2022, March 19). *Xenta-M1, Xenta-M3 & Xenta-M5* [Online]. Available: https://dkkn97s94if1u.cloudfront.net/wp-content/uploads/2021/04/XENTA-Brochure-Air-Defense.pdf

[36] CSG Aerospace. (Accessed: 2022, March 19). *Short Range Air Defence Radar* [Online]. Available: https://csgaerospace.cz/short-range-air-defence-radar

[37] News24. (Published: 2013, September 27). *Four record breaking spots to visit in SA!* [Online]. Available: https://www.news24.com/you/Archive/four-record-breaking-spots-to-visit-in-sa-20170728